

ulm university universität
uulm

Cooperative phenomena in open quantum systems subject to external control

kumulative Dissertation
zur Erlangung
des Doktorgrades Dr.rer.nat.
der Fakultät für Naturwissenschaften
der Universität Ulm

vorgelegt von
Rebecca Schmidt
aus
Rheinfelden (Baden)

2013

Amtierender Dekan:	Prof. Dr. Joachim Ankerhold
Erstgutachter:	Prof. Dr. Joachim Ankerhold
Zweitgutachter:	Prof. Dr. Tommaso Calarco
Tag der Prüfung:	19. November 2013

meinem Vater

Contents

Ante **1**

I. Optimal control of open quantum systems 3

1. Open quantum systems **7**
1.1. System-plus-reservoir model 7
1.1.1. Caldeira-Leggett model 8
1.2. Path integral formalism 9
1.3. Stochastic Liouville-von Neumann equation 12
1.3.1. Ohmic reservoir 14
1.4. Quantum master equations 14
1.4.1. Projector formalism 15
1.4.2. Born-Markov master equation 15
1.4.3. Lindblad master equation 16

2. Optimal control of quantum systems **17**
2.1. Applications: physical systems, methods, objectives 18
2.1.1. Quantum systems 18
2.1.2. Control methods 20
2.1.3. Objectives 21
2.2. Optimal control and noise 22
2.2.1. Time-optimal control 22
2.2.2. Control in the presence of noise 23
2.2.3. Open vs. closed/feedback control 23
2.2.4. Optimal control to fight decoherence 24
2.2.5. Artificial environments 24
2.2.6. Real environments 25
2.3. Dissipative optimal control 25

3. Gaussian states **29**
3.1. Cumulant description of Gaussian states 29
3.2. Wigner functions 30
3.3. Physical quantities of Gaussian states 30

3.3.1. Entropy of Gaussian states 31
3.3.2. Entanglement for bipartite Gaussian states 31

4. Cooperative effects of driving and dissipation: Applications and results 33
4.1. Common state-to-state transfer 33
4.2. Cooling by optimal control 35
4.3. Generating entanglement by optimal control 37

5. Summary and conclusion 41

II. Publications 43

6. Summary of published articles 45
6.1. General remarks 45
6.2. Optimal Control of Open Quantum Systems: Cooperative Effects... . 47
6.3. Cooling of quantum systems through optimal control and dissipation 50
6.4. Quasi-local generation of EPR entanglement in non-equilibrium . . . 52
6.5. Conclusion 55

7. Publications 57
7.1. PRL 107, 130404 (2011) 57
7.2. Phys. Scr. T151, 014034 (2012) 71
7.3. arXiv:1305.6566 [quant-ph] 79

III. Appendix 95

A. Cumulant dynamics 97
A.1. one harmonic mode 97
A.2. two harmonic modes 100

B. Dissipative optimal control algorithm 103

Bibliography 105

Curriculum vitae 117

Publications and conference contributions 117

Thanks 121

Formalities 122

List of Figures

1.1. System-plus-reservoir model 8
1.2. Countour path integral formalism (adapted from [Sto06]) 10
1.3. Contributions to the influence action (adapted from [Wei12]) 11
1.4. Lindblad operator and strong driving (adapted from J. Stockburger) . 16

2.1. Gradient control scheme (adapted from [SRL$^+$03]) 20
2.2. Open vs. closed loop control 23

4.1. Cooling of an open system by optimal control 36
4.2. Entangling of a bipartite Gaussian system 37

6.1. Control signals (taken from [SNA$^+$11a]) 48
6.2. Cooling by optimal control (taken from [SNA$^+$11a]) 49
6.3. Features of the optimal control designed for cooling (taken from [SRAS12]) 50
6.4. Classical cooling by optimal control (taken from [SRAS12]) 51
6.5. Covariance matrices taken from [SSA13a]) 53
6.6. Wigner functions of the normal modes taken from [SSA13a]) 54
6.7. Steady state with control (taken from [SSA13a]) 55

B.1. Dissipative optimal control 103

ἐπεὶ δὲ τὸ ἔκ τινος σύνθετον οὕτως ὥστε ἓν εἶναι τὸ πᾶν,
ἀλλὰ μὴ ὡς σωρὸς ἀλλ' ὡς ἡ συλλαβή·
ἡ δὲ συλλαβὴ οὐκ ἔστι τὰ στοιχεῖα,
οὐδὲ τὸ βα ταὐτὸ τῷ β καὶ α,
οὐδ' ἡ σὰρξ πῦρ καὶ γῆ.

Aristotele, meta physics VII[1]

Understanding the fascinating features of quantum systems, or even more to influence these systems in a directed way, i.e. to control them, is a challenging task, worth the effort.
Quantum systems, as any real system, are unavoidably in contact with their surroundings; yet normal environments, in particular in condensed matter scenarios, do lack a little in positive attitude towards objectives for quantum systems popular with physicists. However, the detrimental influence such a reservoir has on quantum interference effects, relies on the general ability of the environment to impact all observables of the system. This ability offers great possibilities: Our work is focused on making use of this idle resource by applying tailored external controls. In fact, in our case, the environment is not only not disturbing and provides even more than simple noise assisted control: the reservoir is essential to fulfill the given tasks at all.
Basically, we take two ingredients, the unavoidable thermal reservoir and external control, which are both incapable of reaching the objective on their own. Only the combined effort gives rise to our results: We were able to cool a thermalized state below the reservoir temperature and even to generate such a pure quantum feature as entanglement due to a cooperative effort of driving and dissipation.

[1]In short: The whole is greater than the sum of its parts.

This thesis, as requested for a cumulative one, is divided into two parts:
The purpose of Part I, that is Chapters 1 to 5, is to set our work in the context of related work. Beginning with the methods used to describe open quantum system dynamics in Chapter 1, the applicability of these methods for optimal control is discussed. Chapter 2 presents an overview of the state of the art in optimal control of quantum systems, both for closed and open quantum systems. Here, we also present our method for the optimal control of non-Markovian open quantum systems, treating driving and dissipation consistently. The experimental significance of Gaussian states and some mathematical tools to describe Gaussian continuous variable systems are discussed in Chapter 3. The objectives considered for our optimal control tasks and the results we achieved are topic of Chapter 4, while Chapter 5 provides the conclusion.
Part II, that is Chapters 6 and 7, is dedicated to the publications, building the core of this cumulative thesis. Chapter 6 gives a summary of the publications, while Chapter 7 consists of the published articles.
In the last years, I had the chance to learn from many wonderful physicists in discussions and talks, both on conferences and, in particular, 'back home' at this university. For giving me a deeper understanding of the fascinating field of controlled open quantum systems and of physics in general, I would like to thank all these colleagues and professors.
May the reader find this work on 'cooperative phenomena in open quantum systems subject to external controls' as interesting and inspiring as I do.

Part I.

Optimal control of open quantum systems

There has been great progress in the fabrication of tailored quantum systems, increasing in scale from atomic systems up to solid state devices. These tailored systems, such as atoms and ions in traps [SKHR+03, ARJ+12], Bose-Einstein condensates [AEM+95, JBA+03], superconducting devices [VAC+02, YPA+03, SG08, HWA+09], nanomechanical systems [OHA+10, STP+10] or NV-centers in diamonds [JGP+04], offer a great variety of controllable quantum systems. This progress comes with the demand to control these systems, i.e. to drive them to desired objectives with a high fidelity, in order to use them for instance for quantum computation or quantum simulations.
Optimal control aims to determine the best possible external controls, which are actively disrupting the systems dynamics, to drive the system to a favored objective. In order to find these optimal controls, an exact description of the dynamics of the system, that, in particular, includes the driving consistently, is needed.
Real quantum systems are open systems [Wei12, BP06], they interact with their environment; even in the most sophisticated experimental realisations, the systems can never fully be isolated. Therefore, the interaction with the environment has to be taken into account, when it comes to the description of the dynamics of such a system. Moreover, controlled systems are driven systems, they are more or less far from equilibrium. Depending on the strength of the intervention into the dynamics of the system, performed by the applied control, even the stationary state might change. Common approximations made in the context of open system dynamics have to be re-evaluated in this light, concerning their validity. We do describe the driven dynamics of non-Markovian open systems by an exact stochastic Liouville-von Neumann equation (SLN) [SG02], treating both driving and dissipation on the same footing.
In many works, employing control schemes aims for reducing the interaction time of the system of interest and its environment, such as the search for the quantum speed limit [CMC+09], or for mitigating the detrimental effect of dissipation. On the other hand, based on the notion that an environment can also have positive effects on a quantum system, there are works with artificial environments, carefully designed reservoirs, such as in [MHdC+13, ACVM13, WC13], which are acting as an effective control, driving the system to a desired stationary state.
However, standard environments, in particular in condensed matter scenarios, do usually counteract the quantum interference phenomena, physicists are interested in. Due to dissipation and decoherence effects these thermal baths tend to make the system more classical. Furthermore, heat baths are an unavoidable part of the setting and therefore not simply replaceable by an artificial reservoir. Nevertheless, ordinary reservoirs come free of charge and possess in principle the possibility to influence any system observable, an idle resource asking for utilization. We were successful in completing optimal control tasks by a combined effort of environment and controls, where neither part was capable of achieving the result alone. Therefore, in order to learn about the complex interplay between system, environment and

control, we restrict ourselves to Gaussian systems and ohmic reservoirs, keeping our components as simple as possible. In fact, it is due to the simplicity of our settings, that we can definitely attribute our achievements, like cooling a quantum system and generating entanglement, to a cooperative effect of driving and dissipation.

1. Open quantum systems

Real quantum systems are open systems [Wei12, BP06][1], they can never fully be separated from their environment. This is in particular true for condensed matter systems, even for such a highly elaborate system like the quantronium; though any efforts have been made to isolate this system, there are still unavoidable noise sources [ICJ+05]. Also quantum optical systems can never fully be decoupled from the surroundings, e.g. atoms and ions in traps are still exposed to comparatively hot surfaces [THS+04].
Derivation of the dynamics of open quantum systems usually starts from the so-called system-plus-reservoir model presented in the next Section 1.1. In this frame, any reservoir with Gaussian statistics and in thermal equilibrium, is described by the Caldeira-Leggett model (Section 1.1.1). Both path integral methods (Section 1.2), and quantum master equations (Section 1.4) are used to calculate open systems dynamics, differing in the approximations made for their derivations. Based on the path integral formalism, we employ the stochastic Liouville-von Neumann equation (Section 1.3) derived by Stockburger and Grabert [SG02], for alternative stochastic approaches to dissipative dynamics cf. the review articles of Tanimura [Tan06] and Biele and D'Agosta [BD12].

1.1. System-plus-reservoir model

Open quantum systems are generally described by the system-plus-reservoir model, where a system of interest S interacts with a reservoir R. The total system is conservative and can therefore be quantized easily. For the density matrix W of the total system the Liouville-von Neumann equation holds:

$$\dot{W} = \mathcal{L}\, W \tag{1.1}$$

where $\mathcal{L}$ is the Liouville operator, a superoperator which is defined by is action on an operator A. As the total system is conservative, here the Liouvillian acts as $\mathcal{L}\, A = -\frac{i}{\hbar}[H, A]$. The Hamilton operator H of the whole system:

$$H = H_S + H_I + H_R, \tag{1.2}$$

is the sum of the Hamiltonian of the relevant system H_S, the interaction part between system and reservoir H_I and the reservoir part H_R.

[1] In what is textbook knowledge in this Chapter, I roughly follow the book of Ulrich Weiss [Wei12].

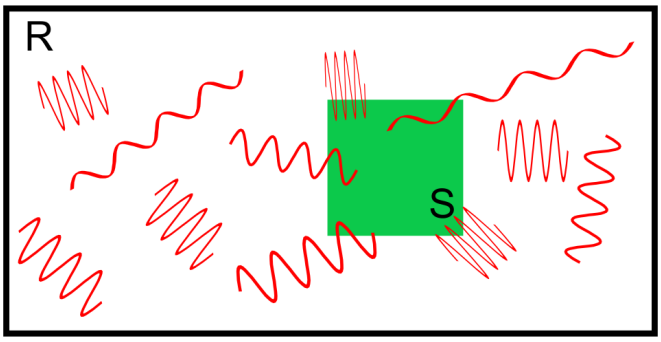

Figure 1.1.: System-plus-reservoir model: The quantum system S, we are interested in, is embedded into a large reservoir R; they interact with each other. Only the total system is conservative, and can therefore be quantized easily.

The full dynamics, while being exact, contains an arbitrary amount of degrees of freedom, we are not interested in, making the calculation of the full dynamics needlessly cumbersome or impossible. Instead, one can gain an effective description for the relevant degrees of freedom, namely for the reduced density matrix ρ of the relevant system S, by tracing out the reservoir degrees of freedom:

$$\rho = tr_R\{W\}, \tag{1.3}$$

where tr_R signifies the trace with respect to the reservoir degrees of freedom.

1.1.1. Caldeira-Leggett model

Caldeira and Leggett [CL83] have shown, that any thermal reservoir in equilibrium, given its statistics is Gaussian, can be modeled by a set $\{k\}$ of harmonic oscillators with mass m_k and frequency ω_k. The reservoir is then fully described by its inverse thermal energy β and spectral density $J(\omega)$:

$$J(\omega) = \frac{\pi}{2}\sum_k \frac{c_k^2}{m_k\omega_k}\delta(\omega - \omega_k), \tag{1.4}$$

where c_k is the coupling constant of the k-th reservoir degree of freedom to the systems coordinate. For a large number of bath degrees of freedom, the Poincaré recurrence time is infinitely larger than any relevant time scale of the system. In this continuums limit $J(\omega)$ becomes a smooth function.
For strictly linear dissipation, the system coordinate[2] q couples bilinearly to the

[2]for the sake of readability, we stick here to one degree of freedom q of the system. Generalization is straightforward.

reservoir:

$$f_k = c_k \cdot q, \tag{1.5}$$

where f_k is the force acting on the system due to the reservoir degree of freedom k. As the reservoir needs to consist of many harmonic modes, coupling a comparably small system to the reservoir does not disturb the reservoir. Nonetheless, from the point of view of the system the interaction can be strong, so the model is not restricted to weak coupling.
Given q, p, are the coordinates of the system and x_k, p_k are the ones of the reservoir, the Hamilton operator (1.2) takes the form:

$$H = H_S + q\sum_k c_k x_k + \sum_k \frac{p_k^2}{2m_k} + \sum_k \frac{1}{2} m\omega_k^2 x_k^2 + \underbrace{\sum_k \frac{c_k^2}{2m_k\omega_k^2} q^2}_{\text{counter term}} \tag{1.6}$$

The last term,$\sum_k \frac{c_k^2}{2m_k\omega_k^2} q^2 = \frac{\mu}{2} q^2$, called counter term, is an additionally added potential term which cancels out the potential renormalisation arising due to the linear coupling term. As we wish to introduce only dissipation, not a quasi-static effect, we take this term into account. This modeling is motivated by a vast class of condensed matter realisations, such as in [MSS01], where the reservoir gives rise to a dynamic dissipation effect only.
The Caldeira-Leggett model has been successfully used for some thirty years for modeling dissipation [Wei12] and is a standard model in condensed matter physics: the model provides an ergodic description, i.e. the system thermalizes to exact thermal limes $\rho_{therm} = tr_R e^{-\beta H}$, and includes low temperature effects, such as the nonexponential decay of correlation functions.

1.2. Path integral formalism

One exact way to formulate quantum mechanics is the path integral method of Feynman and Vernon [FV63],[FH65]. In this frame, the time evolution of the full density matrix:

$$W(t) = \mathrm{e}^{-\frac{i}{\hbar}Ht}\, W(0)\, \mathrm{e}^{\frac{i}{\hbar}Ht}, \tag{1.7}$$

is represented as:

$$\langle q_f, \mathbf{x}_f | W(t) | q_f', \mathbf{x}_f' \rangle = \int \mathrm{d}q_i\, \mathrm{d}q_i'\, \mathrm{d}\mathbf{x}_i\, \mathrm{d}\mathbf{x}_i'\, K(q_f, \mathbf{x}_f, t; q_i, \mathbf{x}_i, 0)\, \langle q_i, \mathbf{x}_i | W(0) | q_i', \mathbf{x}_i' \rangle\, K^*(q_f', \mathbf{x}_f', t; q_i', \mathbf{x}_i', 0) \tag{1.8}$$

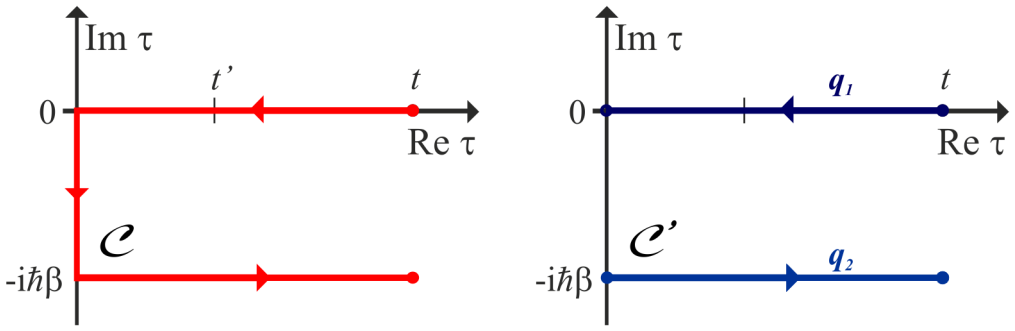

Figure 1.2.: Left: Contour for the imaginary path integral, right: for factorizing initial conditions, the contour can be divided into two real time paths integrals (adapted from [Sto06]).

where the indices i and f signify the initial and final value respectively. The propagator K is given by:

$$K(q_f, \mathbf{x}_f, t; q_i, \mathbf{x}_i, 0) = \int \mathcal{D}q\ \mathcal{D}\mathbf{x}\ \mathrm{e}^{\frac{i}{\hbar}S[q,\mathbf{x}]} \tag{1.9}$$

and

$$K^*(q'_f, \mathbf{x}'_f, t; q'_i, \mathbf{x}'_i, 0) = \int \mathcal{D}q'\ \mathcal{D}\mathbf{x}'\ \mathrm{e}^{-\frac{i}{\hbar}S[q',\mathbf{x}']}. \tag{1.10}$$

The classical action $S[q, \mathbf{x}]$, weighting the individual paths in the Equations (1.9) and (1.10), can be divided into a system, interaction, and reservoir part:

$$S[q, \mathbf{x}] = S_S[q] + S_I[q, \mathbf{x}] + S_R[\mathbf{x}]. \tag{1.11}$$

For factorizing initial conditions and the reservoir in thermal equilibrium, the initial density matrix of the total system, $W(0)$, takes the form:

$$W(0) = \rho(0) \otimes W_R(0) = \rho(0) \otimes \frac{1}{Z_R}\mathrm{e}^{-\beta H_R}\ , \tag{1.12}$$

where Z_R is the partition sum of the undisturbed reservoir. Factorizing initial conditions neglect any correlations between system and reservoir (at $t = 0$), but allows for real time path integration, cf. Figure 1.2. For a rigorous treatment of non-factorizing initial conditions, see [GSI88].
Having established the initial conditions, we can proceed to the actual path integration. For that purpose, one first defines the path variables q_1 and q_2, cf. Figure 1.2 [FV63],[Sto06]:

$$q_1(t) = q(t - \mathrm{i}\hbar\beta) \tag{1.13}$$

$$\text{und } q_2(t) = q(t) \tag{1.14}$$

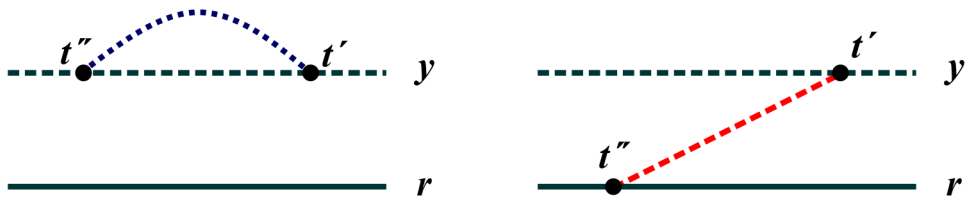

Figure 1.3.: Contributions to the influence action. Left: Self-interaction of the antisymmetric path $y(t)$, where the exchange line (blue) is the propagator $\mathrm{Re}\big(L(t'-t'')\big)$, i.e. the quantum fluctuations. Right: Correlations between the symmetric $r(t)$ and the antisymmetric path $y(t)$, here the exchange line (red) is the propagator $\mathrm{Im}\big(L(t'-t'')\big)$, i.e. the friction (adapted from [Wei12]).

Taking the trace with respect to the reservoir degrees of freedom (eq. (1.3)):

$$\rho\left(q_f, q_f'; t\right) = \int \mathrm{d}\mathbf{x}_f \langle q_f, \mathbf{x}_f | W(t) | q_f', \mathbf{x}_f' \rangle, \tag{1.15}$$

provides us with a path integral for the reduced density matrix:

$$\begin{aligned}\rho\left(q_f, q_f'; t\right) &= \int \mathrm{d}q_i \int \mathrm{d}q_i' \int_{q_i}^{q_f} D[q_1] \int_{q_i'}^{q_f'} D[q_2] \exp\left\{\frac{i}{\hbar}\left(S_s[q_1] - S_s[q_2]\right)\right\} \\ &\quad \times F\big[q_1 - q_2, \frac{q_1+q_2}{2}\big] \rho\left(q_i, q_i'; 0\right)\end{aligned} \tag{1.16}$$

The influence functional $F\big[q_1 - q_2, \frac{q_1+q_2}{2}\big]$ contains the interaction between system and reservoir. In general, when the reservoir is non-Markovian, it is non-local in time, containing memory terms, i.e. information about the common history of system and reservoir. As a consequence, the path integral is in general not analytically solvable. Numerically it can be treated in terms of path integral quantum Monte Carlo methods (cf. e.g. [Suz93]).
We introduce new coordinates $r = \frac{q_1+q_2}{2}$ and $y = q_1 - q_2$. The symmetric path $r(t)$ is the so-called quasiclassical path, while the antisymmetric path $y(t)$ describes quantum fluctuations, cf. Figure 1.3. Hence, the influence functional takes the form:

$$F\left[y, r\right] = \exp\big\{-\frac{1}{\hbar}\Phi[y, r]\big\}, \tag{1.17}$$

where:

$$\begin{aligned}\Phi[y,r] &= \int_{t_0}^{t} \mathrm{d}t' \int_{t_0}^{t'} \mathrm{d}t'' y(t')\ \mathrm{Re}\big(L(t'-t'')\big)\ y(t'') \\ &\quad + \int_{t_0}^{t} \mathrm{d}t' \int_{t_0}^{t'} \mathrm{d}t'' y(t') 2\mathrm{i}\ \mathrm{Im}\big(L(t'-t'')\big) r(t'') \\ &\quad + \frac{i}{\hbar}\mu \int_{t_0}^{t} \mathrm{d}t' \int_{t_0}^{t} \mathrm{d}t'' y(t')\delta(t'-t'') r(t'') \end{aligned} \tag{1.18}$$

The integral kernel[3] $L(t-t')$ is the correlation matrix of the undisturbed reservoir with the elements $L_{jk}(t-t') = \langle x_j x_k \rangle_\beta$. $L(t-t')$ contains the full physical information of the reservoir interaction. The imaginary part of $L(t-t')$ can be identified with friction, as the response function $\chi_R(t-t')$ of the reservoir is given by $\chi_R(t-t') = \frac{2}{\hbar}\Theta(t-t') \cdot \mathrm{Im}(L(t-t'))$. The real part of $L(t-t')$ are the quantum fluctuations (cf. Figure 1.3). $L(t)$ only depends on the inverse thermal energy β and the spectral density $J(\omega)$ of the reservoir:

$$L(t) = \frac{\hbar}{\pi} \int_0^\infty \mathrm{d}\omega J(\omega) \big(\coth \frac{\hbar\omega\beta}{2} \cos\omega t - i \sin\omega t \big). \tag{1.19}$$

The kernel $L(t-t')$ contains therefore a statistic description of the bath and the memory of the interaction history, as it is non-local in time. For solving the path integral analytically, an expression local in time is needed, without loosing the information of the progress made. Therefore, an 'outsourcing' of the memory is required.

1.3. Stochastic Liouville-von Neumann equation

As shown by Stockburger and Grabert [SG02, Sto03, Sto04, Sto06], the influence functional (1.17) can be replaced by a stochastic one:

$$\begin{aligned} F[y,r] &= \int D^2[\xi] \int D^2[\nu]\ W[\xi,\xi^*,\nu,\nu^*] \\ &\quad \times \exp\Big\{ \frac{i}{\hbar} \int_{t_0}^{t} \mathrm{d}t'\ \xi(t')y(t') + \frac{\hbar}{2}\nu(t')r(t') \Big\}, \end{aligned} \tag{1.20}$$

[3] As the reservoir is assumed to be in thermal equilibrium, L only depends on the time difference $t-t'$, not on t, t' individually, i.e. $L(t,t') \equiv L(t-t')$.

where $\xi(t)$ and $\nu(t)$ are two complex valued noise variables and $W[\xi, \xi^*, \nu, \nu^*]$ is a normalized Gaussian functional, which can be seen as probability density of the real valued noise fluctuations $\frac{\xi+\xi^*}{2}$, $\frac{\xi-\xi^*}{2\mathrm{i}}$, $\frac{\nu+\nu^*}{2}$ and $\frac{\nu-\nu^*}{2\mathrm{i}}$.
The replacement of the Feynman-Veron influence functional in eq. (1.17) with the stochastic one in eq. (1.20) is *exact* if the correlation functions of $\xi(t)$ and $\nu(t)$, reproduce the statistics of the reservoir:

$$\begin{aligned}
\mathbb{E}\left[\xi(t)\xi(t')\right] &= \mathrm{Re}(L(t-t')) && (1.21)\\
\mathbb{E}\left[\xi(t)\nu(t')\right] &= 2\frac{i}{\hbar}\Theta(t-t')\cdot \mathrm{Im}(L(t-t')) + \frac{i}{\hbar}\,\mu\,\delta(t-t') \\
&= -i\chi_R(t-t') + \frac{i}{\hbar}\,\mu\,\delta(t-t') && (1.22)\\
\mathbb{E}\left[\nu(t)\nu(t')\right] &= 0, && (1.23)
\end{aligned}$$

and, additionally:

$$\mathbb{E}\left[\xi(t)\right] = \mathbb{E}\left[\nu(t)\right] = 0. \qquad (1.24)$$

The $\mathbb{E}\left[\cdot\right]$ indicates stochastic averaging. So, the autocorrelation function of $\xi(t)$ eq. (1.21) matches the quantum noise of the reservoir, while the crosscorrelations eq.(1.22) match the dynamical response of the environment. That is, both contributions non-local in time to the influence functional (cf. Figure 1.3), are replaced by stochastic variables. To fulfill eq. (1.23), $\nu(t)$ has to be a complex variable with random phase.
Now, the memory terms are stored in the correlation functions of the noise variables, which allows for a stochastic unravelling of the path integral eq. (1.16): the sequence of path integration and stochastic averaging can be changed. For a single stochastic realisation $z(t) = \{\xi(t), \nu(t)\}$ the path integral is solvable, resulting in the stochastic Liouville-von Neumann equation (SLN):

$$\begin{aligned}
\dot{\rho}_z &= \mathcal{L}\rho_z \\
&= -\frac{i}{\hbar}[H_S, \rho_z] + \frac{i}{\hbar}\xi(t)[q, \rho_z] + \frac{\mathrm{i}}{2}\nu(t)\{q, \rho_z\} && (1.25)
\end{aligned}$$

This equation can be solved numerically for a large number of realisations. The physical reduced density matrix $\rho(t)$ is gained by averaging over all realisations:

$$\rho(t) = \mathbb{E}\left[\rho_z(t)\right] \qquad (1.26)$$

The SLN equation (1.25) provides an exact description of non-Markovian open system dynamics: The quantum mechanical dissipation fluctuation theorem is fulfilled by the SLN and in the classical limit it reduces to the Langevin equation.
Here, we use this method only in the context of systems consisting of harmonic modes coupled to ohmic reservoirs. Nevertheless, the SLN is not restricted to these systems, as has been shown in [SG02, KGSA08, KGAS09]. However, for our systems the method is numerically more stable and easier to implement.

1.3.1. Ohmic reservoir

For an ohmic spectral density the SLN (1.25) reduces to the stochastic Liouville equation for dissipation (SLED) [SM99], we introduce in this Subsection.

The spectral density of an ohmic bath is given by $J(\omega) = m\gamma_0\omega$, where γ_0 is the damping constant. However, any physical system has a high frequency cut-off ω_c. There are several ways to avoid an unphysical modeling, i.e. to take into account, that $J(\omega) \to 0$ for $\omega \to \infty$. One way is to take an ohmic spectral density with algebraic cut-off:

$$J(\omega) = \frac{m\gamma_0\omega}{\left(1 + \frac{\omega^2}{\omega_c^2}\right)^2}. \tag{1.27}$$

The cut-off frequency ω_c has to be chosen in such a way, that it is much larger than any relevant system frequencies. It defines the shortest physical time scale in our system, and it is the relevant time scale for the correlations $\mathbb{E}\left[\xi(t)\nu(t')\right]$. Without loss of generality for the ohmic setting, this allows for performing a Markovian approximation for the *imaginary* part of L, i.e. the friction, only. The relevant time scale for the quantum fluctuations, i.e. the *real* part of L, is the thermal time scale $\hbar\beta$, which, at low temperatures, is substantially larger than $\frac{1}{\omega_c}$. Here, the Markovian assumption would come with a substantial loss of generality.

However, memory-less friction comes with a simplification for the noise realisations (eqs. (1.21) - (1.23)). The SLED equation [SM99, Sto06] only depends on realisations of one, real-valued noise variable $\xi(t)$:

$$\frac{\mathrm{d}}{\mathrm{d}t}\rho_\xi = -\frac{i}{\hbar}[H_S, \rho_\xi] + \frac{i}{\hbar}\xi(t)[q, \rho_\xi] - \frac{i}{\hbar}\frac{\gamma_0}{2}\left[q, \{p, \rho_\xi\}\right] \tag{1.28}$$

For the stetting of a reservoir with ohmic spectral density, coupled to a system consisting of harmonic modes, this is an exact stochastic equation of motion. Again, it has to be solved numerically, averaging over all realisations to get the physics. In the extreme high temperature limit, this equation gets fully Markovian and identical with the Caldeira-Leggett master equation.

1.4. Quantum master equations

Starting from the system-plus-reservoir model, i.e. the Hamiltonian eq. (1.1), and the dynamics of the total system eq. (1.2), so-called quantum master equations can be derived. In order to trace out the irrelevant part, usually a projector formalism is employed.

1.4.1. Projector formalism

The projection on the relevant part only is performed by a projection operator $\mathcal{P}$, defined by:

$$\mathcal{P}W(t) = \rho(t) \tag{1.29}$$

with: $\mathcal{P}+\mathcal{Q} = \mathbb{1}$ and $\mathcal{P}^2 = \mathcal{P}$. This results in the exact Nakajima-Zwanzig equation:

$$\frac{\mathrm{d}}{\mathrm{d}t}\rho(t) = \mathcal{P}\mathcal{L}\rho(t) + \int_0^t \mathrm{d}t' \; \mathcal{P}\mathcal{L}e^{\mathcal{Q}\mathcal{L}t'}\mathcal{Q}\mathcal{L}\rho(t-t') + \mathcal{P}\mathcal{L}e^{\mathcal{Q}\mathcal{L}t}\mathcal{Q}W(0), \tag{1.30}$$

which, for non-trivial systems, cannot be solved without further assumptions. Neglecting the initial value of the irrelevant part $\mathcal{Q}W(0)$ and assuming $[\mathcal{P}, \mathcal{L}_S] = 0$, with $\mathcal{L}_S$ being the system part of the Liouville operator[4], gives the homogenous time-retarded quantum Master equation:

$$\frac{\mathrm{d}}{\mathrm{d}t}\rho(t) = \mathcal{P}(\mathcal{L}_S + \mathcal{L}_I)\rho(t) + \int_0^t \mathrm{d}t' \; \mathcal{P}\mathcal{L}_I e^{\mathcal{Q}\mathcal{L}t'}\mathcal{Q}\mathcal{L}_I\rho(t-t'). \tag{1.31}$$

Again, as in eq. (1.3) the resulting equation is non-local in time. This is the price to be payed for getting an equation solely for the relevant degrees of freedom. The information about the common history of bath and system has to be stored somewhere, as it is needed for the full description of the reduced system.

1.4.2. Born-Markov master equation

In order to gain a differential equation from the integro-differential equation (1.31) suitable for practical purposes, further assumptions have to be made. To derive the Born-Markov master equation from eq. (1.31), the kernel is only considered up to second order in $\mathcal{L}_I$ (Born approximation) and the retardation effects are neglected (Markov assumption). This yields to the Born Markov master equation:

$$\frac{\mathrm{d}}{\mathrm{d}t}\rho(t) = \mathcal{P}(\mathcal{L}_S + \mathcal{L}_I)\rho(t) + \int_0^t \mathrm{d}t' \; \mathcal{P}\mathcal{L}_I e^{\mathcal{Q}(\mathcal{L}_S+\mathcal{L}_R)t'}\mathcal{Q}\mathcal{L}_I\rho(t). \tag{1.32}$$

If this equation is formulated in the energy eigenstate basis of H_S, this equation is also known as Redfield equation. Due to the Born approximation, its applicability is restricted to weakly damped systems, i.e. $\gamma_0 \ll \omega_0$ and $\hbar\gamma_0 \ll k_B T$ [GWT84]. Omitting the Markov approximation leads to a master equation non-local in time, which can be replaced by a hierarchy of coupled equations, solvable with some numerical effort, as has been done, in the context of optimal control, in [XYO+04, HG12].

[4] Assuming $\mathcal{L}$ can be divided into a system, interaction and reservoir part $\mathcal{L} = \mathcal{L}_S + \mathcal{L}_I + \mathcal{L}_R$

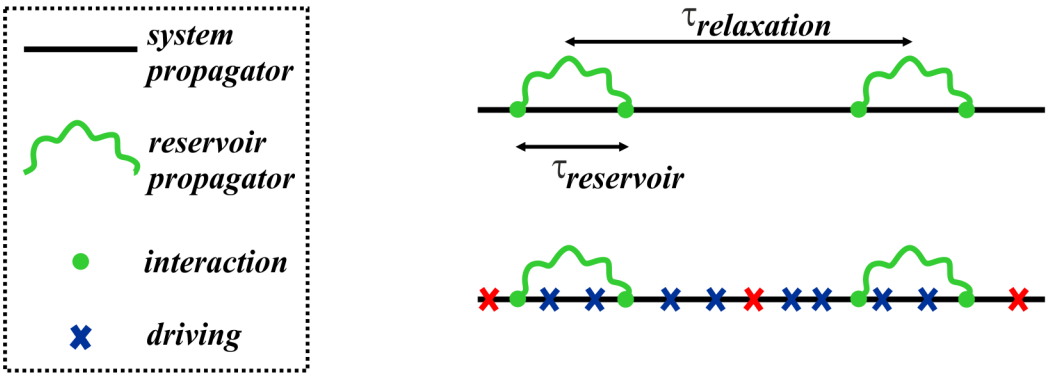

Figure 1.4.: The Lindblad dissipator L consists of three parts: system and reservoir propagator and interaction. Without driving (top), the Lindblad master equation holds, as long as $\tau_{relaxation} \gg \tau_{reservoir}$ (separation of time scales). Bottom: For weak driving (red crosses) nothing changes, but strong driving (blue crosses) changes the dissipator (adapted from J. Stockburger).

1.4.3. Lindblad master equation

If the time scales of reservoir and system separate (cf. Figure 1.4), that is the relevant dynamics of the system is faster than the relaxation time, the rotating wave approximation (RWA) can be applied additionally to the Born-Markov assumption, and the Lindblad master equation is derived:

$$\frac{\mathrm{d}}{\mathrm{d}t}\rho(t) = -\frac{i}{\hbar}[H_S, \rho(t)] + \frac{1}{2}\sum_j \left(\left[L_j \rho(t), L_j^\dagger \right] + \left[L_j, \rho(t) L_j^\dagger \right] \right) \tag{1.33}$$

where L_j are the Lindblad operators, describing the effect of the environment on the system in Born-Markov approximation.
Unfortunately, the RWA does not hold in strongly driven systems [KK04], cf. Figure 1.4. As driving is the purpose of optimal control, the Lindblad master equation might not be the best use for optimal control in open quantum systems. In fact, for a standard Lindblad master equation, with Lindblad operators fixed in time, we were able to show its failure [SNA+11a].
However, there are master equations for driven systems in use with dissipation operators changing in time, depending on the driving, cf, e.g., [BBG+91]. In the context of optimal control, where the pulses are not known beforehand, this has to be done 'en route', i.e. alongside and consistently with the control update, which turns out to be quite cumbersome.

2. Optimal control of quantum systems

Optimal control aims for driving a system to a desired objective. To realize that aim, external control signals are applied, which are disrupting the original dynamics of the system. Finding the best of all possible control pulses is the central focus of optimal control theory.
Formally (cf. [Kro96]), the desired objective is defined in terms of an objective functional $J[w]$ for an admissible process $w = (\mathbf{x}(t), \mathbf{u}(t))$. A process w consists of a state $\mathbf{x}(t)$ of the system and the corresponding controls $\mathbf{u}(t)$. The controlled dynamics of the system are governed by:

$$\dot{\mathbf{x}}(t) = f(\mathbf{x}(t), \mathbf{u}(t), t) \tag{2.1}$$

Optimal control is the search for the control signals $\mathbf{u}(t)$ which extremizes the objective functional $J[w]$ under the constraint, that the equations of motions (2.1) hold, i.e.

$$J[d] = \min_{w \in D} J[w]. \tag{2.2}$$

$D = \{w\}$ is the set of admissible processes.
The objective functional

$$J[w] = F(\mathbf{x}(T)) + \int_0^T \mathrm{d}t \; L(t, \mathbf{x}, \mathbf{u}(t)) \tag{2.3}$$

consists of two contributions: $F(\mathbf{x}(T))$ represents the part of the functional depending on the final value of $\mathbf{x}$, while the running costs L give the dependence on the process. Both F and L need to be functions, which are two times continuously differentiable and are defined for all $\mathbf{x}$, $\mathbf{u}$ and t. We are interested in driving the system to a certain objective at a fixed final time T, but time-optimal control is also possible in this frame.
In the next section, a short overview is given for which quantum systems optimal control is used, which methods are commonly employed and which objectives are pursued. Before we present our method for optimal control of non-Markovian open systems, the context of related work in optimal control of open systems is sketched.

2.1. Applications: physical systems, methods, objectives

The advent of the laser and achievements in tailoring quantum systems made controlled quantum dynamics accessible and created at the same time increasing demand for systematic controls. Inspired by the success optimal control schemes were having since long in classical physical systems, see, e.g., [BH69, Kro96, Dav02], there have been great efforts made to transfer such schemes to quantum systems. Typical objectives for the optimization are to drive the respective system into a desired state, to do quantum processes in a time-optimized way or to enhance quantum features of a system, like entanglement.

2.1.1. Quantum systems

By now, there are various quantum systems, where optimal control is applied. Employing the possibilities of the laser, early applications of optimal control theory have been to quantum systems at hand, both in quantum chemistry and in spin systems in the context of nuclear magnetic resonance (NMR) spectroscopy. The huge progress made in the design of quantum systems, such as atom and ion-traps, optical lattices, Bose-Einstein condensates and mesoscopic systems, for instance superconducting devices, lead to the advent of a variety of controllable quantum systems. At the same time, this progress creates a demand for optimal control. In particular, the efforts made to realize quantum computation, ask for high fidelity command of the respective systems. In the following a short overview is given, focussing on the possibilities and challenges in the respective area of research.

Quantum chemistry

In the context of quantum chemistry optimal control schemes have been proposed to perform controlled reactions, both to enhance the yield of preferred reaction products, such as Tannor et al. [TKR86], but also to learn about reaction mechanisms, such as Rabitz and Coworkers [PDR88, SR90]. An overview is given in the review article of Brif et al. [BCR10]. The unavoidable environment in chemical settings prevented the success of these schemes, until feedback methods (cf. Subsection 2.2.3) were employed [ABB$^+$98, RdVRMK00, WR03].

Furthermore, building on the progress made in isolating molecules, implementations of a quantum computer in molecular systems have been proposed by Palao and Kosloff [PK02]and by Tesch and de Vivie-Riedle [TdVR02].

Recently, the control of molecules, important in a biological context, came into focus, such as in [CMC$^+$12].

NMR

In the context of NMR spectroscopy, optimal control techniques have been used with great success to fight dephasing. Therefore, the environment is part of the description; the dynamics is usually formulated in terms of a Bloch-Redfield equation, cf., e.g., Glaser, Luy and Coworkers ([GSHS+98, SRL+03, KSK+08]).
Also, proposals for implementations of quantum gates in spin systems, governed by optimal pulses, have been put forward, cf., e.g. Schulte-Herbrüggen et al. [SHSKG05].

Quantum optical systems

Tailored quantum optical systems offer many possibilities for applying controls and for the study of controlled dynamics. Usually in this field, one aims to isolate these systems as much as possible from their surroundings, which can be achieved to a high degree, due to the high quality in preparation. Therefore the influence of the environment is discussed in terms of separation of time scales, i.e. whether a task, measurement, etc., can be performed faster than the typical decoherence times. Rapidness provided, these systems can be treated as isolated ones.
For the purpose of quantum information processing, controls have been designed to perform unitary transformations with high fidelity, such as for atoms [THS+04, CHJ+00] and molecules [MRM+11] in traps. In the context of quantum information processing, special interest lie on reliable quantum gates [CHJ+00, NS09, BMM+10, MMC+11].
Generation and storing of entanglement by the means of optimal control was also investigated, cf, e.g. [Häb08, PMB10, CCM12], as well as phase control of Bose-Einstein condensates [ST02].

Solid state

Solid state systems, such as superconducting circuits and devices, are also promising candidates for the implementation of quantum computing. In these condensed matter quantum devices, the influence of the environment is no longer negligible, there are different strategies to cope, as we will discuss cf. Section 2.2.
Among the systems that have been considered in the context of optimal control, are charge qubits [SSHG+07, MCF07] and transmon qubits coupled to a resonator [EW13]. As a model for control in a dissipative solid state device, Rebentrost et al. [RSSHW09] discussed the control of a qubit coupled to a two-level fluctuator which is exposed to a thermal bath.
Recently, NV-Centers in diamonds, got into the focus of optimal control, such as in [FDT+09].

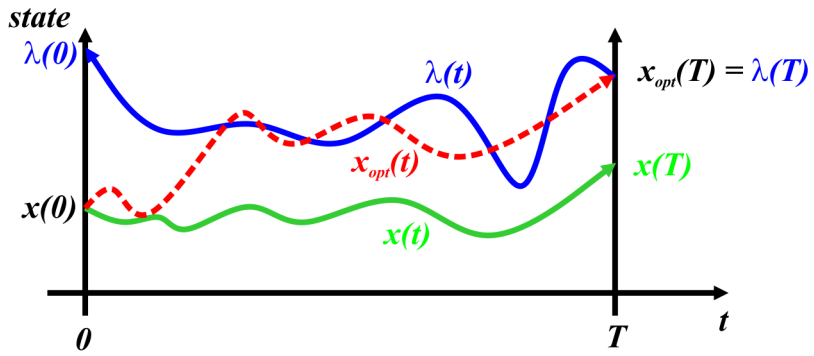

Figure 2.1.: Basic idea of gradient-based control schemes. Forward propagation of state $x(t)$, backward propagation of the Lagrange multiplier, i.e. the costate, $\lambda(t)$. Update of the control $u(t)$ is done by demanding the gradient $\frac{\partial H}{\partial u} \equiv 0$. H is a generalized Hamilton function, $H = L + \lambda \cdot \dot{x}$, depending on the running costs L and the dynamics. Aim of the algorithm is to find the optimal path x_{opt}. To allow for graphical representation, $x_{opt}(T) = \lambda(T)$ is one of the simplifications made (adapted from [SRL+03]).

2.1.2. Control methods

Solving the optimization problem of equation (2.2), can be done in various ways, prominent in use among them are gradient-based methods, evolutionary learning algorithms for feedback control schemes, and simplex algorithms (like Nelder-Mead). For systems, which are well understood, one can employ strategies, which truncate the search space beforehand in a sophisticated way.

Gradient-based methods

Tackling the optimization problem by the means of variational calculus, provides us with gradient type methods, which are widely used in the optimal control context. These numerical methods consist basically of an iteratively solvable set of differential equations for the state, costate (in terms of variation calculus, the Lagrange multiplier) and the control update, cf. Figure 2.1. The control update is found by calculating a gradient with respect to the controls. More sophisticated gradient methods employ a so-called line search, for this the Hesse matrix itself or an approximation of it is computed. Gradient based methods are used by many groups, such as [SR90, WG07], the GRAPE algorithm [SHSKG11] and the SPINACH package for controlled spin dynamics [KKC+11].
A special class of gradient type control schemes are the Krotov-based [Kro96] methods: here the state and the costate are propagated with different iterations of the

control signal. This avoids getting stuck in local minima, inspiring Krotov to call it a 'global' method. To apply this classical method to quantum systems, fundamental contributions were made by Sklarz and Tannor [ST02], Palao and Kosloff [PK02] and Koch and Coworkers, as in [RNK12]. We extended the method to stochastic open system dynamics [SNA+11a], cf. Section 2.3.
Some comparisons have been made of the performance of the different types of control algorithms in use in the optimal control community (cf., e.g., [SdF11, NLKS13]). It has been shown, that the Krotov method is turning into an ordinary gradient method for higher iteration numbers. And, while Krotov's method provides rather dramatic improvements of the performance in the early iteration steps, it is outperformed by the other methods, when it comes to highest fidelity requests.
In any case, for our problem of open system control, which comes with a numerically rather expensive stochastic dynamics, the feature, that a Krotov-based method offers good results for comparatively few iteration steps, is quite convincing for us. Of equal importance is another feature: The Krotov-based algorithm is almost insensitive to the initial guess of the control signals [RNK12], and it can be a considerable challenge to guess a neat initial control pulse.

Basis sets

Searching for the optimal control in the whole search space can be cumbersome. However, given that the experimental setting, control pulses are searched for, is well known, the basis of functions for the control fields can be truncated in a sophisticated way. This comes with the additional benefit of pulses, which are easily implementable in experiments. In the context of NMR this is done by allowing only for a few system frequencies [Min12]. As a more general method Calarco, Montagero and Coworkers developed the chopped random basis method (CRAB) [DCM11, CCM11]. It has been successfully applied to various experimental settings, as in [MKL+13]. To avoid the cumbersome gradient calculations, CRAB employs the Nelder-Mead algorithm, a simplex downhill method, also used by other control groups, e.g. [EW13].

2.1.3. Objectives

Objectives considered in the context of optimal control of quantum systems are in particular the maximization of the overlap with a desired target state ('state-to-state transfer'), time-optimal control and the enhancement of quantum features like entanglement. All the controlled gate operations and the NMR applications are state-to-state transfers. Time-optimal control, i.e. performing the given task in the shortest possible time, is one promising way to deal with noise [WG07, MJKC09, CMC+09]. Optimal control has also been applied to generate entanglement, e.g. in [PK02, Häb08, PMB10].

2.2. Optimal control and noise

There are different strategies to deal with the fact, that the system, we want to control, is coupled to an environment. First, one might think of being fast in performing the desired tasks, to simply give the environment not enough time to interfere. Such schemes are called time-optimal control. Then, one can ask, how the performance of the control pulses, calculated without noise, will change, if noise is added. If the pulses are robust, i.e. the task is still performed with the desired fidelity, there will be no reason to take the environment into account.

Since feedback control is a successful way in *classical* systems to treat imperfections, such as noise, in the modeling, one might explore this approach for quantum systems also. However, performing a measurement in a quantum system comes with preparing a new probe, so there is a trade-off between experimental effort and labor invested in the theoretical modeling. Control can also be actively used, to fight decoherence, e.g. to drive the system towards decoherence-free subspaces.

All these strategies imply, that the environment is 'hostile', i.e., working against the pursued goal. However, it is known, that there are 'friendly' reservoirs, as discussed in the context of engineered reservoirs, carefully designed baths, driving the system to the aimed for target. As these are artificial environments, they are not the typical unavoidable ones we are faced with in condensed matter. Indeed, we were able to show, that it might not be necessary to invest the effort of engineering a reservoir, but that optimal control pulses can turn a hostile environment into a friendly one.

2.2.1. Time-optimal control

Assuming that noise is detrimental, the natural demand for a control scheme is to perform the desired task quickly, at least faster than the relaxation time scale. Spörl et al. [SSHG$^+$07] proposed time optimized pulses for Josephson charge qubits. Murphy et al. [MJKC09] showed that optimal controlled quantum transport can be faster than the adiabatic case, without losing fidelity.

This gives rise to the question, how fast a given task can be performed by the means of optimal control. Caneva et al. [CMC$^+$09] showed that a quantum speed limit exists, i.e. there is actually a lower bound to the time needed to achieve a defined goal.

However, Schirmer and Coworkers [FdFS12] showed in a general frame, that for minimizing detrimental noise effects, being as quick as possible is the best way only for Markovian environments. For systems with such an environment, the control signal found for the isolated system is still the optimal one. In agreement with our result [SNA$^+$11a], they found, that for non-Markovian environments, given the coupling mechanisms are known, the memory effects of the environment can be used.

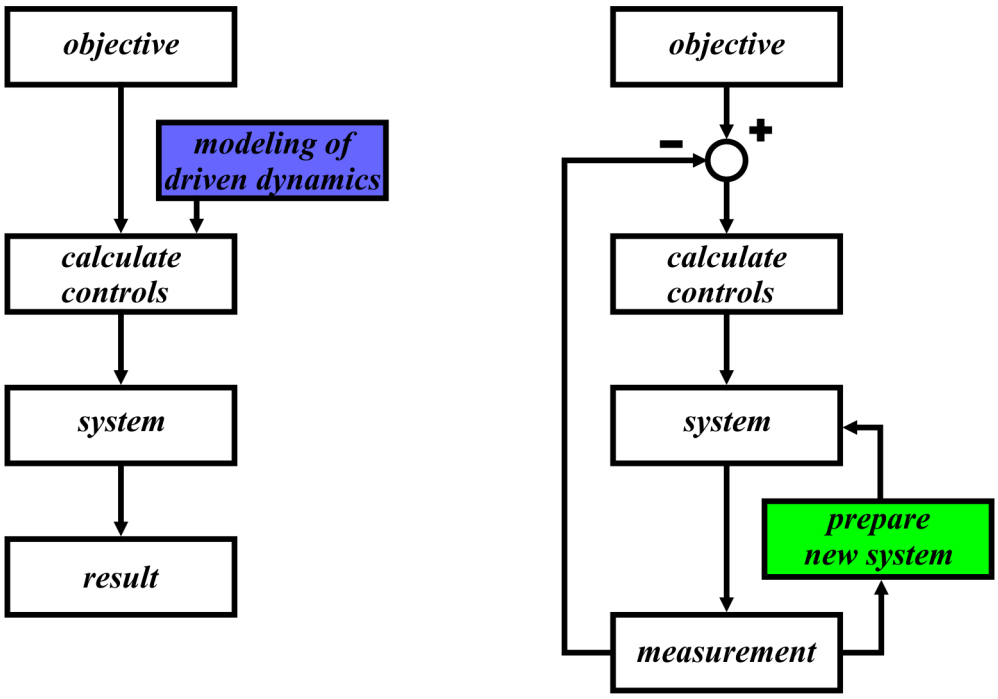

Figure 2.2.: Optimal control schemes in quantum systems. While for open loop control (left) the main effort comes with the *exact* modeling needed, closed loop, also called feedback, control (right) comes with a high experimental effort.

2.2.2. Control in the presence of noise

Sometimes, the environment can not be ignored, e.g. if there is no way to perform the desired task faster than the typical interaction times or if either the system or the control pulses themselves are subject to imperfections. Then, a natural question is, how the control signals, calculated for an isolated perfect system, will perform. Or, in other words, how robust the pulses are with respect to typical noise sources. This has been done by, e.g., Treutlein et al. [THR+06], Montangero et al. [MCF07] and Murphy et al. [MJKC09], who found their respective pulses to be quite robust against typical noise sources in their respective settings.

2.2.3. Open vs. closed/feedback control

In the classical frame, feedback control, i.e., adjusting the controls by feeding back measurement results of the actual state of the system in a closed loop, is successfully used to take the effects of noise into account. However, as any measurement on a quantum system disturbs this system, the transfer of these closed loop control schemes to quantum systems is not straightforward. Such feedback schemes do

come with a new preparation of the system after each measurement, which can be experimentally costly, cf. Figure 2.2. In quantum chemistry, where the experimental effort to prepare a new probe is managable, there exist successful feedback control experiments, cf. [RdVRMK00, WR03]. Serafini and Mancini proposed a feedback scheme to generate entanglement [SM10]. Also, there are several proposals, for instance [DMB+09], to combine non-demolition measurement, like in [NRO+99], with feedback control schemes.

Admittedly, in particular in an open system, the exact modeling of the total system, including the noise, which is needed for the open loop control, can be elaborate and - numerically - costly. On the other hand, there comes a reward with the effort invested: If the control pulses work, they not only confirm the modeling but allow for a deeper understanding of the driven dynamics.

For an actual experimental implementation, there can be specific noise sources, not taken into account in the modeling, because this noise is not of fundamental interest, yet fatal for applications with highest fidelity demands. Egger and Wilhelm [EW13] suggested a combined schemes of open and closed loop control, where the controls signals gained in the open loop are adjusted to the imperfections of the actual experimental setting by the means of an additional feedback scheme.

2.2.4. Optimal control to fight decoherence

A prominent goal for optimal control in open systems has been to reverse the detrimental effects of decoherence and dissipation, e.g., by driving the system into a decoherence free subspace: Viola and Lloyd [VL98] employed a bang-bang control scheme to fight decoherence of a two-level system. Kofman and Kurizki [KK04] showed that suitably chosen controls can dynamically suppress decoherence of a qubit in a thermal bath, using generalized Bloch equations, including explicitly non-RWA effects. Schulte-Herbrüggen et al. [SHSKG11] investigated driving of systems subject to Markovian environments into subspaces of weak relaxation.

2.2.5. Artificial environments

It is known, however, that the interaction with an environment can be helpful in special cases. This gave rise to the exciting field of engineered reservoirs, cf., e.g., [MHdC+13, ACVM13, WC13], that is coupling a system to a carefully designed environment, where the stationary state of the system is the desired one. In terms of optimal control, 'incoherent controls' are discussed, i.e. noise sources, which interaction with the system can be switched at will, e.g., Barreiro et al. [BMS+11]. Clausen et al.[CBK12] considered a coupling to the reservoir that can be modulated.

2.2.6. Real environments

In a strict sense, the artificial environments, discussed in the previous Subsection, are controls, in the sense that one can not only choose their design, but even whether they are part of the setting at all. These reservoirs are components added to the system fully under the experimentalist's command, and that is not what we are typically faced with in the context of solid state physics. Here, the environment is a non negligible part of the system and generally not helpful.
However, the sought-after features, i.e. an impact on all observables of the system, are in principle inherent to any environment, even an ordinary thermal one. They are just not used in a productive way. We employed driving in order to make use of this idle resources: arbitrary fast and strong driving changes the system and therefore the interplay with the environment. This gives rise to nonequilibrium physics showing cooperative effects of driving and dissipation. We employed the control scheme presented in the next Section, to calculate control pulses, which in a combined effort with the thermal environment are capable to perform tasks, like cooling and generating entanglement, which neither of the components can accomplish alone.

2.3. Dissipative optimal control

We derived a control algorithm, which provides a consistent description of both driving and dissipation. In [Sch09, SNA+11b][1] we extended the work of Sklarz and Tannor [ST02] to open non-Markovian quantum systems. In their method for closed quantum systems, Sklarz and Tannor build up on the work of Krotov and Coworkers [KF83, Kro96, KK99] for classical systems. Here, we give a short overview of the derivation of our control algorithm.
The exact dynamics of an open non-Markovian quantum system can be described by a stochastic Liouville- von Neumann (SLN) equation (for details cf. Section 1.3):

$$\dot{\rho_z} = \mathcal{L}\rho_z, \tag{2.4}$$

valid for one single noise realisation $z(t) = \{\xi(t), \nu(t)\}$. At this point, no specification to our objective $F[\mathbf{u}(t), \{\rho_z(T)\}]$ is made; also we made no other restriction on our controls signals $\mathbf{u}(t)$, than that they act on the relevant system only ($H_S \to H_S + H_C$).
As we do only know the dynamics of a single noise realization z, the control formalism has to be formulated for one realisation also. With an admissible process $w \equiv$

[1] The derivation of the optimal control formalism was topic of my diploma thesis [Sch09]. Part of the results were published in the supplemental material [SNA+11b] of [SNA+11a].

$(\mathbf{u}(t), \{\rho_z(t)\})$, the dissipative objective functional reads:

$$\tilde{J}[w, \phi_z] = G(\rho_z(T)) - \int_0^T R(t, \mathbf{u}(t), \rho_z(t))\mathrm{d}t - \phi_z(0, \rho_z(0)), \tag{2.5}$$

where $\phi_z(t, \rho_z(t))$ is an arbitrary continuously differentiable function Krotov introduces. It can be shown, that $\tilde{J}[w, \phi_z] = J[w]$ for all $\phi_z(t)$ [KF83]. Here, the auxiliary functions of Krotov's formalism G, R and H^{Krotov} take the form:

$$G(\rho_z(T)) := F_z(\rho_z(T)) + \phi_z(T, \rho_z(T)) \tag{2.6}$$

$$\begin{aligned} H^{Krotov}\left(t, \rho_z(t), \mathbf{u}(t), \frac{\partial\phi_z(t, \rho_z(t))}{\partial\rho_z}\right) := \mathrm{tr}\Big\{ &\left(\frac{\partial\phi_z(t, \rho_z(t))}{\partial\rho_z}\mathcal{L}\rho_z\right) \\ &+ \left(\rho_z^\dagger \mathcal{L}^\dagger \Big(\frac{\partial\phi_z(t, \rho_z(t))}{\partial\rho_z}\Big)^\dagger\right)\Big\} \end{aligned} \tag{2.7}$$

$$\begin{aligned} R(t, \mathbf{u}(t), \rho_z(t)) := &H^{Krotov}\left(t, \rho_z(t), \mathbf{u}(t), \frac{\partial\phi_z(t, \rho_z(t))}{\partial\rho_z}\right) \\ &+ \frac{\partial}{\partial t}\phi_z(t, \rho_z(t)) \ , \end{aligned} \tag{2.8}$$

where $F_z(\rho_z(T))$ is the objective for one realisation z.
The functional (2.5) is subjected to variational calculus:

$$\delta\tilde{J}[w, \phi_z] = \delta\left(G(\rho_z(T)) - \int_0^T R(t, \mathbf{u}(t), \rho_z(t))\mathrm{d}t - \phi_z(0, \rho_z(0))\right) \stackrel{!}{=} 0, \tag{2.9}$$

in order to find the minimum of $\tilde{J}[w, \phi_z]$. For fixed controls $\mathbf{u}(t)$, the auxiliary function ϕ_z is chosen in such a way, that $\tilde{J}[w, \phi_z]$ is maximized with respect to ρ_z for any admissible process w. This provides, that afterwards, now with fixed ϕ_z any change in $\mathbf{u}(t)$ will achieve an improvement. That implies, that we calculate in each iteration step j of our control algorithm:

$$R(t, \rho_z{}^{(j)}(t), \mathbf{u}^{(j)}(t)) = \min_{\rho_z,\ \rho_z^\dagger} R(t, \rho_z(t), \mathbf{u}^{(j)}(t)) \tag{2.10}$$

and

$$G(\rho_z{}^{(j)}(T)) = \max_{\rho_z(T),\ \rho_z^\dagger(T)} G(\rho_z(T)) \tag{2.11}$$

to fix ϕ_z^j. Then, the new control and the new state have to be calculated consistently:

$$\mathbf{u}^{(j+1)}(t) = \arg\max_{\mathbf{u}} \mathbb{E}\left[R_z(t, \rho_z^{(j+1)}, \mathbf{u})\right] \tag{2.12}$$

$$\frac{\mathrm{d}}{\mathrm{d}t}\rho_z^{(j+1)}(t) = \mathcal{L}^{(j+1)}\rho_z^{(j+1)}(t) \tag{2.13}$$

With the definition of the costate, i.e. the Lagrange multiplier, Λ_z:

$$\Lambda_z^{(j)} := \left.\frac{\partial \phi_z^{(j)}}{\partial \rho_z^\dagger}\right|_{\rho_z=\rho_z^{(j)}} \tag{2.14}$$

the variational calculus with respect to the state ρ_z provides us with a stochastic equation of motion for the costate Λ_z:

$$\mathcal{L}^\dagger\Lambda_z + \frac{\mathrm{d}}{\mathrm{d}t}\Lambda_z(t) = 0 \tag{2.15}$$

with the end time boundary condition:

$$\Lambda_z(T) = \frac{\partial}{\partial \rho_z^\dagger(T)} F_z(\rho_z(T)). \tag{2.16}$$

Variation with respect to the costate Λ_z regains eq. (2.4) and finally, variation with respect to the controls, results in the update formula for these controls:

$$u_{(i)}^{(new)}(t) = u_{(i)}^{(old)}(t) + \frac{1}{\lambda_{(i)}(t)}\,\mathbb{E}\left[\frac{\partial H^{Krotov}}{\partial u_{(i)}(t)}\right] \tag{2.17}$$

where i is the respective component of the vector $\mathbf{u}(t)$, and λ is a tuning parameter, which can be suitably chosen in order to enhance numerical stability. The contribution of each noise realisation to the new control signal is given by:

$$\begin{aligned}\frac{\partial H^{Krotov}}{\partial u_{(i)}} &= 2\cdot \mathrm{Re}\left[tr\left\{\Lambda_z^\dagger \frac{\partial \mathcal{L}}{\partial u_i}\rho_z\right\}\right] \\ &= \frac{2}{\hbar}\mathrm{Im}\left[tr\left\{\Lambda_z^\dagger\left[\frac{\partial H_C}{\partial u_i}, \rho_z\right]\right\}\right]\end{aligned} \tag{2.18}$$

where H_C is the part of the Hamiltonian of the system describing the influence of the controls. Note, that $\Lambda_z(t)$ is propagated with the old control signals, while $\rho_z(t)$ is propagated with the new ones. In detail, the algorithm can be found in Appendix B.

3. Gaussian states

Many quantum systems are continuous variable systems (CVS) such as the different degrees of freedom of the electromagnetic field, vibrational modes of solids, atomic ensembles, nuclear spins in a quantum dot, Josephson junctions and Bose-Einstein condensates [WPGP+12]. These systems can be described in terms of quantized harmonic modes, which can be represented by Gaussian functions, as the ground state, the thermal, squeezed and coherent states of a harmonic oscillator are Gaussian. Therefore, the research of Gaussian quantum information is a field of great interest, cf. the review articles of Braunstein and van Loock [BvL05] and of Weedbrock et al. [WPGP+12].
While being relevant for many experimental realisations, Gaussian states can be treated rather straightforward in terms of mathematics. Also, the Wigner functions, introduced below, of Gaussian states are Gaussians and are a beneficial tool for visualizing, and, hence, for understanding the driven dissipative dynamics. The mathematical description in terms of first and second cumulants can be used to find expressions for all physical quantities of interest, such as entropy and entanglement. In fact, while for mixed states, it is in general not easy to define an entanglement measure, for bipartite Gaussian states it is given by the logarithmic negativity [VW02].

3.1. Cumulant description of Gaussian states

A system, consisting of N harmonic modes can be described by the operators of the conjugated variables of each mode k, i.e. $\{q_k, p_k\}_{k=1}^{N}$, with $[q_i, p_j] = i\hbar\delta_{ij}$, which can be arranged in a vector:

$$\mathbf{x} = (q_1, p_1, \ldots, q_N, p_N)^T \tag{3.1}$$

Gaussian states can fully be described by the first and second cumulants of the q_k and p_k. The first cumulants are of course the first moments. The second cumulants are the elements of the covariance matrix σ, with:

$$\sigma_{ij} = \frac{1}{2}\langle x_i x_j + x_j x_i\rangle - \langle x_i\rangle\langle x_j\rangle \equiv \left\langle \frac{x_i x_j + x_j x_i}{2} \right\rangle_c . \tag{3.2}$$

Therefore, in the context of Gaussian states, there is no need to invest the numerical effort to propagate the full density matrix, but, one can propagate the cumulants

instead. As long as the applied driving couples at most quadratically to the system, the Gaussian nature of the state is preserved. Anyhow, even for the one-dimensional harmonic mode subjected to driving and damping, parametric, i.e. quadratically coupled, control is a challenge. Only in the case of restricting to periodic driving fields [ZH95], the problem is analytically solvable in terms of Matthieu functions [McL64]. This is of course an unacceptable constraint to the search for *optimal* control pulses.

3.2. Wigner functions

In phase space, any density operator can be represented in terms of a Wigner function, i.e. a quasiprobability distribution [Sch01]. With the symplectic form $\mathbf{\Omega}$

$$\mathbf{\Omega} := \bigoplus_{k=1}^{N} \omega, \qquad \omega = \begin{pmatrix} 0 & 1 \\ -1 & 0 \end{pmatrix} \tag{3.3}$$

the Weyl operator $D(\zeta)$ is given by $D(\zeta) := \exp(i\mathbf{x}^T\mathbf{\Omega}\zeta)$ and the Wigner characteristic function takes the form:

$$\chi(\zeta) = \mathrm{tr}\{\rho \mathrm{D}(\zeta)\}. \tag{3.4}$$

The Wigner function is then gained by a Fourier transformation of $\chi(\zeta)$. For a Gaussian state the Wigner function $W(x)$ is also Gaussian [Hol75]:

$$W(\mathbf{x}) = \frac{1}{(2\pi)^N \sqrt{\det \sigma}} \exp\left\{-\frac{1}{2}(\mathbf{x}-\bar{\mathbf{x}})^T \sigma^{-1} (\mathbf{x}-\bar{\mathbf{x}})\right\}. \tag{3.5}$$

We employed this phase space representation in [SRAS12, SSA13a] to visualize our results and gain a deeper understanding of the driven dissipative dynamics.

3.3. Physical quantities of Gaussian states

As the full information of the Gaussian state is represented in the first and second cumulants, any physical quantity of interest can be expressed with them. For the case of open systems, quantities only depending on the second cumulants are of particular interest, such as entropy or entanglement. The second cumulants can only be influenced by controls, which couple at least quadratically to the system's coordinate.

3.3.1. Entropy of Gaussian states

The von Neumann entropy for one harmonic mode is given by [HSH99]:

$$S(\rho) = g\left(\sqrt{\langle q^2\rangle_c \langle p^2\rangle_c - \langle qp - pq\rangle_c^2 /4}\right) \tag{3.6}$$

with $g(x) = (x + \frac{1}{2})\log(x + \frac{1}{2}) - (x - \frac{1}{2})\log(x - \frac{1}{2})$. We used this expression to quantify the cooling of a thermalized state by optimal control in [SNA+11a].

3.3.2. Entanglement for bipartite Gaussian states

Entanglement is the resource of quantum information.[1] It is the quantum part of the non-local information in system of at least two subsystems [NC00, Aud05]. However, for an open system, measuring entanglement is a non-trivial task, which is in general not solved yet. Information to be gained by a measurement, occurs in mixed states as classical and as well as quantum information, both of them come in the flavors local and nonlocal. For the quantum part, both local and nonlocal, the term 'quantum discord' has been coined [OZ01]. For bipartite Gaussian systems quantum discord has been investigated in [GP10, AD10].
Entropy based entanglement measures, which are successfully used for pure states, also count for the classical correlations when it comes to mixed states. Though, entanglement measures are sought for, which indicates the violation of the Bell inequality, however there are mixed entangled states which do not violate local realism [BvL05]. It has been shown, that it is necessary for separability [Per96, HHH96], that the partially transposed density matrix is positive (positive partial transpose (PPT) criterion). Physically, this operation corresponds to a local time reversal of the partially transposed subsystem, mathematically, it results in a sign change in the respective p operator. For Gaussian bipartite systems, it has been shown, that the violation of the PPT criterion is sufficient and necessary for entanglement. Various theoretical aspects of Gaussian bipartite entanglement have been investigated, e.g., in [EP02, ASI04, OP11], experiments have been done by, e.g., [DFP+09, LKOH+05].

Logarithmic negativity

For a bipartite Gaussian state, consisting of the substates A and B, the covariance matrix σ (eq. (3.2)) can be grouped in the following way:

$$\sigma = \begin{pmatrix} \alpha & \gamma \\ \gamma^T & \beta \end{pmatrix}, \tag{3.7}$$

[1] Actually, the original paper of Einstein, Podolsky and Rosen [EPR35] considered a continuous variable system to discuss entanglement. The term 'Verschränkung', i.e. entanglement, on the other hand, was coined by Schrödinger [Sch35]

where α, β correspond to the covariance matrices of the respective sub-units A and B, while γ (transpose γ^T) carries the mixed cumulants and therefore the non-local information of the system. Unitary transformations do not change entanglement [Ade06], therefore, the first cumulants can be set to zero without loss of generality. The PPT-criterion can then be rephrased to be:

$$\tilde{\nu}_- \geq 1, \tag{3.8}$$

where $\tilde{\nu}_-$ is the smallest symplectic eigenvalue of the covariance matrix corresponding to the partially transposed density matrix [VW02]. Expressed by the covariance matrix, it is given by[2]:

$$\tilde{\nu}_- = \sqrt{2}\sqrt{\det\alpha + \det\beta - 2\det\gamma - \sqrt{(\det\alpha + \det\beta - 2\det\gamma)^2 - 4\det\sigma}}. \tag{3.9}$$

The determinantes $\det\sigma$, $\det\alpha$, $\det\beta$ and $\det\gamma$ are symplectic invariants. Based on this, the logarithmic negativity, $E_{\mathcal{N}}$, the entanglement measure for Gaussian bipartite systems [VW02] is defined as[3]:

$$E_{\mathcal{N}} = \max\{0, -\ln(\tilde{\nu}_-)\}. \tag{3.10}$$

The subsystems A and B are entangled, if $E_{\mathcal{N}} > 0$, while $E_{\mathcal{N}} = 0$ corresponds to purely classical and/or local quantum correlations. If A and B are entangled, then $\det\gamma$ is negative [Sim00].

[2]Other than widely used in the literature of Gaussian quantum information particularly in the context of Gaussian entanglement, we do *not* use $\hbar \equiv 2$, but $\hbar \equiv 1$ instead.

[3]First published in a journal by Vidal and Werner [VW02], Plenio [Ple05] proved the logarithmic negativity to be a full entanglement monotone.

4. Cooperative effects of driving and dissipation: Applications and results

We apply the optimal control method (cf. Section 2.3), we derived for open non-Markovian systems, to harmonic modes (cf. Chapter 3) coupled to a reservoir with ohmic spectral density (cf. Subsection 1.3.1). First, we concentrate on a system consisting of a single harmonic mode, for which we investigated both a common state-to-state transfer scenario and a cooling scenario. Secondly, we extended our method to a bipartite system, in order to examine entanglement generation by optimal control. The results, we highlight in this Chapter, have been published in the articles forming Part II of this dissertation[1].

4.1. Common state-to-state transfer

Assuming that we start with a wavepacket with initially minimal width, the dissipative dynamics without any external control will lead to a damped oscillation of the first cumulants, while the second cumulants would thermalize. That is, in phase space, the center of our wavepacket would perform a spiral motion to the origin, while the wavepacket itself broadens isotropically, in agreement with the inverse thermal energy of the reservoir β. Basically, we are losing irretrievable our carefully prepared initial state. Therefore the task, we wanted to fulfill by optimal control, is to restore the initial state at the time T, i.e., we want to rewind the dissipative dynamics by the means of optimal control.

State-to-state transfer is a very common task in the context of optimal control (cf. Section 2.1). We were able to show that for the condensed matter scenario, we consider, neither the control pulses of the corresponding closed system were robust, nor standard Lindblad dynamics would provide accurate results. Our method, on the contrary, provides results with high fidelity.

[1] As Chapter 6 provides the detailed summary of the published articles requested for a cumulative dissertation, there is some overlap with this Chapter (due to aiming for completeness of Part I of this thesis, also).

Stochastic dynamics

For a single harmonic mode, with $H_S = \frac{p^2}{2m} + \frac{m\omega_0^2}{2}q^2$, coupled to a reservoir with ohmic spectral density (for details cf. Subsection 1.3.1), the stochastic dynamics is governed by the SLED equation:

$$\frac{\mathrm{d}}{\mathrm{d}t}\rho_\xi = -\frac{i}{\hbar}[H_S + H_C, \rho_\xi] + \frac{i}{\hbar}\xi(t)[q, \rho_\xi] - \frac{i}{\hbar}\frac{\gamma_0}{2}\left[q, \{p, \rho_\xi\}\right]. \tag{4.1}$$

The stochastic equations of motion, which arise for the cumulants, are to be found in Appendix A.1.
The control Hamiltonian H_C is chosen to be:

$$H_C = -F(t)q + \Delta(t)\frac{q^2}{2}. \tag{4.2}$$

$F(t)$ is a linear force control field, which acts only on the first cumulants, i.e. in phase space, it shifts the center of the wavepacket. The second cumulants are only influenced by the parametrical tuning control field $\Delta(t)$. It changes the potential, acting on the harmonic mode, by changing the frequency $\omega^2 = \omega_0^2 + \Delta$. Hence, in phase space it changes the width of the wavepacket, including squeezing effects. Being at most quadratic in the coupling to the system, this driving preserves the Gaussian nature of the state.

Objective

The objective of a state to state transfer is to maximize the overlap with a target state $A = |\alpha\rangle\langle\alpha|$, where A is a projection operator onto the target state, here a coherent state. In order to formulate a minimizing task, we ask for reducing the remaining error $M = 1 - A$:

$$F\left[\mathbf{u}(t), \{\rho_z\}\right] = \mathbb{E}\left[\mathrm{tr}\left\{M\rho_z(t_f)\right\}\right]. \tag{4.3}$$

The equations for the backward propagation of the cumulants of the co-state and the control update, calculated according to Section 2.3, can be found in Appendix A.1.

Results

Our initial state is a wave packet of minimal uncertainty centered around $q = 1$ and $p = 0$ which we want to restore at $T = 20$[2]. We choose the final time to be of the order of the relaxation time of the uncontrolled system and explicitly not to be a multiple of 2π.

[2] We use natural units, i.e. $\hbar = 1$, $k_B = 1$, units ω_0 for energies, angular frequencies, or rates; lengths are given in $1/(\sqrt{m\omega_0})$, momenta in $\sqrt{m\omega_0}$ and we set: $\omega_c = 50$, $m = 1$, $\omega_0 = 1$

As can be seen in the article constituting Section 7.1, we explored a typical range for solid state quantum devices of both damping constant γ_0, varied between $\gamma_0 = 0.005 \ldots 0.1$, and inverse thermal energy β, varied between $\beta = 50 \ldots 0.5$, gaining fidelities up to 99%. Better results are gained for higher β and lower γ_0, that is for cold baths and weak damping. Nonetheless, fidelities for other parameters are also satisfactory. For $\gamma_0 = 0.05$ and $\beta = 1$, Figure 6.1 shows exemplarily the windowed Fourier transformations of the control signals.

Comparison with a Lindblad master equation

For the comparison with a Lindblad master equation, we took the standard form[3] for the damped harmonic oscillator [BP06]:

$$\frac{\mathrm{d}}{\mathrm{d}t}\rho = -i[H_S + H_C, \rho] + \gamma_0(N_\beta + 1)\left(a\rho a^\dagger - \frac{1}{2}\{a^\dagger a, \rho\}\right) + \gamma_0 N_\beta \left(a^\dagger \rho a - \frac{1}{2}\{aa^\dagger, \rho\}\right) \tag{4.4}$$

in dimensionless units, where a, $a^\dagger$ are the annihilation and the creation operator of the harmonic oscillator, respectively, and $N_\beta = \frac{1}{e^\beta - 1}$ is the thermal occupation number of the unperturbed oscillator. The equations of motion for the first and second cumulants, arising from this master equation, are given in Appendix A.1. The control signals gained by this RWA dynamics are shown in Figure 6.1 (middle), and the fidelities predicted are high. However, the RWA control pulses differ substantially from the SLN ones, and feeding these RWA control signals into the full stochastic dynamics, which is an *exact* description of how the system will actually evolve subjected to driving and dissipation, leads to a performance considerably worse. Therefore, we were able to show, that the standard Lindblad dynamics is not suitable to investigate driven open system dynamics.

4.2. Cooling by optimal control

An initially thermalized state would stay thermalized forever, if no external controls were applied. However, a maximally mixed state is in terms of quantum information processing quite useless. The challenge, we face with our control algorithm here, is to purify our system, that is to cool our system through driving.
Cooling a quantum system is an important task. Many schemes use internal degrees of freedom as, e.g., in [PH07, RSK+07] also, utilizing optimal control, [ST04, Pec11]. In our system the cooling has to be achieved by a cooperative effect of driving and dissipation, there are no inner degrees to be explored. Cooling by optimal control pulses is also possible for the analogous classical system [Roh11].

[3] Where the driving is not taken into account for the construction of the Lindblad operators, cf. Subsection 1.4.3

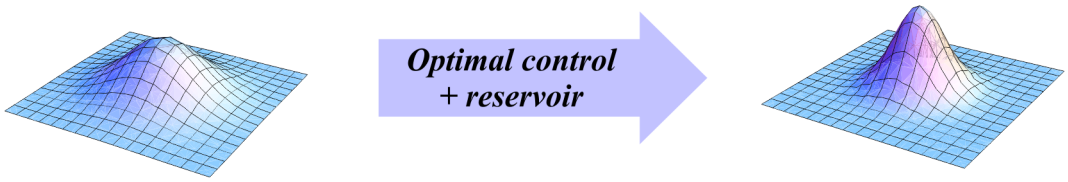

Figure 4.1.: Schematic representation of our control aim. Cooling an initially thermalized state (left) by a cooperative effort of driving and dissipation to the ground state (right).

Stochastic dynamics

The dynamics are basically the same as in the previous section, except that we only take the parametrical control part into account $H_C = \Delta(t)\frac{q^2}{2}$, as the von Neumann entropy of the system is only a function of the second cumulants (cf. Subsection 3.3.1).

Objective

We also perform a state-to-state transfer, projecting on the ground state of an isolated harmonic mode. This is not the ground state of the open system, the ground state of the damped harmonic oscillator is not a pure state, but a mixed one, as has been shown in [GWT84]. Nevertheless, the bare ground state is a suitable objective, as the cooling is of course a nonequlibrium effect, switching off the controls would lead to a renewed thermalization with the reservoir.

Results

Our initial wavepacket is thermalized, and at $T = 20$ we want to have a wavepacket of minimal uncertainty. As can bee seen in Figure 6.2, we do achieve cooling, i.e. a reduction of the von Neumann entropy by control signals as shown in Figure 6.3 (left, upper). The reservoir is needed, because for a closed system, the entropy would be conserved. Therefore, in our parameter range, stronger coupling, i.e. larger γ_0, increases the effect.

Comparison with a Lindblad master equation and the Caldeira-Leggett master equation

As we showed in the article constituting Section 7.1 the standard Lindblad equation fails completely in reproducing this cooling effect. Used to describe the dynamics in the control algorithm, it predicts, the best solution would be no control at all. While

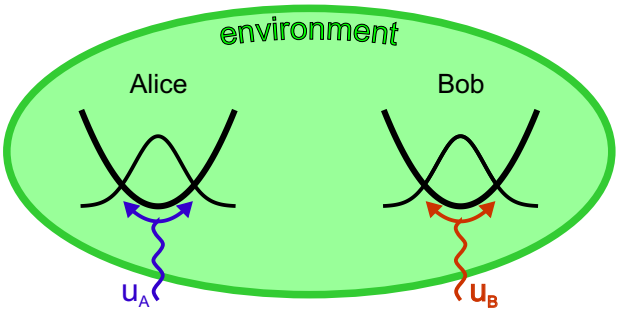

Figure 4.2.: Schematic representation of our setting. Two harmonic modes, not directly coupled to each other, share the same reservoir. The system can be influenced by external parametric controls, acting *locally* on the subsystems. Neither the local controls, nor the reservoir alone can generate entanglement between Alice and Bob, but together, they succeed.

feeding the SLN control pulses into the Lindblad dynamics, heating is predicted. Other than that, we were able to show in the article constituting Section 7.2, that the Caldeira-Leggett master equation:

$$\frac{\mathrm{d}}{\mathrm{d}t}\rho = -\frac{i}{\hbar}[H_S + H_C, \rho] - \frac{i\eta}{2m\hbar}\,[q, \{p, \rho\}] - \frac{\eta}{\hbar^2\beta}\,[q, [q, \rho]] \tag{4.5}$$

is in principle capable of calculating cooling pulses. However, the Caldeira-Leggett master equation is not sufficient to calculate low temperature quantum dynamics [Vac00]; we monitored the violation of Heisenbergs uncertainty principle. The equations of motion for the first and second cumulants implemented for the Caldeira-Leggett master equation are to be found in appendix A.1.

4.3. Generating entanglement by optimal control

The minimal setting needed for generating entanglement are two subsystems and a non-local interaction. However, not any non-local interaction gives rise to entanglement, in particular, a thermal heat bath, shared by the subunits and appropriately modeled for a condensed matter setting, does not. Well knowing, that local operations can not generate entanglement either, we went for finding control pulses driving an initially separated bipartite system, only coupled via a common reservoir, into an entangled state. From the onset, it is perfectly clear, that this is only possible as a cooperative effect of driving and dissipation.

State-of-the-art

Due to the important role, that entanglement plays for quantum information, the dynamics of entanglement in the presence of reservoirs is a well-studied topic for different scenarios. For a bipartite open system, consisting of two subunits A and B, the non-local interaction, necessary to generate entanglement, can in principle be provided from three different sources: a direct coupling of the subsystems, a control acting nonlocally, or a common reservoir. For some settings, a common thermal reservoir mediates a quasi-static direct coupling between the subsystems [PR08, BFP03, Bra02, WDCK$^+$11], which gives rise to a static entanglement effect. Also, entanglement can be preserved in a decoherence free subspace, if the subsystems are initially squeezed, as in [HB08]. These findings stimulated investigations of engineered reservoirs, i.e. artificial environments, driving the system in a favored stationary state, as in [LGL$^+$11, MHdC$^+$13, SMSP10, ACVM13].
Explicit driving on the other hand, has been taken into account, e.g., in [GPZ10], where the direct coupling is periodically driven, in [ZPAI13], where a non-classical driving is considered, and in a feedback scheme in [SRP09].

Stochastic dynamics

As for entanglement at least two subsystems are necessary, our formalism needed to be adjusted for two harmonic modes A and B. Therefore, the Hamiltonian of the total system (cf. Equation (1.2)) takes the form:

$$H = H_{S_A} + H_{S_B} + H_{S_A,S_B} + H_I + H_R. \tag{4.6}$$

The system part, *without* any direct coupling between the subunits, is given by:

$$H_{S_A} + H_{S_B} = \sum_{i=A,B} \frac{p_i^2}{2m_i} + \frac{m_i\omega_i^2}{2} q_i^2 + \frac{u_{2,i}}{2} q_i^2 \tag{4.7}$$

where the control fields u_A, u_B, to be determined, act *locally* on the respective subunit. The driving is modeled parametrically, only the second cumulants are relevant for entanglement and, as mentioned, linear control does not change them. The common reservoir is again modeled by a large set of harmonic modes:

$$H_R = \sum_\alpha \frac{p_\alpha^2}{2m_\alpha} + \frac{m_\alpha\omega_\alpha^2}{2} x_\alpha^2, \tag{4.8}$$

where the interaction Hamiltonian between the system and the reservoir is given by:

$$H_I = (q_A + q_B) \sum_\alpha c_\alpha x_\alpha + (q_A + q_B)^2 \sum_\alpha \frac{c_\alpha^2}{2m_\alpha\omega_\alpha^2}. \tag{4.9}$$

Only the symmetric mode of the system $Q_+ = (q_A + q_B)/\sqrt{2}$ couples to the reservoir, the antisymmetric mode $Q_- = (q_A - q_B)/\sqrt{2}$ is not subjected to dissipation. The last term of the equation may seem like a direct coupling between the subsystems mediated by the bath. On the contrary, it cancels out such an effect. In our modeling, the adiabatic elimination would lead to a vanishing influence of the reservoir, allowing only for dynamic dissipation. If this counterterm (cf. Subsection 1.1.1) is missing, its absence may give rise to a quasi-static entanglement effect [PR08, Bra02]. However, for the condensed matter applications we consider, this would be an inappropriate modeling.
For our Gaussian bipartite system, the SLN equation then takes the form:

$$\begin{aligned}\frac{\mathrm{d}}{\mathrm{d}t}\rho_{AB} &= -\frac{\mathrm{i}}{\hbar}[(H_{S,A} + H_{C,A}) \otimes \mathbb{1}_B, \rho_{AB}] - \frac{\mathrm{i}}{\hbar}[\mathbb{1}_A \otimes (H_{S,B} + H_{C,B}), \rho_{AB}] \\ &\quad + \frac{\mathrm{i}}{\hbar}\xi(t)[q_A + q_B, \rho_{AB}] - \frac{\mathrm{i}}{\hbar}\frac{\gamma_0}{2}[q_A + q_B, \{p_A + p_B, \rho_{AB}\}] \end{aligned} \tag{4.10}$$

The equations of motion for the first and second cumulants of this bipartite Gaussian system can be found in Appendix A.2.

Objective

Our goal is maximizing the entanglement of our subsystems at the final time $T = 6\pi$, which is measured by the logarithmic negativity (details cf. Subsection 3.3.2):

$$E_{\mathcal{N}} = \max\{0, -\ln(\tilde{\nu}_-)\}. \tag{4.11}$$

However, minimizing the argument of a logarithm (and the reciprocal of it, due to the derivative) with a numerical method, is not the best of all ideas. For the setting we looked into here, it appears, that minimizing $\det\gamma$ (remember, $\det\gamma < 0$ is a necessary condition for entanglement), is both sufficient and numerical stable.
In principal, one can question the goal of maximizing entanglement for a continuous variable system: The maximally entangled state for a Gaussian system is the infinitely squeezed EPR-state, which can not be normalized and is therefore unphysical. In praxis, the limit of numerical accuracy shelters us from having such problems.

Results

We choose A and B to be identical harmonic modes[4], initially prepared in their bare ground states. As we show in the article constituting Section 7.3, for the uncontrolled dynamics the two sub-states stay separated. There is no entanglement created by the mere coupling to the reservoir. We want to maximize the entanglement between

[4] i.e. $m_A = m_B = 1$, $\omega_A = \omega_B = 1$

the two subunits at the final time T, both with symmetric controls, i.e. $u_A = u_B$, and single-site control, i.e., u_A only, $u_B \equiv 0$. For the exemplary parameters $\beta = 1$ and $\eta = 0.1$, the entanglement achieved is $E_{\mathcal{N}}(T) = 4.37$ for the symmetric controls and $E_{\mathcal{N}}(T) = 2.33$ for single-site driving. While in continuous variable system, there is no upper bound for entanglement, values of $E_{\mathcal{N}}$ considered necessary for utilization in experimental realisations are of the order of one, cf., e.g. [GPZ10].
Figure 6.5 presents the covariance matrices, clearly showing $\det \gamma < 0$ for the driven cases. In the normal modes, squeezing is necessary for entangled states. We succeed, in particular, in squeezing the antisymmetric mode as can be seen in Figure 6.6. As this mode decouples from the reservoir, the effect is lasting (cf. Figure 6.7). Also, we found the results to be quite robust against temperature rise.
Neither local controls alone, nor a thermal reservoir without potential renormalisation, can generate entanglement. We were able to show, that by a combined effort of both reservoir and local driving, entanglement can be created. As any condensed matter system comes with a thermal bath, the experimental effort reduces to applying local driving; in a totally minimalistic setting, even single-site driving is sufficient. We believe, that this presents a promising new possible scheme for experimental generation of entanglement.

5. Summary and conclusion

The progress made in fabrication of tailored quantum devices provides a variety of controllable quantum systems and simultaneously creates a demand for optimal control of these systems. As any real system, these quantum systems are open systems, interacting with their environment. The exact description of the dynamics of driven open systems is highly non-trivial, yet necessary, as in driven systems commonly applied approximations fail. Therefore, such an exact description is essential to correctly capture the features of this dynamics, which is necessary to gain a deeper understanding of the underlying processes. We provided an optimal control algorithm based on an exact description of non Markovian open quantum systems, which treats both driving and dissipation on the same footing.
The ability of impacting all system observables is inherent to the concept of a reservoir. In a standard reservoir in a typical condensed matter scenario this ability is normally used to counteract quantum interference effects. By the means of optimized control pulses, we employ this idle resource in a productive way, generating cooperative effects of driving and dissipation.
For rather simple, but elementary systems, we were able to reveal fascinating aspects of nonequilibrium physics, succeeding both in cooling a thermalized quantum system and in entangling two subsystems. Having understood the underlying principles both the experimental realisation and the generalization to larger systems are the next issues to be tackled.
We have shown, that the whole is greater than the sum of its parts, namely driving and dissipation can cooperatively perform tasks, neither part is capable alone.

Part II.

Publications

6. Summary of published articles

6.1. General remarks

Inspired by the possibilities to design and control quantum devices, we aim to determine control signals which drive these systems to desired objectives. However, as real quantum systems are always open quantum systems [Wei12, BP06], the interaction of the system of interest with the surrounding environment has to be taken into account. Driving changes the system of interest, in particular arbitrary strong and fast driving, resulting in a backaction on the interaction with the environment. Therefore a consistent description of both driving and dissipation is needed.
Such an optimal control method for non-Markovian open quantum systems based on an exact, consistent description of both driving and dissipation we derived in the first article [SNA$^+$11a]. We employ this method in all articles on different quantum systems in order to drive them to reasonable objectives and learn more about the driven nonequilibrium dynamics of our systems [SNA$^+$11a, SRAS12, SSA13a].
The scenario we are interested in, is in fact, the common one in condensed matter physics: Our quantum system of interest is embedded into an environment, which has great impact on our system and is beyond our control. For low temperatures (i.e., if the system's relaxation times are *not* much longer than the thermal time of the reservoir $\hbar\beta$) neither the Markovian nor the Born approximation holds [Wei12]. As the uncontrolled dynamics of the respective system is far from reaching desirable objectives, we apply additional controls, which are calculated by optimal control techniques, to drive the system in the desired way. Allowing for arbitrary strong and fast driving, also the rotating wave approximation (RWA) is no longer applicable [KK04].
System and environment are described by a system-plus-reservoir model: The Hamiltonian of the total system can be divided into a system part, H_S, a reservoir part H_R and an interaction part between the former two, H_I, i.e. $H = H_S + H_I + H_R$. Now, we can add a control Hamiltonian H_C, which acts only locally on the relevant system to the system Hamiltonian $H_S \to H_S + H_C$. For an exact description of the non-Markovian dynamics, we use the stochastic Liouville-von Neumann equation (SLN) (details cf. Section 1.3, originally published in [SG02]):

$$\dot{\rho}_{\xi,\nu} = \mathcal{L}\rho_{\xi,\nu} = -\frac{i}{\hbar}[H_S + H_C, \rho_{\xi,\nu}] + \frac{i}{\hbar}\xi(t)[q, \rho_{\xi,\nu}] + \frac{\mathrm{i}}{2}\nu(t)\{q, \rho_{\xi,\nu}\} \tag{6.1}$$

holding for one stochastic realisation $\{\xi(t), \nu(t)\}$. The correlation functions of these

complex-valued noise variables $\xi(t)$ and $\nu(t)$ reproduce the quantum correlation function $L(\tau)$ of the total environmental force, which is fully determined by the spectral density $J(\omega)$ and the inverse thermal energy β of the reservoir. The physical density matrix is given by a stochastic averaging:

$$\rho(t) = \mathbb{E}\left[\rho_{\xi,\nu}(t)\right]. \tag{6.2}$$

Using this stochastic equation of motion (6.1) as constraint, we extended the optimal control work of Krotov [Kro96] and Sklarz and Tannor [ST02] to non-Markovian open systems (for details cf. Section 2.3). This provides us with a system of equations for the state $\rho_{\xi,\nu}(t)$, the co-state $\Lambda_{\xi,\nu}(t)$ (i.e. the Lagrange multiplier) and the control update to be solved consistently and iteratively by numerical means:

$$\begin{aligned}
\dot{\rho}_{\xi,\nu} &= \mathcal{L}\rho_{\xi,\nu} \\
\dot{\Lambda}_{\xi,\nu} &= -\mathcal{L}^{\dagger}\Lambda_{\xi,\nu}, \text{ with the final time boundary condition:} \\
\Lambda_{\xi,\nu}(T) &= \frac{\partial}{\partial \rho^{\dagger}_{\xi,\nu}(T)} F_{\xi,\nu}(\rho_{\xi,\nu}(T))
\end{aligned} \tag{6.3}$$

$$u_{(i)}^{(new)}(t) = u_{(i)}^{(old)}(t) + \frac{1}{\lambda_{(i)}(t)}\mathbb{E}\left[\frac{2}{\hbar}\mathrm{Im}\left[tr\left\{\Lambda_{\xi,\nu}^{\dagger(old)}\left[\frac{\partial H_C}{\partial u_i}, \rho_{\xi,\nu}^{(new)}\right]\right\}\right]\right].$$

Concerning the control update, Krotov's method differs slightly, but substantially from the usual gradient method (the forward propagation of $\rho_{\xi,\nu}(t)$ takes place with the new control signals, while the backward propagation of $\Lambda_{\xi,\nu}(t)$ is done with the old ones, cf. 2.1.2).

In order to gain a deeper understanding of the interplay and cooperative effects of both dissipation and driving in applying our general valid method, we stick to rather simple settings. But, while the components of our settings (harmonic modes for the reduced system, ohmic spectral density for the environment, linear and parametric controls) are not very complex, their interplay is nevertheless non-trivial and reveals quite interesting physics. As these systems are Gaussian, their description is mathematically rather straightforward (for details cf. Chapter 3). Nonetheless, the systems are not analytically solvable anymore, as we are not restricting the parametric control to periodic signals, which can be treated in terms of Matthieu functions [ZH95]. We do allow for arbitrary strong and fast driving. Despite the simplicity, the systems shows interesting features of non-equilibrium physics. In fact, it is due to the simplicity, that we can definitely attribute these features to cooperative effects of driving and dissipation.

We use natural units throughout our publications, i.e. $\hbar = 1$, $k_B = 1$, units ω_0 for energies, angular frequencies, or rates; lengths are given in $\frac{1}{\sqrt{m\omega_0}}$, as for momenta

$\sqrt{m\omega_0}$. This is the general setting for all of the three publications; we now turn to the individual projects.

6.2. Optimal Control of Open Quantum Systems: Cooperative Effects of Driving and Dissipation[1]

The system, we considered in this publication, is a single harmonic mode, with $H_S = \frac{p^2}{2m} + \frac{m\omega_0^2}{2}q^2$, which is coupled to a reservoir with ohmic spectral density $J(\omega) = m\gamma_0\omega/\left(1+\frac{\omega^2}{\omega_c^2}\right)^2$ and a high frequency cutoff ω_c (with: $\omega_c = 50$, $m = 1$ and $\omega_0 = 1$). Then, the SLN equation is given by (for details cf. Subsection 1.3.1):

$$\frac{\mathrm{d}}{\mathrm{d}t}\rho_\xi = -\frac{i}{\hbar}[H_S + H_C, \rho_\xi] + \frac{i}{\hbar}\xi(t)[q, \rho_\xi] - \frac{i}{\hbar}\frac{\gamma_0}{2}\left[q, \{p, \rho_\xi\}\right]. \tag{6.4}$$

For this system we want to maximize the overlap with a coherent state at a fixed end time T, i.e., we want to minimize $M = 1 - A$, where $A = |\alpha\rangle\langle\alpha|$ is a projector onto a coherent state. Our control Hamiltonian takes the form $H_C = -F(t)q + \Delta(t)\frac{q^2}{2}$, with $F(t)$ being a linear force control field and $\Delta(t)$ represents a parametrical tuning control field, modifying the instantaneous resonance frequency to be $\omega^2 = \omega_0^2 + \Delta$. Being at most quadratic in their coupling, these control fields do not change the Gaussian nature of the states.

We investigated two issues in this paper, both formulated as a state-to-state transfer control problem. On the one hand, we ask for restoring the initial state at the final time T, it is, fighting the detrimental effects of the environment. And, on the other hand, we want to drive an initially thermalized state to the ground state, i.e. cooling by optimal control.

First, we succeeded to determine control signals for a typical state-to-state transfer task: Our initial state is a wave packet of minimal uncertainty centered around $q = 1$ and $p = 0$ which we want to restore at $T = 20$. We explored a typical range for solid state quantum devices of both for damping constants $\gamma_0 = 0.005 \ldots 0.1$, and inverse thermal energies $\beta = 50 \ldots 0.5$, gaining fidelities up to 99%.

We also compared our SLN results with control pulses gained with other descriptions of the dynamics, Figure 6.1 shows the windowed Fourier transformations of the control signals for $\gamma_0 = 0.05$ and $\beta = 1$.

As can be seen, the control pulses for the dissipative system (upper) differs substantially from the one for the closed system (lower), indicating, that the later are not robust against dissipation. In fact, feeding the controls for the undisturbed system into the exact SLN open system dynamics leads to poor results.

[1] [SNA+11a]: Rebecca Schmidt, Antonio Negretti, Joachim Ankerhold, Tommaso Calarco, and Jürgen T. Stockburger, PRL 107, 130404 (2011)

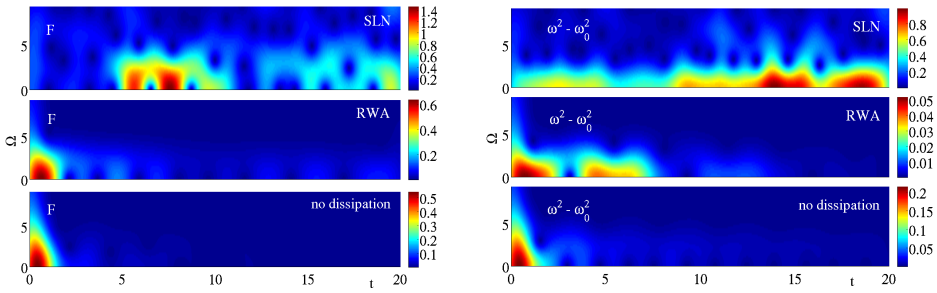

Figure 6.1.: Windowed Fourier transformation of the optimal control signals for state-to-state-transfer, restoring initial state at final time T ($\gamma_0 = 0.05$ and $\beta = 1$). L.h.s. force control field $F(t)$, r.h.s. tuning control field $\Delta(t)$. SLN dynamics (upper, respectively) shows detailed features over the total propagation time, while for the closed system (lower, respectively) the control signals only in the beginning give a push in the right direction. Control signals gained for RWA dynamics (middle, respectively) perform poorly, when applied to the exact dynamics (taken from [SNA+11a]).

We also investigated the performance of a standard Lindblad master equation [BP06], cf. Subsection 1.4.3:

$$\frac{\mathrm{d}}{\mathrm{d}t}\rho = -i[H_S + H_C, \rho] + \gamma_0(N_\beta + 1)\left(a\rho a^\dagger - \frac{1}{2}\{a^\dagger a, \rho\}\right) + \gamma_0 N_\beta\left(a^\dagger \rho a - \frac{1}{2}\{aa^\dagger, \rho\}\right) \tag{6.5}$$

in dimensionless units, where a, $a^\dagger$ are the annihilation and the creation operator of the harmonic oscillator, respectively, and $N_\beta = \frac{1}{e^\beta - 1}$ is the thermal occupation number of the unpertubated oscillator. The control signals gained by this RWA dynamics are shown in Figure 6.1 (middle), and the fidelities predicted are high. However, the RWA control pulses differ substantially from the SLN ones, and feeding these RWA control signals into the full stochastic dynamics, which is an *exact* description of the system, leads to a performance considerably worse. Therefore, we were able to show, that the standard Lindblad dynamics is not suitable for investigate driven open system dynamics.
Second, we also achieved cooling of our system by the means of optimal control, an aim not reachable in a closed system, due to entropy conservation. Here we started with our system thermalized with the reservoir, aiming for maximal overlap with the ground state. Our results can be visualized in terms of von Neumann entropy, which for Gaussian states is given by (cf. [HSH99]):

$$S(\rho) = g\left(\sqrt{\langle q^2\rangle_c \langle p^2\rangle_c - \langle qp - pq\rangle_c^2 / 4}\right) \tag{6.6}$$

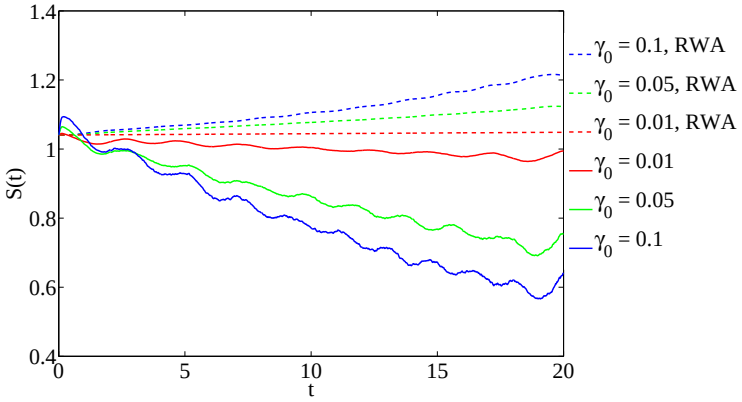

Figure 6.2.: Dynamics of the von Neumann entropy of an initially thermalized state under application of optimal control signals ($\beta = 1$). SLN dynamics (solid lines) shows a reduction of entropy due to driving. RWA dynamics (dashed lines) for these controls predicts an incorrect heating effect (taken from [SNA+11a]).

with $g(x) = (x + \frac{1}{2}) \log(x + \frac{1}{2}) - (x - \frac{1}{2}) \log(x - \frac{1}{2})$. Given that only the parametric control $\Delta(t)$ has an impact on the second cumulants, and the entropy is a function of them, the control Hamiltonian considered here is $H_C = \Delta(t)\frac{q^2}{2}$ only. Figure 6.2 shows, that the RWA approach here not only is less successful, but fundamentally wrong. The method itself fails to calculate control signals, and, inducting the ones calculated for the SLN dynamics, heating instead of cooling is predicted. This reveals the 'hard-coding' of the thermalized state of the uncontrolled oscillator into the Lindblad operators. This strikingly demonstrates, that the effort, we have to invest in our numerical method, is justified by its success.

As mentioned, in a closed system, no cooling can be achieved by optimal controls, and there are no internal degrees of freedom in our system, which can be exploited for the effect. This clearly shows, that the cooling is a cooperative effect of both driving and dissipation.

Scientific contribution: We provide an exact optimal control algorithm for non-Markovian open quantum systems, which is successfully applied both to state-to-state transfer and to cooling of an originally thermalized mode below the reservoir temperature. We also showed, that a standard Lindblad approach fails. We demonstrated that there is more for optimal control in open systems than fighting dissipation. The interplay of driving and dissipation gives rise to new possibilities: the thermal environment is needed to cool via optimal control.

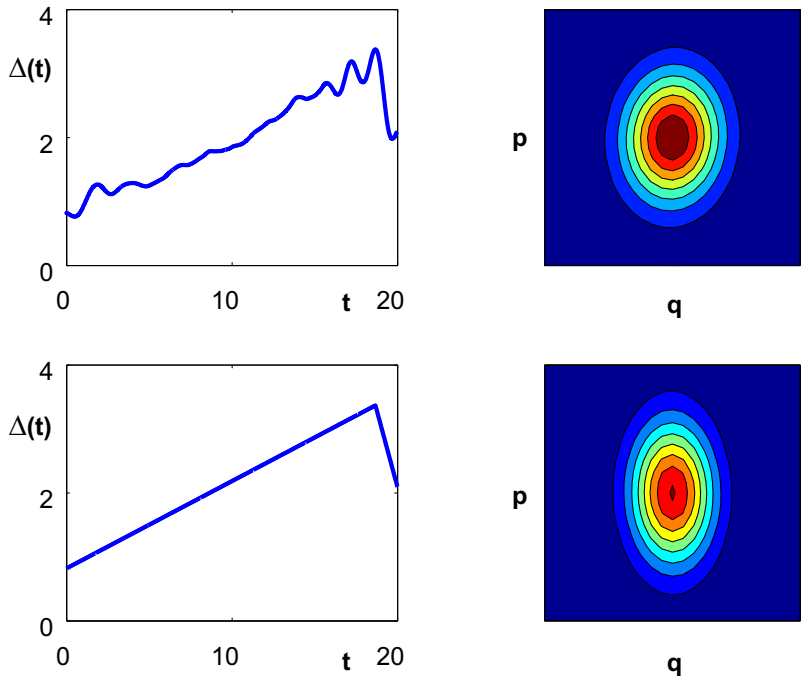

Figure 6.3.: Comparison of the performance of a simplified version (l.h.s., lower) of the optimal control signal $\Delta(t)$ (l.h.s., upper) with the original one in terms of the contour plot of the Wigner function at the final time T. While the simplified signal still achieves cooling, it fails to reduce the squeezing of the final state (taken from [SRAS12]).

6.3. Cooling of quantum systems through optimal control and dissipation[2]

In this publication, we took a closer look at the cooling scenario of the previous Section, in order to gain a deeper understanding, why the calculated control signal looks like that. Therefore, we here focused on the way the control signals actually works in terms of Wigner functions and gain a deeper understanding of the constituent parts of the control pulse. We also had a closer look into the performance of the Caldeira-Leggett master equation, which constitutes the high temperature limit of our method. In order to understand the driven dynamics, we visualized the dynamics of the Wigner function of our system, which, as $\langle q \rangle_c = \langle p \rangle_c = 0$, takes the

[2][SRAS12]: Rebecca Schmidt, Selina Rohrer, Joachim Ankerhold, and Jürgen T. Stockburger, Phys. Scr. T151, 014034 (2012)

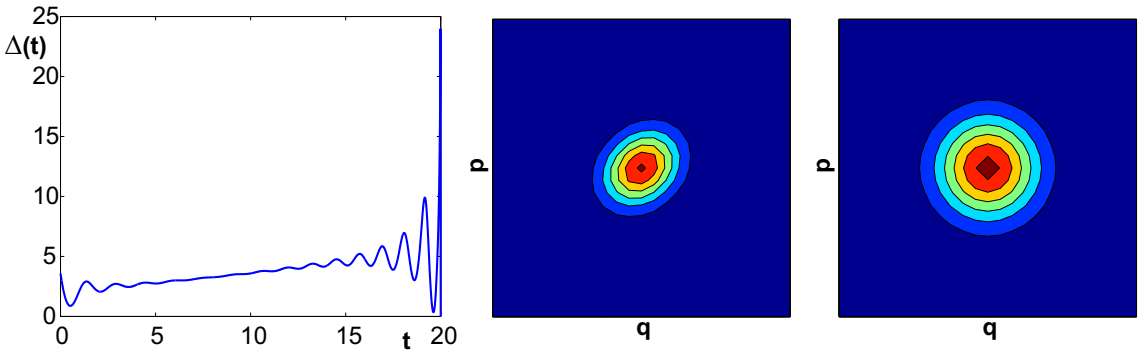

Figure 6.4.: Optimal control field $\Delta(t)$ gained by a Caldeira-Leggett Master equation (left). While it shows the main features of the quantum control signal, and cooling is achieved (middle), it violates the uncertainty relation: The ground state (right) covers a larger area in phase space (taken from [SRAS12]).

form:

$$W(q,p) = \frac{1}{2\pi\sqrt{\det\sigma}} \cdot \exp\left\{\frac{1}{2\det\sigma}\left(q^2\left\langle p^2\right\rangle_c - (qp+pq)\left\langle\frac{qp+pq}{2}\right\rangle_c + p^2\left\langle q^2\right\rangle_c\right)\right\} \tag{6.7}$$

where $\det\sigma = \left\langle q^2\right\rangle_c\left\langle p^2\right\rangle_c - \left\langle\frac{qp+pq}{2}\right\rangle_c^2$ is the determinant of the covariance matrix σ. The system is, as mentioned, subjected to parametric control only, i.e. the control Hamiltonian reads $H_C = \Delta(t)\frac{q^2}{2}$. Figure 6.3 l.h.s., upper, shows the control pulse $\Delta(t)$ we calculated. When this control pulse is applied to an initially thermalized, i.e. isotropic, Wigner function, the system gets more and more squeezed during the gradual rise of the control. The work performed is dissipated to the reservoir and entropy is transferred also, as shown in Figure 6.2 in the previous Section. The final release happens on a rather short time scale, not allowing the system to get fully thermalized again. The modulation of the signal, both on the timescale of the unpertubated system $\omega_0 = 1$ and the thermal time scale of the reservoir $\hbar\beta = 1$, 'massages' the Wigner function during propagation in order to reduce the squeezing of the final state. The simplified control signal shown in Figure 6.3 (lower) reproduces only the ramp-like ascent and the steep descent on a short timescale, that quench and release. This rudimental signal preserves the main effect of the control in achieving a comparable overlap with the target state. Nevertheless, this simplified version fails in reducing the squeezing.
In contrast to the Lindblad master equation, which fails to reproduce our results, the Caldeira-Leggett master equation [CL83]:

$$\frac{\mathrm{d}}{\mathrm{d}t}\rho = -\frac{i}{\hbar}[H_S + H_C, \rho] - \frac{i\eta}{2m\hbar}[q,\{p,\rho\}] - \frac{\eta}{\hbar^2\beta}[q,[q,\rho]] \tag{6.8}$$

does not rely on the RWA, and the Born-Markov approximation is replaced by a stronger Markov approximation, assuming an instantaneous decay of the environmental fluctuations. While the control algorithm for this way of describing dynamics is able to find a control signal capable to reduce the entropy of the system, it is not a valid description of the quantum dynamics, the predicted target state would cover a smaller area in phase space than the ground state (Figure 6.4). This comes with no surprise: For the harmonic potential considered here, the *classical* Klein-Kramers equation is the equation of motion for the Wigner function corresponding to the density matrix governed by eq. 6.8, therefore quantum features are not included in this description.
Nevertheless, cooling by optimal control for classical systems, both Markovian and non-Markovian, is also possible, as has been shown by Rohrer [Roh11].
Scientific contribution: We gain a deeper understanding in the nonequilibrium driven dynamics. We basically learned, why control signal looks like that. While cooling by optimal control can also be achieved in classical systems, this less elaborate method is not suitable to deal with quantum systems, violating features as elementary as the uncertainty principle.

6.4. Quasi-local generation of EPR entanglement in non-equilibrium[3]

The system we considered in this publication consists of two harmonic modes coupled to a common reservoir. Our objective is to generate entanglement between the initially separated states. The environment, which we consider, is the generic thermal bath for solid state devices, which does not create entanglement between the subunits (for details cf. Subsection 1.1.1). We apply our control pulses only locally to the two subsystems, well knowing, that entanglement can not be generated by local operations and classical communication (LOCC) alone. As the two subunits are not directly coupled, the only source of non-locality in the setting is the common reservoir. However, we demonstrate that in the combined system, entanglement can be generated, due to a cooperative effect of driving and dissipation.
The relevant system, consisting of the subsystems A and B, is described by the Hamiltonian:

$$H_S(t) \equiv H_A(t) + H_B(t) = \sum_{j=A,B} \frac{p_j^2}{2M} + \frac{M\Omega^2}{2} q_j^2 + \frac{u_j(t)}{2} q_j^2. \tag{6.9}$$

where we only consider parametric controls $u_j(t)$ $(j = A, B)$, acting *locally* on the respective subsystems. Logarithmic negativity $E_{\mathcal{N}}$, the entanglement measure for

[3][SSA13a]: Rebecca Schmidt, Jürgen T. Stockburger, and Joachim Ankerhold, arXiv:1305.6566 [quant-ph]

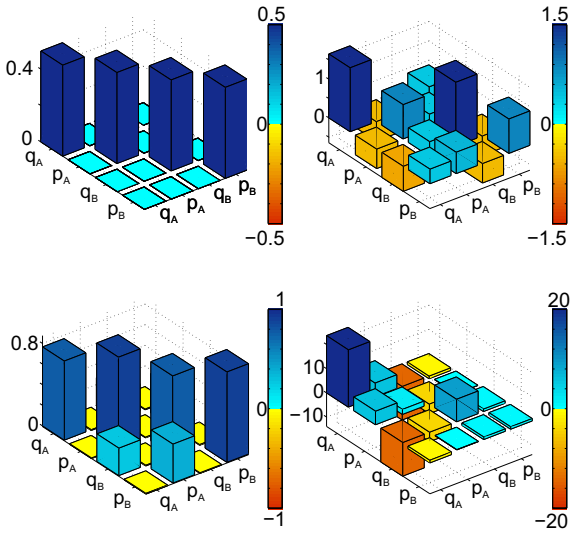

Figure 6.5.: Covariance matrices of the system for $\beta = 1$, $\eta = 0.1$, $\omega_c = 50$ and $T = 6\pi$. Initially, both A and B are prepared in the ground state (upper left). At $t = T$, without driving (lower left) the stationary state is still separated ($\det\gamma > 0$), while applying control signals both symmetrically ($u_A = u_B$, upper right) and single-site (u_A only, $u_B \equiv 0$, lower right) generate entanglement. $E_{\mathcal{N}}(T)$ achieved is 4.37 and 2.33, respectively (taken from [SSA13a]).

bipartite Gaussian states, is a function of the second cumulants only, which are not changed by linear control signals [VW02]:

$$E_{\mathcal{N}} = \max\{0, -\ln(\tilde{\nu}_-)\}. \tag{6.10}$$

Here, $\tilde{\nu}_-$ is the smallest symplectic eigenvalue of the covariance matrix corresponding to the partially transposed density matrix. Gaussian states are fully described by their first and second cumulants, where the later are grouped in the covariance matrix σ with $\sigma_{ij} = \frac{1}{2}\langle x_i x_j + x_j x_i\rangle - \langle x_i\rangle\langle x_j\rangle$. In the 2×2 block structure

$$\sigma = \begin{pmatrix} \alpha & \gamma \\ \gamma^T & \beta \end{pmatrix}, \tag{6.11}$$

α, β correspond to the covariance matrices of the respective sub-units A and B, while γ (transpose γ^T) carries the mixed cumulants and therefore the non-local information of the system.
Entanglement only exists if $E_{\mathcal{N}} > 0$ while $E_{\mathcal{N}} = 0$ corresponds to purely classical and/or local quantum correlations. Note that $\det\gamma < 0$ is necessary for $E_{\mathcal{N}}$ to be positive [Sim00].

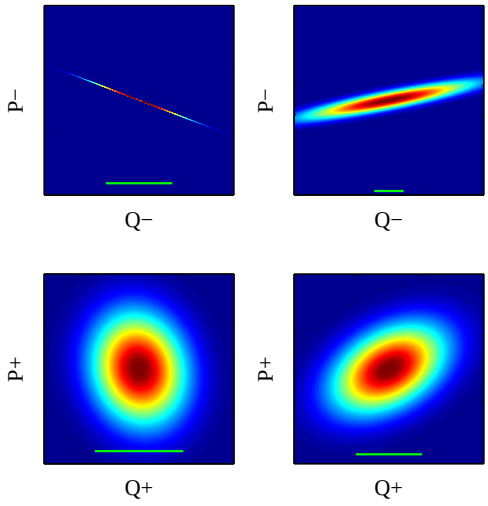

Figure 6.6.: Reduced Wigner functions for the anti-symmetric Q_-, P_- (top) and symmetric Q_+, P_+ (bottom) normal modes at $T = 6\pi$ for two-site (left) and single-site (right) control. The green line indicates the ground state width; parameters as in Figure 6.5 (taken from [SSA13a]).

A and B are embedded in a common reservoir:

$$H_R = \sum_k \frac{p_k^2}{2m_k} + \frac{m_k\omega_k^2}{2}x_k^2 \tag{6.12}$$

$$H_I = (q_A + q_B)\sum_k c_k x_k + (q_A + q_B)^2 \sum_k \frac{c_k^2}{2m_k\omega_k^2}\,. \tag{6.13}$$

Only the symmetric mode $Q_+ = (q_A + q_B)/\sqrt{2}$ couples to the reservoir, the Q_- decouples and therefore does not suffer from dissipation. In this setting, the last term in Equation 6.13, the counterterm, plays a crucial role: if it is not taken into account, the effect is a quasi-static direct coupling between the subsystems, which may give rise to an environment-induced entanglement (as in [Bra02, PR08]). For the typical solid state system, there is no such effect. Therefore, modeling the interaction according to the Caldeira-Leggett model, this counter term ensures, that we only allow for a dynamic dissipation effect. Here, the reservoir has a vanishing net effect, when an adiabatic elimination is carried out.
This interaction alone, even though it is non-local, does not generate entanglement. In fact, the steady state of the uncontrolled system can be calculated to be $\tilde{\nu}_-^2 = \langle(q_A + q_B)^2\rangle_\beta\langle(p_A + p_B)^2\rangle_\beta/(\hbar/2)^2$, i.e. $\tilde{\nu}_-^2 > 1$ if $\beta < \infty$. So, without additional driving the subsystems stay separated forever, as can be seen in fig. 6.5.

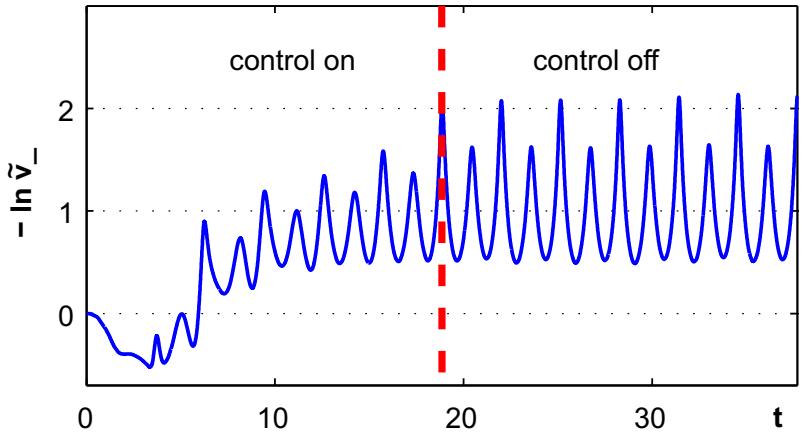

Figure 6.7.: Entanglement dynamics for $\beta = 0.1$ for a protocol where the control is switched off at $t_f = 6\pi$. Other parameters are as in Fig. 6.5 (taken from [SSA13a]).

We calculated control signals both for symmetric control pulses, i.e. $u_A = u_B$ and for single-site control, i.e. u_A only ($u_B \equiv 0$), succeeding in the generation of entanglement in both cases, as $\det \gamma$ is negative (cf. fig. 6.5) and the logarithmic negativity achieved is $E_{\mathcal{N}}(T) = 4.37$ and $E_{\mathcal{N}}(T) = 2.33$, respectively.
The resulting entanglement is also reflected in a squeezing of normal modes, the necessary condition $\det \gamma < 0$ can be recasted (for symmetric controls) as:

$$4 \det \gamma = \Delta_P \, \Delta_Q - [\langle Q_+ P_+ \rangle - \langle Q_- P_- \rangle]^2. \tag{6.14}$$

Other than the standard EPR entanglement, where the squeezing is antisymmetric in the normal modes $r_- = -r_+$, Fig. 6.6 shows, that our control pulses only squeeze the non-dissipative antisymmetric mode strongly.
We were also able to show, cf. Fig.6.7, that the effect is quite robust against temperature rising of the bath, and, due to the decoupling of the antisymmetric mode, lasting.
Scientific contribution: We extend our method to treat bipartite systems, showing that entanglement can be generated in a minimal setting: the non-local interaction provided by the reservoir is exploited by the help of local controls only. The achieved entanglement is a cooperative effect of driving and dissipation.

6.5. Conclusion

In order to perform optimal control in open quantum systems, we derived an optimal control method for non-Markovian open quantum systems, which treats both driving and dissipation consistently.

Starting from using optimal control as a tool to fight the detrimental effect of a non-Markovian environment we get quite a long way in discovering cooperative effects of driving and dissipation, not available with only one of the components at hand. Focussing on conceptual rather simple, yet relevant, fundamental systems, we were able to gain a deeper understanding of the rich interplay between a non-Markovian environment and designed control pulses.
We were able to cool a thermalized quantum system below the temperature of the reservoir and were furthermore able to generate a pure quantum mechanical feature, i.e. entanglement, by the combined effort of both driving and dissipation.

7. Publications

7.1.

Title:	Optimal Control of Open Quantum Systems: Cooperative Effects of Driving and Dissipation
Authors:	R. Schmidt, A. Negretti, J. Ankerhold, T. Calarco and J.T. Stockburger
Journal:	Physical Review Letters 107, 130404
Year:	2011
Copyright[1]:	American Physical Society (APS)
Online journal:	`http://prl.aps.org/abstract/PRL/v107/i13/e130404`

[1]The use of the article in the framework of a PhD thesis is kindly allowed by APS, according to the copyright policies of APS: http://publish.aps.org/copyrightFAQ.html.

PRL 107, 130404 (2011) PHYSICAL REVIEW LETTERS week ending 23 SEPTEMBER 2011

Optimal Control of Open Quantum Systems: Cooperative Effects of Driving and Dissipation

R. Schmidt,[1] A. Negretti,[2] J. Ankerhold,[1] T. Calarco,[2] and J. T. Stockburger[1]

[1]*Institut für Theoretische Physik, Universität Ulm, Albert-Einstein-Allee 11, 89069 Ulm, Germany*

[2]*Institut für Quanteninformationsverarbeitung, Universität Ulm, Albert-Einstein-Allee 11, 89069 Ulm, Germany*

(Received 5 October 2010; revised manuscript received 22 August 2011; published 21 September 2011)

We investigate the optimal control of open quantum systems, in particular, the mutual influence of driving and dissipation. A stochastic approach to open-system control is developed, using a generalized version of Krotov's iterative algorithm, with no need for Markovian or rotating-wave approximations. The application to a harmonic degree of freedom reveals cooperative effects of driving and dissipation that a standard Markovian treatment cannot capture. Remarkably, control can modify the open-system dynamics to the point where the entropy change turns negative, thus achieving cooling of translational motion without any reliance on internal degrees of freedom.

DOI: 10.1103/PhysRevLett.107.130404 PACS numbers: 03.65.Yz, 02.30.Yy, 03.67.−a, 05.70.Ln

Introduction.—The control of quantum dynamics for the accurate preparation of a prescribed quantum state by a tailored time-dependent field is a task of key importance in quantum physics and related disciplines. With increasing complexity of devices for quantum information processing the destructive role of environmental fluctuations has become a severe limitation to further progress. For example, neutral atoms or ions in electromagnetic traps are exposed to fluctuations of (comparatively hot) chip surfaces [1], while in superconducting circuits diffusing charges and electromagnetic fluctuations affect fidelities quite substantially [2].

In this context, optimal control theory (OCT) has emerged as a key ingredient in strategies to tame the effect of decoherence and other imperfections either directly by mitigating their effect or indirectly by speeding up operations. In limiting cases or under idealized conditions OCT has already been used to increase the fidelity of simple quantum gates [3–7] or to construct more complex protocols [8]. Generally, however, OCT has treated environmental interactions mostly by heuristic or approximate methods so far. A simple strategy has been followed in Ref. [9], where the impact of a heat bath was taken into account by assuming an initial thermal state while neglecting its effect completely during its dynamics. Some progress has been achieved within fully dynamical approaches based on standard Markovian master equations. Unfortunately, these schemes have severe drawbacks: First, they become inconsistent for strong control fields unless additional field-dependent memory terms in the dissipator are introduced [10,11]. Second, the rotating-wave approximation (RWA), which is usually performed on the system-environment interaction in order to obtain a master equation with complete positivity, is known to be unreliable in driven systems [10]. Third, at sufficiently low temperatures or for reservoirs with structured spectral mode densities the true dynamics of open quantum systems is non-Markovian. These errors in the dynamics may be further amplified by OCT search algorithms. As a result, OCT computations using standard master equations yield mismatched fields, which perform poorly when applied to a realistic setting.

In this Letter we present a treatment of optimal control of open quantum systems which is not susceptible to these problems. Stochastic Liouville–von Neumann (SLN) equations [12,13] provide an approach to quantum dissipation in a driven system which is both conceptually transparent and formally exact. Field-induced modifications of environmental effects are thus included *a priori*. From the SLN equations one arrives naturally at the definition of a state-costate pair [14] of dynamical variables with the simple first-order equations of motion required by gradient-based and related OCT methods.

We outline the salient features of our OCT technique (for details see Supplemental Material [15]) and apply it to a simple model. Notably, it turns out that control fields extracted from a RWA-based master equation differ substantially from exact ones obtained within the SLN scheme. This leads even to the counterintuitive phenomenon of control-induced cooling, which is completely missing in the RWA approach.

Open-system dynamics and control algorithm.—We start with the exact stochastic equation of motion [12]

$$\dot{\varrho}_{\xi,\nu}(t) = -\frac{i}{\hbar}[H_s, \varrho_{\xi,\nu}(t)] - \frac{i}{\hbar}[H_c, \varrho_{\xi,\nu}(t)] + \frac{i}{\hbar}\xi(t)[q, \varrho_{\xi,\nu}(t)] + \frac{i}{2}\nu(t)\{q, \varrho_{\xi,\nu}\} \quad (1)$$

for noisy samples $\varrho_{\xi,\nu}(t)$ of the density matrix of an open quantum system. The system is characterized by a Hamiltonian H_s governing its autonomous motion, augmented by a term $H_c(t)$ describing the influence of time-dependent control fields $u_j(t)$. It interacts bilinearly with a dissipative environment whose quantum statistical force-force correlation function is mapped to the noise statistics as follows [12]: (i) the autocorrelation of ξ matches the

 © 2011 American Physical Society

Copyright American Physical Society

PRL 107, 130404 (2011) PHYSICAL REVIEW LETTERS week ending 23 SEPTEMBER 2011

quantum noise of the reservoir, (ii) the cross correlations of ξ and ν match the dynamical response of the environment, and (iii) the correlations $\langle \nu(t)\nu(t')\rangle$ vanish identically. According to the last condition $\nu(t)$ is a complex variable with random phase. The nonvanishing correlations are identical to the real and imaginary parts of the kernel defining the Feynman-Vernon influence functional [16,17], from which Eq. (1) can be derived without approximations.

The fluctuations and the dynamical response of the thermal environment are fully characterized by its temperature and spectral density $J(\omega)$, which in the present case will be taken as Ohmic (proportional to ω up to a UV cutoff ω_c). Both $1/\omega_c$ and, more important, the thermal time $\hbar\beta$ are intrinsic time scales of the environmental fluctuations. Equation (1) now simplifies to

$$\dot{\varrho}_\xi(t) = \Omega\varrho_\xi(t) := -\frac{i}{\hbar}[H_s, \varrho_\xi(t)] - \frac{i}{\hbar}[H_c, \varrho_\xi(t)] - \frac{i}{2\hbar}\gamma_0[q, \{p, \varrho_\xi(t)\}] + \frac{i}{\hbar}\xi(t)[q, \varrho_\xi(t)], \tag{2}$$

where γ_0 is the damping rate of a Brownian particle of mass m [18]. The physical density matrix is a stochastic average of the form $\varrho(t) = \mathbb{E}[\varrho_\xi(t)]$.

At the price of introducing an explicit noise variable $\xi(t)$, Eq. (2) represents the exact non-Markovian dynamics in terms of a stochastic ensemble with time-local equations of motion. All memory effects inherent in the reservoir dynamics are contained in the time-dependent correlations. There is no decomposition of the environment into additional degrees of freedom and a secondary, Markovian environment [19]. In an extreme high-temperature limit, Eq. (2) becomes Markovian and reduces to the master equation of Caldeira and Leggett [20].

Optimal control means searching for control signals which drive desirable characteristics of the dynamics to extremal values. Here we consider optimization objectives defined by minimization of an expectation value $\langle M\rangle$ at a specified end time T. This leads to a search for extrema of the objective functional

$$\mathsf{B}[\mathbf{u}(t)] = \mathbb{E}[\mathrm{tr}\{M\varrho_\xi(T)\}] = \mathrm{tr}\{M\varrho(T)\}, \tag{3}$$

where the first equality relies on the map $\mathbf{u} \mapsto \varrho_\xi(T)$ implicit in the initial-value problem of Eq. (2). Alternatively, Eq. (2) can be interpreted as a constraint on simultaneous variations of $\mathbf{u}(t)$ and $\varrho_\xi(t)$. This constraint needs to be taken into account through a time-dependent Lagrange multiplier $\Lambda_\xi(t)$, which also depends on the particular noise realization $\xi(t)$. Variational calculus leads to the equation of motion

$$\dot{\Lambda}_\xi(t) = -\Omega^\dagger\Lambda_\xi(t) = -\frac{i}{\hbar}[H_s, \Lambda_\xi(t)] - \frac{i}{\hbar}[H_c, \Lambda_\xi(t)] - \frac{i}{2\hbar}\gamma_0\{p, [q, \Lambda_\xi(t)]\} + \frac{i}{\hbar}\xi(t)[q, \Lambda_\xi(t)] \tag{4}$$

for $\Lambda_\xi(t)$, called the costate of the optimal control problem in this context. Equation (4) is not an initial value problem; it needs to be solved with the terminal boundary condition $\Lambda_\xi(T) + M = 0$ arising from variation of the final state.

Now the gradient of the objective functional under the above constraint is given by

$$\frac{\delta\mathsf{B}}{\delta u_j(t)}\bigg|_{\text{constr.}} = \mathbb{E}\Big[\mathrm{tr}\Big\{\Lambda_\xi(t)\frac{\partial\Omega}{\partial u_j}\varrho_\xi(t)\Big\}\Big], \tag{5}$$

where $\varrho_\xi(t)$ and $\Lambda_\xi(t)$ obey the stochastic equations of motion (2) and (4).

The preceding considerations show that the SLN approach treats quantum memory effects in a mathematical language which integrates seamlessly into the state-costate framework of standard OCT techniques. For numerical computations, we have adapted the monotonically convergent algorithm of Krotov [21,22] to the present case of non-Markovian stochastic propagation. This algorithm improves performance by substituting gradient search steps with a nonlocal generalization of Eq. (5). Key performance characteristics are improved by this change (see [15]).

Application.—As a common model we consider a harmonic oscillator, i.e., $H_s = \frac{p^2}{2m} + \frac{m\omega_0^2}{2}q^2$, which is subject to an additional potential $H_c(t) = -F(t)q + \frac{m}{2}\Delta(t)q^2$ depending on a force control field $F(t) \equiv u_1(t)$ and a tuning control field $\Delta(t) \equiv u_2(t)$, which modifies the instantaneous resonance frequency, $\omega^2 = \omega_0^2 + \Delta$. This choice is not only a model for typical realizations as, e.g., trapped atoms or ions or low energy dynamics of Josephson junctions, it also offers itself as a simple test case where an intuitive interpretation of numerical results may be feasible. It is nontrivial since it includes the nonlinear response of the system to parametric driving, and it is fairly generic as it applies to potentials with harmonic minima.

Under the equation of motion (2), the individual samples ϱ_ξ remain Gaussian for Gaussian initial states. This allows us to rephrase the equation of motion (2) as a system of ordinary stochastic differential equations for the first and second cumulants (means and variances) associated with ϱ_ξ, i.e., $\langle q\rangle_c$, $\langle p\rangle_c$, $\langle q^2\rangle_c$, $\langle p^2\rangle_c$, and $\langle\frac{1}{2}(qp + pq)\rangle_c$. A similar consideration holds for the costate dynamics (4) if a maximal overlap with a Gaussian target state is chosen as optimization objective, i.e., $M = 1 - A$, where $A = |\alpha\rangle\langle\alpha|$ projects onto a coherent state. We thus obtain closed equations of motion for the first two cumulants in the propagation of both the state $\varrho_\xi(t)$ and the costate $\Lambda_\xi(t)$. While the effect of the linear control $F(t)$ alone is given by linear response theory, the dynamical squeezing through a time-dependent $\Delta(t)$ leads to nontrivial dynamics, as does the combined action of both controls. We have explored these effects numerically, computing the expectation values in Eq. (5) explicitly through a large number of samples

 Copyright American Physical Society

(typically 10^4). This has the advantage of being securely based on first principles, without resorting to approximations of the dynamics.

In the following, we use natural units ($\hbar = k_B = 1$, units ω_0 for energies, angular frequencies, or rates, $1/\sqrt{m\omega_0}$ for lengths, and $\sqrt{m\omega_0}$ for momenta). We choose a minimal-uncertainty wave packet centered around $q = 1$ and $p = 0$ as both initial and target state. Values of the temperature and the damping constant are chosen in the range typical of superconducting solid-state devices [2]. The propagation time $T = 20$ is roughly comparable to the relaxation time in the examples to be discussed.

We compare the results of iteratively determined control fields for three types of dynamics inserted for state and costate in Eq. (5): (a) SLN dynamics; (b) the standard Markovian master equation of the harmonic oscillator [23], with the usual raising and lowering operators associated with H_s as Lindblad operators; (c) quantum dynamics without dissipation.

Figures 1 and 2 show time-frequency signatures of the controls $F(t)$ and $\Delta(t)$ obtained through the windowed Fourier transform (also short-time Fourier transform, STFT) using a Gaussian window. Both controls show marked differences between the SLN and RWA cases. The tendency for more pronounced and more complex high-frequency features in the SLN case indicates the importance of exercising control also on time scales of the environmental fluctuations (of order β), similar to a known strong-field approach to the suppression of decoherence known as ''bang-bang control'' [24]. A second tendency seen in the SLN results is the application of fields spread out over the entire time interval, as compared to the emphasis on a stronger initial perturbation in the cases of RWA dissipation or no dissipation.

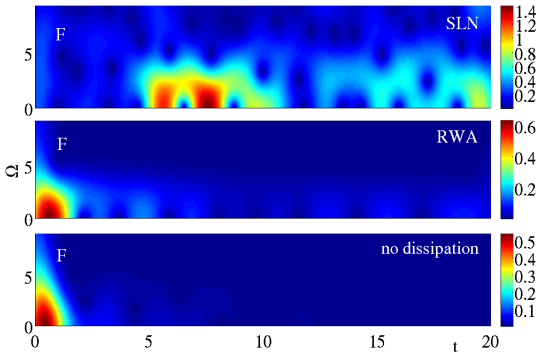

FIG. 1 (color online). Windowed Fourier transform of the optimal control force $F(t)$ obtained using different dynamical equations: (a) SLN equation (2), SLN, (b) a simple generalization of the standard master equation to driven systems, RWA, and (c) unitary propagation. Parameters are $\gamma_0 = 0.05$, $\omega_c = 50$, $\beta = 1$.

Values of the objective functional achieved with the SLN fields for different temperatures and damping constants are compared in Table I. Free dynamics (no control) would result in values roughly equal to $1/2$ for all parameters listed. A test of the control fields obtained in RWA, inserted in the exact equation of motion, typically yields values of the objective functional which are up to 100% larger than for controls computed using SLN dynamics. The algorithmic property of monotonic convergence is confirmed by our numerical results.

Dynamical cooling.—Optimal control for closed systems conserves entropy like any unitary time evolution. Quantum dissipation invariably creates mixed states in the subsystem of interest; i.e., if the initial state is pure the entropy of the open system will increase. But can optimal control of an open system prevent this or even lower the entropy in other cases? To investigate this question, we choose the oscillator ground state as target and prepare both system and environment as thermal states with equal inverse temperature $\beta = 1$. In this symmetric setting, the field $F(t)$ is not needed, since it changes the position, but not the shape of the wave packet. We therefore consider only the control field $\Delta(t)$ in the following. The von Neumann entropy of the mixed state is given by [25] $S(\varrho) = g(\sqrt{\langle q^2\rangle_c\langle p^2\rangle_c - \langle pq + qp\rangle_c^2/4})$ with $g(x) = (x + \frac{1}{2})\log(x + \frac{1}{2}) - (x - \frac{1}{2})\log(x - \frac{1}{2})$. We thus obtain the counterintuitive result that a time-dependent control field can modify dissipative dynamics to the point where its entropy change turns negative (Fig. 3). We attribute this phenomenon to the cooperative effect of driving and dissipation, since neither of the two alone can cause this. The subsystem energy of the final state decreases below its original thermal value, indicating a dynamical cooling effect. In contrast, it can be shown (see Supplemental Material [15]) that commonly used RWA methods predict heating above the environmental temperature for nonzero driving. Consistent corrections of master equations for

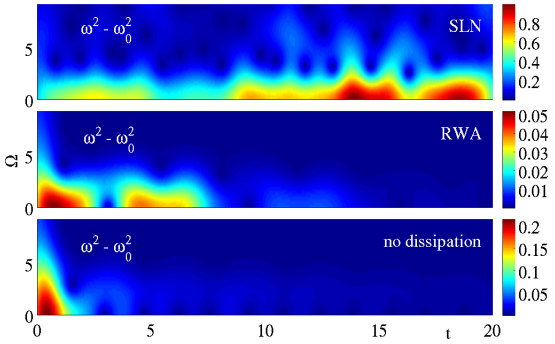

FIG. 2 (color online). Windowed Fourier transform of the optimal tuning field $\Delta = \omega^2 - \omega_0^2$ obtained using dynamical equations as in Fig. 1. Different color scales apply to the three scenarios.

Copyright American Physical Society

TABLE I. Results for the minimization of $\mathrm{tr}\{M\rho(T)\}$ for various inverse temperatures β and different damping constants γ_0 in the range typical of mesoscopic quantum circuits or condensed-phase chemical reactions.

$\beta\backslash\gamma_0$	0.005	0.01	0.05
0.5	0.1036	0.1582	0.3351
1.0	0.0477	0.0688	0.1432
5.0	0.0059	0.0109	0.0245
50.0	0.0037	0.0072	0.0133

finite H_c prove to be a formidable challenge [11]. Moreover, even if H_c could be used in the construction of the dissipator, the distinction between co- and counter-rotating terms would hardly be justified. If the control fields change on the time scale of the reservoir fluctuations, a ''wobbly frame'' rather than a rotating frame results.

In contrast to recent proposals for quantum refrigerators [26,27], which rely on intricate band or level structures, we have chosen a model with minimal structure. The cooling effect found here seems to be a feature of temporal patterns, not of a specifically designed system. We also note that no internal degree of freedom is needed for the effect to occur.

Conclusions.—The present SLN approach to optimal control enjoys two natural advantages compared to control theory based on standard Markovian master equations: (i) its noise statistics are by construction independent of the quantum dynamics, i.e., strong external driving introduces no need for correction terms, and (ii) one arrives at the usual state-costate picture required by OCT methods in a straightforward way. Numerical control of a harmonic degree of freedom is demonstrated with varying parameters and objectives. Most results show marked differences compared to the RWA approach, where the influence of driving on dissipation is neglected. Efficient computations are feasible for environmental couplings from weak damping up to a quality factor as low as $Q \approx 10$. This allows applications to solid-state devices such as superconducting circuits with Josephson junctions and condensed-matter phenomena such as reactive dynamics of small molecules in a solvent or on a surface. Optimal control of a dissipative quantum system can extract entropy from a system initially at the same temperature as its environment. Dynamical cooling in a simple system without special structural features may be considered as a likely strategy for mesoscopic quantum refrigeration.

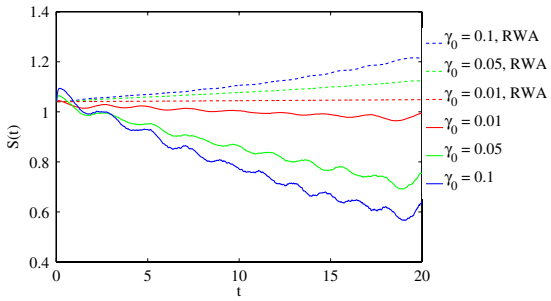

FIG. 3 (color online). An open quantum system initially equilibrated with its surroundings loses entropy S under an optimized control field (solid). In contrast, the standard Markovian/RWA master equation leads to increased entropy under driving (dashed, see [15]).

We gratefully acknowledge helpful conversations with S. Montangero and M. Murphy as well as financial support from Land Baden-Württemberg, DFG (SFB569, SFB/TRR21), EU (Marie Curie FP7-IEF, AQUTE, DIAMANT, PICC), and Ulm University/UUG.

[1] P. Treutlein *et al.*, Phys. Rev. Lett. **92**, 203005 (2004).
[2] G. Ithier *et al.*, Phys. Rev. B **72**, 134519 (2005).
[3] S. Montangero, T. Calarco, and R. Fazio, Phys. Rev. Lett. **99**, 170501 (2007).
[4] C. M. Tesch and R. de Vivie-Riedle, Phys. Rev. Lett. **89**, 157901 (2002).
[5] A. Spörl *et al.*, Phys. Rev. A **75**, 012302 (2007).
[6] R. Nigmatullin and S. G. Schirmer, New J. Phys. **11**, 105032 (2009).
[7] J. P. Palao and R. Kosloff, Phys. Rev. Lett. **89**, 188301 (2002).
[8] T. Schulte-Herbrüggen, A. Spörl, N. Khaneja, and S. J. Glaser, Phys. Rev. A **72**, 042331 (2005).
[9] P. Treutlein, T. W. Hänsch, J. Reichel, A. Negretti, M. A. Cirone, and T. Calarco, Phys. Rev. A **74**, 022312 (2006).
[10] A. G. Kofman and G. Kurizki, Phys. Rev. Lett. **93**, 130406 (2004).
[11] R. Xu, Y. Yan, Y. Ohtsuki, Y. Fujimura, and H. Rabitz, J. Chem. Phys. **120**, 6600 (2004).
[12] J. T. Stockburger and H. Grabert, Phys. Rev. Lett. **88**, 170407 (2002); J. T. Stockburger, Chem. Phys. **296**, 159 (2004).
[13] W. Koch, F. Großmann, J. T. Stockburger, and J. Ankerhold, Phys. Rev. Lett. **100**, 230402 (2008).
[14] See Eq. (4) and preceding paragraph.
[15] See Supplemental Material at http://link.aps.org/supplemental/10.1103/PhysRevLett.107.130404 for details on our OCT approach and a comparison with standard RWA methods.
[16] U. Weiss, *Quantum Dissipative Systems* (World Scientific, Singapore, 2008), 3rd ed..
[17] Y. Tanimura, J. Phys. Soc. Jpn. **75**, 082001 (2006).
[18] J. T. Stockburger and C. H. Mak, J. Chem. Phys. **110**, 4983 (1999).
[19] P. Rebentrost *et al.*, Phys. Rev. Lett. **102**, 090401 (2009); T. Schulte-Herbrüggen *et al.*, J. Phys. B **44**, 154013 (2011).
[20] A. O. Caldeira and A. J. Leggett, Physica (Amsterdam) **121A**, 587 (1983).
[21] V. F. Krotov, *Global Methods in Optimal Control Theory* (Marcel Dekker, New York, 1996).

 Copyright American Physical Society

[22] S. E. Sklarz and D. J. Tannor, Phys. Rev. A **66**, 053619 (2002).
[23] H.-P. Breuer and F. Petruccione, *The Theory of Open Quantum Systems* (Oxford University Press, Oxford, 2002).
[24] L. Viola and S. Lloyd, Phys. Rev. A **58**, 2733 (1998).
[25] A. S. Holevo, M. Sohma, and O. Hirota, Phys. Rev. A **59**, 1820 (1999).
[26] J. P. Pekola and F. W. J. Hekking, Phys. Rev. Lett. **98**, 210604 (2007).
[27] M. Rey, M. Strass, S. Kohler, P. Hänggi, and F. Sols, Phys. Rev. B **76**, 085337 (2007).

Copyright American Physical Society

EPAPS for "Optimal control of open quantum systems: cooperative effects of driving and dissipation"

R. Schmidt,[1] A. Negretti,[2] J. Ankerhold,[1] T. Calarco,[2] and J. T. Stockburger[1]

[1]*Institut für Theoretische Physik, Universität Ulm, Albert-Einstein-Allee 11, 89069 Ulm, Germany.*

[2]*Institut für Quanteninformationsverarbeitung, Universität Ulm, Albert-Einstein-Allee 11, 89069 Ulm, Germany.*

This document serves as a supplement to our article "Optimal control of open quantum systems: cooperative effects of driving and dissipation" [Physical Review Letters (2011)]. It describes the numerical algorithm used, a generalization of the Krotov iterative algorithm to open quantum systems evolving under a stochastic equation of motion. A comparison with the Markovian dynamics of a commonly used quantum master equation shows that the latter cannot reproduce the cooperative cooling effect described in the main text.

I. OBJECTIVE AND CONSTRAINT

We outline a modification of Krotov's algorithm for the optimization of final-state properties of an open quantum system governed by the stochastic differential equation

$$\dot{\hat{\varrho}}_\xi(t) = \hat{\mathfrak{L}}\hat{\varrho}_\xi(t) := -\frac{i}{\hbar}[\hat{H}_\mathrm{s}, \hat{\varrho}_\xi(t)] - \frac{i}{\hbar}[\hat{H}_\mathrm{c}(t), \hat{\varrho}_\xi(t)] - \frac{i}{2\hbar}\gamma_0[\hat{q}, \{\hat{p}, \hat{\varrho}_\xi(t)\}] + \frac{i}{\hbar}\xi(t)[\hat{q}, \hat{\varrho}_\xi(t)]\,, \qquad (1)$$

which must be considered as a dynamical constraint in the context of the optimization problem. Here γ_0 is the damping rate of a Brownian particle in the (ohmic) environment, and $\xi(t)$ is a noise variable whose statistics are governed by the quantum correlation function of the environmental fluctuations.

The objective functionals to be minimized is assumed to depend linearly on the terminal state, i.e., the functional is the expectation value of an observable $\hat{M}$ at the final time T, typically a projection operator. The physical terminal state $\hat{\varrho}(T)$ is the stochastic average of the dynamical state $\hat{\varrho}_\xi(T)$, i. e., the objective functional is of the form

$$\mathsf{B}[\mathbf{u}(t)] = \mathrm{tr}\{\hat{M}\hat{\varrho}(T)\} = \mathbb{E}[\mathrm{tr}\{\hat{M}\hat{\varrho}_\xi(T)\}] \qquad (2)$$

where the vector $\mathbf{u}(t)$ denotes control fields which define the time-dependence of $\hat{H}_\mathrm{c}(t)$, and the first equality implies the equation of motion (1). We use the symbol $\mathbb{E}$ for the expectation value with respect to the noise $\xi(t)$ only, not for the further average given by tracing over $\hat{\varrho}_\xi(t)$.

Copyright American Physical Society

II. EXTENDED OBJECTIVE FUNCTIONAL AND OPTIMAL CONTROL EQUATIONS

Following Refs. [20, 21] (see main text), we use an extended objective functional

$$\mathsf{L}_\xi[\mathbf{u}(t), \hat{\varrho}_\xi(t); \phi_\xi] := \mathsf{G}_\xi(\hat{\varrho}_\xi(T)) - \int_0^T \mathrm{d}t\, \mathsf{R}_\xi(t, \mathbf{u}(t), \hat{\varrho}_\xi(t)) - \phi_\xi(0, \hat{\varrho}_\xi(0)), \tag{3}$$

containing the auxiliary, real-valued function $\phi_\xi(t, \hat{\varrho}_\xi(t))$, which depends on the time t, the noise realization $\xi(t)$, and the state sample $\hat{\varrho}_\xi(t)$. Further auxiliary functions

$$\mathsf{G}_\xi(\hat{\varrho}_\xi(T)) := \mathrm{tr}\{\hat{M}\hat{\varrho}_\xi(T)\} + \phi_\xi(T, \hat{\varrho}_\xi(T)), \tag{4}$$

$$\mathsf{K}_\xi(t, \mathbf{u}(t), \hat{\varrho}_\xi(t), \,\cdot\,) := \mathrm{tr}\{\,\cdot\,\hat{\mathfrak{L}}\hat{\varrho}_\xi(t)\}, \tag{5}$$

$$\mathsf{R}_\xi(t, \mathbf{u}(t), \hat{\varrho}_\xi(t)) := \mathsf{K}_\xi\left(t, \mathbf{u}(t), \hat{\varrho}_\xi(t), \frac{\partial}{\partial\hat{\varrho}_\xi}\phi_\xi(t, \hat{\varrho}_\xi(t))\right) + \frac{\partial}{\partial t}\phi_\xi(t, \hat{\varrho}_\xi(t)) \tag{6}$$

are chosen such that the expectation value $\mathbb{E}[\mathsf{L}_\xi]$ of the extended functional coincides with the ordinary objective functional for *admissible processes*, i. e., pairs $(\mathbf{u}(t), \{\hat{\varrho}_\xi(t)\})$ of a vector of control fields and a stochastic ensemble $\{\hat{\varrho}_\xi(t)\}$ with the property that the equation of motion (1) is obeyed for the given vector $\mathbf{u}(t)$ and for all noise realizations of $\xi(t)$. In this case the partial derivatives in the definition of R_ξ combine to form a total derivative, effectively canceling the boundary terms of ϕ_ξ, contained in Eqs. (3) and (4).

Different choices of ϕ_ξ modify the objective functional for non-admissible processes, such as the combination of control fields and states from different iterations. For Krotov's algorithm it is necessary to choose a function ϕ_ξ with the following property: For any admissible process, L_ξ is at a *maximum* with respect to variations of $\hat{\varrho}_\xi$ with the function $\mathbf{u}(t)$ kept fixed, i. e., variations away from the submanifold of admissible processes decrease L_ξ. This means that an appropriate choice of ϕ_ξ must conform to the two conditions

$$\mathsf{G}_\xi(\hat{\varrho}_\xi^{(j)}(T)) = \max_{\hat{\varrho}_\xi}\{\mathsf{G}_\xi(\hat{\varrho}_\xi(T))\}, \tag{7}$$

$$\mathsf{R}_\xi(t, \mathbf{u}^{(j)}(t), \hat{\varrho}_\xi^{(j)}(t)) = \min_{\hat{\varrho}_\xi}\{\mathsf{R}_\xi(t, \mathbf{u}^{(j)}(t), \hat{\varrho}_\xi(t))\}, \tag{8}$$

where the superscript (j) denotes the admissible process resulting from an initial guess or a previous iteration.

After making such a choice of $\phi_\xi^{(j)}$, we demand that, in addition to being admissible, the new process $(\mathbf{u}^{(j+1)}(t), \{\hat{\varrho}_\xi^{(j+1)}(t)\})$ is taken from the class of pairs $(\tilde{\mathbf{u}}(t), \{\tilde{\varrho}_\xi(t)\})$ which fulfill the condition

$$\tilde{\mathbf{u}}(t) = \arg\max_{\mathbf{u}(t)} \mathbb{E}\left[\mathsf{R}_\xi(t, \mathbf{u}(t), \tilde{\varrho}_\xi(t))\right] \tag{9}$$

Copyright American Physical Society

at any time t. This condition selects a specific pair $(\mathbf{u}^{(j+1)}(t), \{\hat{\varrho}_\xi^{(j+1)}(t)\})$ from the set of admissible process. Using Eq. (9), the update $\mathbf{u}^{(j)}(t) \to \mathbf{u}^{(j+1)}(t)$ can be performed locally in conjunction with the propagation of the new state $\hat{\varrho}_\xi^{(j+1)}(t)$ since the dependence of the dynamical state on the control fields obeys causality.

What remains to be specified is a mathematical construction which defines specific computational steps using the function ϕ_ξ. For the linear dynamics of Eq. (1), it turns out that the function $\phi_\xi(t, \hat{\varrho}_\xi)$ appears in the conditions (7) and (8) only in form of its derivative with respect to the state, and since a complete derivative can be formed from them, the *co-state* $\hat{\Lambda}_\xi = \partial\phi_\xi/\partial\hat{\varrho}_\xi$ can be characterized as an additional dynamical variable with the equation of motion

$$\dot{\hat{\Lambda}}_\xi(t) = -\hat{\mathfrak{L}}^\dagger\hat{\Lambda}_\xi(t) = -\frac{i}{\hbar}[\hat{H}_\mathrm{s}, \hat{\Lambda}_\xi(t)] - \frac{i}{\hbar}[\hat{H}_\mathrm{c}(t), \hat{\Lambda}_\xi(t)] - \frac{i}{2\hbar}\gamma_0\{\hat{p}, [\hat{q}, \hat{\Lambda}_\xi(t)]\} + \frac{i}{\hbar}\xi(t)[\hat{q}, \hat{\Lambda}_\xi(t)]. \quad (10)$$

Solving this equation with the end-time boundary condition $\hat{\Lambda}_\xi(T) + \hat{M} = 0$, resulting from (7), amounts to a (fully sufficient) construction of ϕ_ξ to first order in variations of $\hat{\varrho}_\xi$ around $\hat{\varrho}_\xi^{(j)}$.

In a variant of the algorithm, described by Sklarz and Tannor [21], the implicit condition (9) is substituted by an explicit form

$$u_k^{(j+1)}(t) = u_k^{(j)}(t) + \frac{1}{\lambda_k(t)}\mathbb{E}\left[\mathrm{tr}\left\{\hat{\Lambda}_\xi^{(j)}(t)\frac{\partial\hat{\mathfrak{L}}}{\partial u_k}\hat{\varrho}_\xi^{(j+1)}(t)\right\}\right], \quad (11)$$

which is equivalent to Eq. (9) if a suitable (j-dependent) cost functional is added to B. It is to be noted that the simultaneous appearance of j and $j+1$ on the r.h.s. of this equation gives this update law properties quite different from a simple gradient search. The functions $\lambda_k(t)$ arising from this cost functional may be adjusted to tune convergence properties. In summary, the algorithm works as follows:

1. An initial guess for the control fields $\mathbf{u}^{(0)}(t)$ is chosen.

2. The equation of motion (1) with $\mathbf{u}^{(0)}(t)$ is solved with initial condition $\hat{\varrho}(0)$ for an ensemble of trajectories $\{\hat{\varrho}_\xi(t)\}$.

3. The co-state ensemble is initialized using the condition $\hat{\Lambda}_\xi(T) + \hat{M} = 0$ and then propagated backwards to the initial time with Eq. (10).

4. The ensembles $\{\hat{\varrho}_\xi(t)\}$ and $\{\hat{\Lambda}_\xi(t)\}$ are propagated forward until the end time T, but at each time step the co-states are propagated with the old control fields, that is, the ones obtained from the j-th iteration, whereas the states $\hat{\varrho}_\xi(t)$ are propagated with the new control fields given by the update law (11). (Alternatively, stored values from step 3 can be used).

Copyright American Physical Society

5. The objective functional (2) is computed, and steps 3 and 4 are repeated until the value of objective functional is in the desired range.

This optimization algorithm applies not only to Eq. (1), but to any type of linear dynamics subject to additive or multiplicative noise.

III. PROOF OF MONOTONIC CONVERGENCE

The procedure outlined above guarantees that each step of the iteration reduces the objective functional, that is, $\mathbb{E}[\mathsf{B}_\xi[\mathbf{u}^{(j+1)}(t), \hat{\varrho}_\xi^{(j+1)}(t)]] \leq \mathbb{E}[\mathsf{B}_\xi[\mathbf{u}^{(j)}(t), \hat{\varrho}_\xi^{(j)}(t)]]$. This becomes evident if the change of the objective functional is decomposed into three terms,

$$\mathbb{E}[\mathsf{L}_\xi[\mathbf{u}^{(j)}(t), \hat{\varrho}_\xi^{(j)}(t), \phi_\xi]] - \mathbb{E}[\mathsf{L}_\xi[\mathbf{u}^{(j+1)}(t), \hat{\varrho}_\xi^{(j+1)}(t), \phi_\xi]] = \Delta_1 + \Delta_2 + \Delta_3, \tag{12}$$

where

$$\Delta_1 = \int_0^T \mathrm{d}t\, \mathbb{E}\left[\mathsf{R}(t, \mathbf{u}^{(j)}(t), \hat{\varrho}_\xi^{(j+1)}(t)) - \mathsf{R}(t, \mathbf{u}^{(j)}(t), \hat{\varrho}_\xi^{(j)}(t))\right] \tag{13}$$

$$\Delta_2 = \int_0^T \mathrm{d}t\, \mathbb{E}\left[\mathsf{R}(t, \mathbf{u}^{(j+1)}(t), \hat{\varrho}_\xi^{(j+1)}(t)) - \mathsf{R}(t, \mathbf{u}^{(j)}(t), \hat{\varrho}_\xi^{(j+1)}(t))\right] \tag{14}$$

$$\Delta_3 = \mathbb{E}\left[\mathsf{G}(\hat{\varrho}_\xi^{(j)}(T)) - \mathsf{G}(\hat{\varrho}_\xi^{(j+1)}(T))\right] \tag{15}$$

Now $\Delta_1 \geq 0$ and $\Delta_3 \geq 0$ follow from Eq. (8) and Eq. (7), respectively, whereas $\Delta_2 \geq 0$ is a property of the update law (9). We have thus demonstrated monotonicity for the modified algorithm, which ensures convergence for an arbitrary initial guess with any objective functional bounded from below.

Recent work by S. Schirmer and P. de Fouquieres [New J. Phys. **13**, 073029 (2011)] points out that proofs of monotonicity for Krotov-type iteration methods are not rigorous if time-discrete approximations are substituted for the dynamics of state and co-state. For all practical purposes, however, the typical benefits of the Krotov method persist, i. e., convergence for a wide range of initial guesses and rapid improvement during the first iteration steps.

IV. DRIVEN DYNAMICS WITH FIXED RWA DISSIPATOR: EFFECTIVE RESERVOIR

For comparison, we study the control problem of the parametrically driven harmonic oscillator, modeling the open system dynamics through a Lindblad Master equation. From a system-reservoir model, this equation results from performing the Born, Markov, and RWA approximations on the

Copyright American Physical Society

system-reservoir interactions. In the dimensionless units introduced in the main text, the Master equation reads

$$\begin{aligned}\frac{d}{dt}\hat{\rho} &= -i[\hat{H}(t),\hat{\rho}] \\ &+ \gamma_0(N_\beta+1)\left(\hat{a}\hat{\rho}\hat{a}^\dagger - \tfrac{1}{2}\{\hat{a}^\dagger\hat{a},\hat{\rho}\}\right) \\ &+ \gamma_0 N_\beta\left(\hat{a}^\dagger\hat{\rho}\hat{a} - \tfrac{1}{2}\{\hat{a}\hat{a}^\dagger,\hat{\rho}\}\right)\end{aligned} \tag{16}$$

with

$$\hat{H}(t) = \hat{a}^\dagger\hat{a} + \frac{1}{2} + \frac{\Delta(t)}{4}(\hat{a}+\hat{a}^\dagger)^2 = \left(1+\frac{\Delta(t)}{2}\right)(\hat{a}^\dagger\hat{a}+\tfrac{1}{2}) + \frac{\Delta(t)}{4}(\hat{a}^2+\hat{a}^{\dagger 2})\,. \tag{17}$$

Following common practice (see, however, Refs. [10, 11]), we have defined the rotating frame of the RWA through the time-independent Hamiltonian $\hat{H}_0 = \hat{a}^\dagger\hat{a} + \frac{1}{2}$, not the full Hamiltonian $\hat{H}(t)$. Accordingly, the dissipative terms of Eq. (16) contain the thermal occupation number $N_\beta = (e^\beta - 1)^{-1}$ of the unperturbed oscillator.

Due to the mismatch between the Hamiltonians of the pre-set rotating frame and of the driven dynamics, oscillatory terms reappear when the dissipative terms are transformed to the interaction picture. In order to show this, we define the interaction picture with respect to $\hat{H}(t)$,

$$\hat{\rho}(t) = \hat{U}(t)\hat{\rho}_{\rm I}(t)\hat{U}^\dagger(t)\,,\quad \dot{\hat{U}} = i\hat{H}\hat{U}\,. \tag{18}$$

The Master equation for $\hat{\rho}_{\rm I}$ then reads

$$\begin{aligned}\frac{d}{dt}\hat{\rho}_{\rm I} &= \gamma_0(N_\beta+1)\left(\hat{b}\hat{\rho}_{\rm I}\hat{b}^\dagger - \tfrac{1}{2}\{\hat{b}^\dagger\hat{b},\hat{\rho}_{\rm I}\}\right) \\ &+ \gamma_0 N_\beta\left(\hat{b}^\dagger\hat{\rho}_{\rm I}\hat{b} - \tfrac{1}{2}\{\hat{b}\hat{b}^\dagger,\hat{\rho}_{\rm I}\}\right)\,,\end{aligned} \tag{19}$$

where $\hat{b} = \hat{U}^\dagger\hat{a}\hat{U}$ and its adjoint are time dependent, following the equations of motion

$$\dot{\hat{b}} = -i\left(1+\tfrac{\Delta}{2}\right)\hat{b} - i\tfrac{\Delta}{2}\,\hat{b}^\dagger \tag{20}$$

$$\dot{\hat{b}}^\dagger = i\tfrac{\Delta}{2}\,\hat{b} + i\left(1+\tfrac{\Delta}{2}\right)\hat{b}^\dagger\,. \tag{21}$$

From this, one easily concludes that b is a linear combination of $\hat{a}$ and $\hat{a}^\dagger$ with $[\hat{b},\hat{b}^\dagger] = 1$, i.e., the map $\hat{a}\mapsto\hat{b}$ is a Bogoliubov transformation

$$\hat{b} = e^{i\theta}\cosh y\;\hat{a} + e^{i\varphi}\sinh y\;\hat{a}^\dagger \tag{22}$$

with real (and, in our case, time-dependent) parameters θ, ϕ, and y. Using this equation, we obtain

Copyright American Physical Society

the form

$$\begin{aligned}\frac{d}{dt}\hat{\rho}_{\mathrm{I}} &= \gamma_0(N_\beta+1)\cosh^2 y\left(\hat{a}\hat{\rho}_{\mathrm{I}}\hat{a}^\dagger - \tfrac{1}{2}\{\hat{a}^\dagger\hat{a},\hat{\rho}_{\mathrm{I}}\}\right)\\ &+ \gamma_0(N_\beta+1)\sinh^2 y\left(\hat{a}^\dagger\hat{\rho}_{\mathrm{I}}\hat{a} - \tfrac{1}{2}\{\hat{a}\hat{a}^\dagger,\hat{\rho}_{\mathrm{I}}\}\right)\\ &+ \gamma_0 N_\beta\cosh^2 y\left(\hat{a}^\dagger\hat{\rho}_{\mathrm{I}}\hat{a} - \tfrac{1}{2}\{\hat{a}\hat{a}^\dagger,\hat{\rho}_{\mathrm{I}}\}\right)\\ &+ \gamma_0 N_\beta\sinh^2 y\left(\hat{a}\hat{\rho}_{\mathrm{I}}\hat{a}^\dagger - \tfrac{1}{2}\{\hat{a}^\dagger\hat{a},\hat{\rho}_{\mathrm{I}}\}\right)\\ &+ \gamma_0(2N_\beta+1)\sinh y\cosh y e^{i(\theta-\varphi)}\left(\hat{a}\hat{\rho}_{\mathrm{I}}\hat{a} - \tfrac{1}{2}\{\hat{a}^2,\hat{\rho}_{\mathrm{I}}\}\right)\\ &+ \gamma_0(2N_\beta+1)\sinh y\cosh y e^{-i(\theta-\varphi)}\left(\hat{a}^\dagger\hat{\rho}_{\mathrm{I}}\hat{a}^\dagger - \tfrac{1}{2}\{\hat{a}^{\dagger 2},\hat{\rho}_{\mathrm{I}}\}\right)\end{aligned} \tag{23}$$

for the Master equation, where all of the prefactors depend on time through θ, φ, and y. Typical solutions lead to oscillating prefactors, meaning that Eq. (23) can be further simplified through time coarse graining. This in itself can be seen as evidence that the initial application of the RWA was not consistent. However, coarse-graining at this point is appropriate if one wants to compare the features of the dynamics predicted by Eqs. (16) and (23) with the exact dynamics. The first four terms of Eq. (23) contain functions of time which are squares of real time-dependent functions, therefore they typically dominate the result of the coarse graining procedure. Collecting the dominant terms results in the simplified Master equation

$$\begin{aligned}\frac{d}{dt}\hat{\rho}_{\mathrm{I}} &= \gamma_0(\tilde{N}+1)\left(\hat{a}\hat{\rho}_{\mathrm{I}}\hat{a}^\dagger - \tfrac{1}{2}\{\hat{a}^\dagger\hat{a},\hat{\rho}_{\mathrm{I}}\}\right)\\ &+ \gamma_0\tilde{N}\left(\hat{a}^\dagger\hat{\rho}_{\mathrm{I}}\hat{a} - \tfrac{1}{2}\{\hat{a}\hat{a}^\dagger,\hat{\rho}_{\mathrm{I}}\}\right)\end{aligned} \tag{24}$$

with

$$2\tilde{N}+1 = (2N_\beta+1)\,\overline{\cosh(2y)} \geq 2N_\beta+1\ , \tag{25}$$

where the bar indicates time coarse graining. The immediate interpretation of this result is obvious: Up to a unitary transform, the dynamics of Eqs. (16) and (23) effectively describes relaxation towards a thermal oscillator state with a higher-than-thermal occupation number $\tilde{N}$. This state therefore has a higher entropy than the thermal state obtained by equilibrating without driving. Accordingly, with the dynamics approximated by Eq. (16), optimal control cannot find solutions which push the system entropy below its equilibrium value. This is consistent with our numerical findings, in particular the observation that optimal control based on Eq. (16), with overlap to the ground state as objective, converges to the trivial result $\Delta \equiv 0$. The alluringly simple method of constructing the dissipator based on a Hamiltonian without driving is an oversimplification which fails to reproduce cooperative effects of driving and dissipation, most notably, the cooling effect reported in the main text.

Copyright American Physical Society

7.2.

Title:	Cooling of quantum systems through optimal control and dissipation
Authors:	R. Schmidt, S. Rohrer, J.T. Stockburger and J. Ankerhold
Journal:	Physica Scripta T151, 014034
Year:	2012
Copyright[2]:	IOP Publishing Limited on behalf of the Royal Swedish Academy of Sciences
Online journal:	`http://iopscience.iop.org/1402-4896/2012/T151/014034`

[2]The use of the article in the framework of a PhD thesis is kindly allowed by IOP, according to the assignment of copyright (3.2.2): http://iopscience.iop.org/1402-4896/page/Assignment%20of%20Copyright%20Form.

IOP Publishing Physica Scripta
Phys. Scr. **T151** (2012) 014034 (5pp) doi:10.1088/0031-8949/2012/T151/014034

Cooling of quantum systems through optimal control and dissipation

Rebecca Schmidt, Selina Rohrer, Joachim Ankerhold and Jürgen T Stockburger

Institut für Theoretische Physik, Universität Ulm, Albert Einstein-Allee 11, D-89069 Ulm, Germany

E-mail: rebecca.schmidt@uni-ulm.de

Received 18 May 2012
Accepted for publication 27 June 2012
Published 30 November 2012
Online at stacks.iop.org/PhysScr/T151/014034

Abstract
Based on an exact non-Markovian open systems quantum dynamics, we demonstrate how to reduce the entropy of an open system through a cooperative effect of driving and dissipation. We illustrate the controlled dynamics in phase space in terms of Wigner functions and discuss the applicability of approximate approaches using master equations.

PACS numbers: 03.65.Yz, 02.30.Yy, 03.67.−a, 05.70.Ln

(Some figures may appear in color only in the online journal)

1. Introduction

Coherent control of quantum dynamics is a powerful tool for driving a system toward desired states and to optimize the properties of the dynamics. Mature numerical methods exist for the control of non-dissipative dynamics [1–5]. Similar approaches to open quantum systems are urgently needed and are evolving rapidly [6–8]. However, particular care is needed in this case, for which commonly used equations of motion are approximate. Strong driving does not only have an impact on the system, but also the interaction between the control-modified system and the reservoir differs substantially from the case of autonomous dynamics. This basically calls Markovian and perturbative approaches into question. Instead of relying on these approaches, we propagate the quantum system using a fully non-Markovian, exact stochastic Liouville–von Neumann equation [9]. Uniting this approach with optimal control theory allows the consideration of control signals of arbitrary strength and complexity [10].

2. Method

In order to derive the exact dynamics, we describe the driven open system by a Hamiltonian of the form

$$H = H_0 + H_C + H_I + H_R, \tag{1}$$

where the individual terms are defined as follows: the system Hamiltonian H_0 governs the autonomous dynamics of the system, which we assume to be characterized by a position q and a momentum p, or equivalent conjugate variables, such as phase and charge in a mesoscopic circuit. The control Hamiltonian $H_C = H_C(\mathbf{u}(t))$ describes the modification of this dynamics through classical controls $\mathbf{u}(t)$, typically fields assumed to be acting on the system only. The vector-valued function $\mathbf{u}(t)$ is the *independent quantity* to be varied in the control problem. The term H_I denotes the Hamiltonian of the system–reservoir interaction, and H_R is the Hamiltonian governing the autonomous dynamics of the reservoir. As shown by Caldeira and Leggett [11], any reservoir with Gaussian fluctuations can be modeled by a set of harmonic oscillators,

$$H_I + H_R = \sum_i \frac{p_i^2}{2m_i} + \frac{m_i\omega_i^2}{2}\left(x_i - \frac{c_i}{m_i\omega_i^2}q\right)^2. \tag{2}$$

Here x_i, p_i, m_i and ω_i are the coordinates and parameters of the respective reservoir mode, q is the coordinate of the system and c_i is the coupling constant of the system and the respective reservoir mode.

An exact expression for the reduced dynamics in closed form requires the path integral formalism [11, 12], which is unsuitable for optimal control theory. However, the *stochastic* equation of motion

$$\dot{\rho}_{v,\xi} = \mathcal{L}\rho_{v,\xi} := -\frac{\mathrm{i}}{\hbar}[H_0 + H_C, \rho_{v,\xi}] + \frac{\mathrm{i}}{\hbar}\xi(t)[q, \rho_{v,\xi}] + \frac{\mathrm{i}}{2}v(t)\{q, \rho_{v,\xi}\}, \tag{3}$$

 © 2012 The Royal Swedish Academy of Sciences Printed in the UK
Copyright Royal Swedish Academy of Sciences

Phys. Scr. **T151** (2012) 014034 R Schmidt *et al*

which can be used in optimal control theory, has been shown to be fully equivalent [9]. The functions $\xi(t)$ and $\nu(t)$ are correlated complex-valued Gaussian stochastic processes [9] exactly matching the fluctuations and the dynamic response of the reservoir as given by the quantum correlation function $L(\tau)$ of the total environmental force,

$$L(t-t') = \left\langle \sum_i c_i x_i(t) \sum_j c_j x_j(t') \right\rangle. \tag{4}$$

Equation (3) introduces the stochastic Liouvillian superoperator $\mathcal{L}$, defined through the second equality. For an environment in thermal equilibrium, $L(t-t')$ is fully determined by the spectral density $J(\omega)$ and the inverse thermal energy β of the reservoir:

$$L(t) = \frac{\hbar}{\pi} \int_0^\infty \mathrm{d}\omega J(\omega) \left(\coth \frac{\hbar\omega\beta}{2} \cos\omega t - \mathrm{i} \sin\omega t \right). \tag{5}$$

The specific properties of the Gaussian processes $\xi(t)$ and $\nu(t)$ are related to $L(t-t')$ as follows:

$$\mathbb{E}\left[\xi(t)\xi(t')\right] = \mathrm{Re}(L(t-t')), \tag{6a}$$

$$\mathbb{E}\left[\xi(t)\nu(t')\right] = 2\frac{\mathrm{i}}{\hbar}\Theta(t-t')\mathrm{Im}(L(t-t')), \tag{6b}$$

$$\mathbb{E}\left[\nu(t)\nu(t')\right] = 0, \tag{6c}$$

$$\mathbb{E}\left[\xi(t)\right] = \mathbb{E}\left[\nu(t)\right] = 0. \tag{6d}$$

For computational purposes, equation (3) is solved multiple times with numerical samples of ξ and ν generated according to equation (6). Averaging over samples yields the physical density matrix

$$\rho = \mathbb{E}\left[\rho_{\nu,\xi}\right], \tag{7}$$

from which any physical observable may be obtained, in particular, the optimization objective.

Based on the exact dynamics we have generalized Krotov's iterative algorithm [13, 14] into a form applicable to equations (3) and (7). Details are provided in [10] (including supplemental material).

The type of objective we are considering is minimizing an expectation value $\langle M \rangle$ of an observable M of the system at a final time t_f (a von Neumann measurement). In the minimization of the corresponding objective functional

$$F[\mathbf{u}(t), \{\rho_{\nu,\xi}\}] = \mathbb{E}\left[\mathrm{tr}\{\mathrm{M}\ \rho_{\nu,\xi}(\mathrm{t_f})\}\right], \tag{8}$$

the equation of motion (3) needs to be introduced as a constraint, valid for any realization of the stochastic variables $\xi(t)$ and $\nu(t)$.

Variational calculus leads to a characterization of local extrema that includes a stochastic equation of motion for the Lagrange multiplier Λ with a *terminal* boundary condition:

$$\dot{\Lambda}_{\nu,\xi}(t) = -\mathcal{L}^\dagger \Lambda_{\nu,\xi}(t), \tag{9a}$$

$$\Lambda_{\nu,\xi}(t_\mathrm{f}) = -M, \tag{9b}$$

where $\mathcal{L}^\dagger$ is the adjoint of the Liouvillian $\mathcal{L}$ (see equation (3)) and $M = -|\alpha\rangle\langle\alpha|$ is defined through a projection operator on a target state $|\alpha\rangle$ at the final time t_f.

The Krotov algorithm relies on the coupled dynamics of the quantum state and a *costate* Λ, which can (for most purposes) be identified with the previously introduced Lagrange multiplier; most importantly, it also obeys the equation of motion (9*a*). The key step of the Krotov algorithm is an iterative update for the control fields, changing the components of the vector $\mathbf{u}(t)$ according to

$$u_i^{(\mathrm{new})}(t) = u_i^{(\mathrm{old})}(t) - \frac{1}{\lambda_i(t)} \times \mathbb{E}\left[\frac{2}{\hbar}\mathrm{Im}\left[\mathrm{tr}\left\{\frac{\partial H_\mathrm{c}}{\partial u_i}\left[\rho_{\nu,\xi}, \Lambda^\dagger_{\nu,\xi}\right]\right\}\right]\right]. \tag{10}$$

Different choices for the function $\lambda_i(t)$ can be made in order to tune the convergence properties of the algorithm [14].

3. Application and results

While coherent control of Hamiltonian dynamics still conserves entropy (a scalar invariant of unitary transformations), open-system dynamics generally brings about a change in entropy. Without external control, this results in thermalization, i.e. a rise in entropy when considering a pure initial state. In the following, we demonstrate that it is possible to *remove* entropy from an open quantum system by applying optimal control fields, without promoting the coupling to a low-temperature reservoir, as is done, e.g., in sideband cooling.

In this context, we look at systems with at most a few bound states thermally accessible, usually well described in the harmonic approximation, with an environment characterized by a spectral density of the form $J(\omega) = \eta\omega/(1+\frac{\omega^2}{\omega_c^2})^2$ with large UV cutoff ω_c, corresponding to Stokes' (or Ohmic) friction with friction constant η in the classical limit. Still, we emphasize that our method is not restricted to harmonic systems. In the following, we use natural units ($\hbar = 1$; $k_\mathrm{B} = 1$). At the initial time $t = 0$, the system is thermalized with the reservoir (inverse thermal energy $\beta = 1$), and a moderate value $\eta = 0.1$ is chosen for the friction constant. The objective is defined by choosing the ground state as the target state $|\alpha\rangle$.

The parametric control

$$H_\mathrm{C}(t) = \frac{\Delta(t)}{2} q^2 \tag{11}$$

is chosen as the simplest time-dependent modification of the potential with non-trivial effects on the dynamics. The single control field $\Delta(t)$ takes the place of $\mathbf{u}(t)$. With a Gaussian initial state, all stochastic samples remain Gaussian over time; therefore, equations (3) and (9*a*) can be replaced by ordinary differential equations for the expectation values of position and momentum and for the matrix elements of the covariance matrix associated with the Wigner function. We emphasize, however, that the more general case of an anharmonic system can be treated on an equal footing. In either case the optimal control dynamics in phase space can be investigated in terms of the Wigner function of the system.

 Copyright Royal Swedish Academy of Sciences

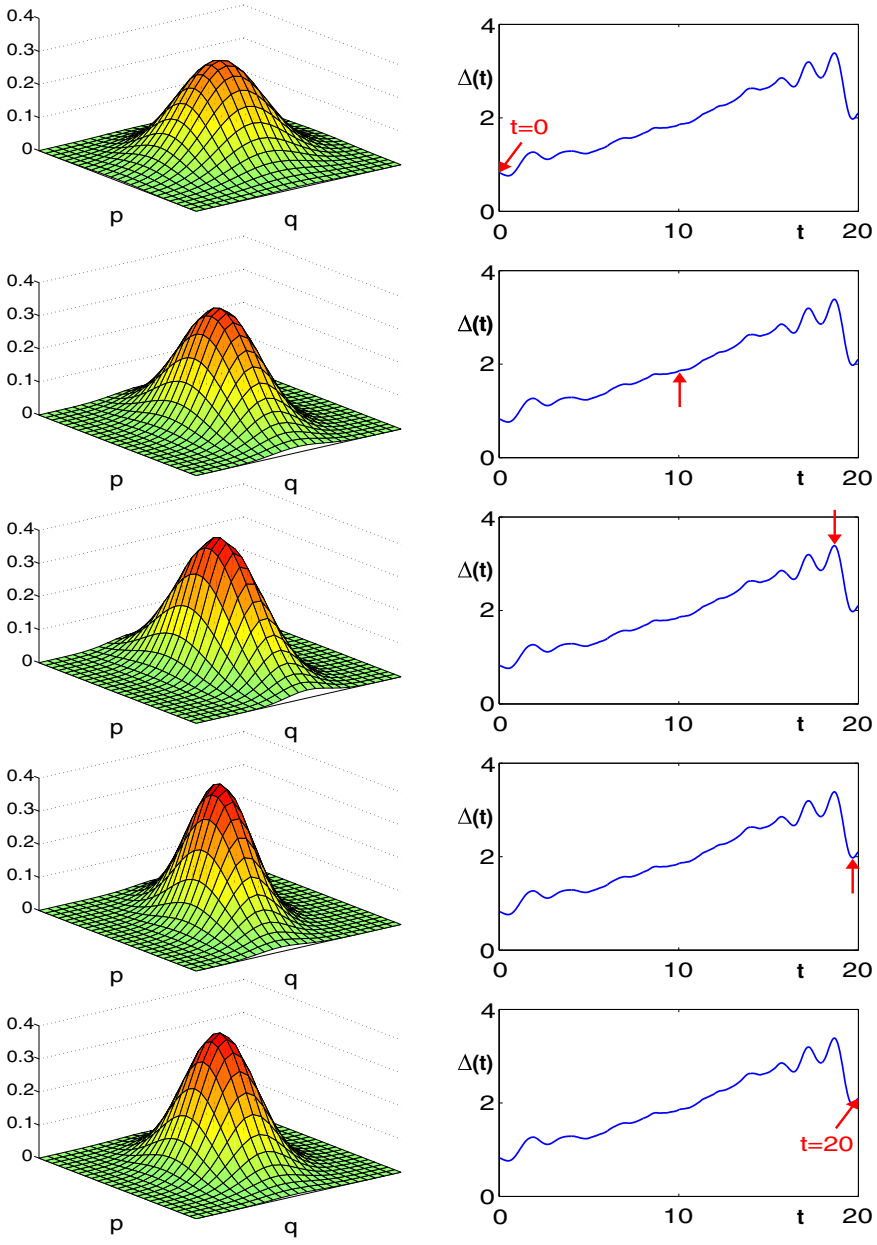

Figure 1. Control of an open quantum system with parametric control: for the time steps $t = 0$, 10, 18.7, 19.7 and 20 each. Left-hand side: the Wigner function; right-hand side: control signal $\Delta(t)$. Parameters: inverse thermal energy of the reservoir: $\beta = 1$; friction constant $\eta = 0.1$.

3.1. The stochastic Liouville–von Neumann equation

In figure 1 we show the time evolution of the Wigner function of the system for the optimal control field obtained from equations (10) and (11). In natural units, the initial Wigner function has rotational symmetry, characteristic of a thermal state, later evolving through various squeezed states. The optimal control solution (figure 1, right) shows two main features: first there is a long ramp-like rise, followed by a steep descent, with virtually no transition. On the other hand, the signal also carries a periodic modulation which, in this case, matches both on the timescale of the original system ($\omega_0 = 1$) and the thermal time $\hbar\beta = 1$. During the gradual rise, the Wigner function gets more and more squeezed in the direction q as the applied control narrows the potential, indicating that the energy added by the work performed is dissipated to the reservoir, also transferring entropy to the environment in the process. The effective temperature of the system, roughly estimated from the level populations and the characteristic energy scale of $H_0 + H_C$, decreases. The rapid

Copyright Royal Swedish Academy of Sciences

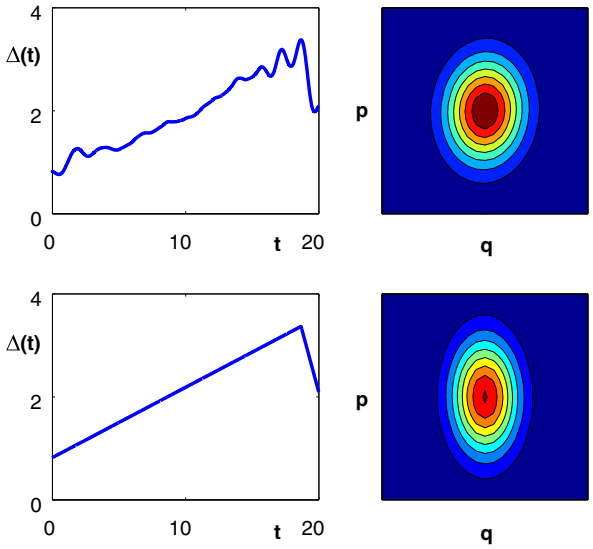

Figure 2. Comparison between the original control signal $\Delta(t)$ (upper left) with the respective contour plot of the Wigner function of the system (upper right) at $t = t_f$ and a simplification of the control signal (lower left) with the respective contour plot of the Wigner function of the system (lower right) at $t = t_f$. While achieving comparable overlap with the objective, the simplified control fails to reduce the squeezing of intermediate states.

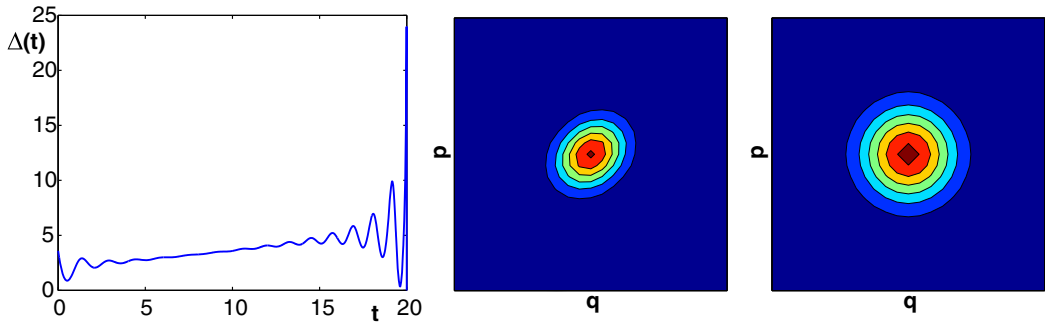

Figure 3. Results of optimal control with a classical Caldeira–Leggett master equation: the computed control signal $\Delta(t)$ (left-hand side) carries the main features of the control signals of the quantum treatment. The Wigner function of the classical dynamics shows cooling (middle), but violates the uncertainty relation: the ground state (right-hand side) covers a larger area in phase space.

decrease of the control toward the end of the propagation is fast enough to preserve this cooling effect (i.e. to prevent the full re-thermalization of the energy levels). In addition, the small modulations visible in the numerically determined optimal control serve to drive the squeezed state back toward a state again isotropic in phase space.

In figure 2 we compared our optimal control signal with a simplified one lacking the oscillatory parts, approximating the numerical solution by two linear ramps. This simplified signal, while also achieving a significant overlap with the ground state, results in a Wigner function that is much less isotropic. One might be interested in replacing the exact but computationally expensive equation of motion, equation (3), with simpler approaches to the dynamics. The consequences will be outlined in the following section.

3.2. The quantum optical master equation

Surprisingly, the quantum optical master equation, one of the standard approaches to the dynamics of open quantum systems, fails to account for the cooling effect described above. Since the level structure of the time-independent Hamiltonian H_0 is, so to speak, 'hard-coded' into the dissipative terms, these terms describe relaxation toward the canonical ensemble, $\rho = Z^{-1}\exp(-\beta H_0)$ even for strong changes to the potential. Using the system Hamiltonian $H_0 + H_C$ and standard Lindblad operators (obtained solely from H_0) cannot reproduce the cooling effect. The fact that the resulting solutions always describe heating, never cooling [10], underscores the inconsistency of this approach.

3.3. The Caldeira–Leggett master equation

The shortcomings of the quantum optical master equation are related to the inapplicability of the Born–Markov approximation and the rotating-wave approximation in their conventional form. One attempt to circumvent this difficulty while maintaining the simplicity of a master equation is the

 Copyright Royal Swedish Academy of Sciences

use of the Caldeira–Leggett master equation [11]

$$\frac{\mathrm{d}}{\mathrm{d}t}\rho = -\frac{\mathrm{i}}{\hbar}[H_0, \rho] - \frac{\mathrm{i}\eta}{2m\hbar}[q, \{p, \rho\}] - \frac{\eta}{\hbar^2\beta}[q, [q, \rho]]. \quad (12)$$

This approach replaces the Born–Markov approximation (separation of time scales between environmental fluctuations and relaxation) with a stronger Markovian approximation, assuming the decay of environmental fluctuations to be virtually instantaneous compared to any other time scale of the dynamics. It does not rely on the rotating-wave approximation.

In figure 3 we show the optimal control solution obtained through the Caldeira–Leggett master equation. The resulting control signal shows some qualitative features of the one calculated without approximations. Again, there is a gradual rise of the control signal, superimposed with oscillations of increasing amplitude. However, the growth of this amplitude is much stronger than in the exact dynamics, and the final drop in the signal is virtually instantaneous. This indicates that the Markovian approximation of the dynamics reproduces the essence of the effect, but overestimates the effectiveness of high-frequency components in the control signal. The final states shown on the rhs of figure 3 also show that the Caldeira–Leggett master equation tends to overstate the effect: the predicted phase-space density is concentrated in a *smaller* area than that of the ground state. In retrospect, this misfeature is less than surprising: when equation (12) is translated into an equation of motion for the Wigner function, the special case of a harmonic potential yields a result identical to the classical Klein–Kramers equation. The quantum mechanical zero-point motion is missing from this picture. This anomalous result is also closely related to the previous observation that the Caldeira–Leggett master equation violates positivity [15]. Reliable results can be expected of the Caldeira–Leggett master equation only for temperatures far above the range of interest for the cooling effect considered here.

However, the observation that cooling can be observed in classical dynamics as well is interesting in itself. Preliminary results indicate that both Markovian and non-Markovian classical dynamics allow cooling through optimal control.

4. Outlook

Controlling an open quantum system not only changes the dynamics of the system but has an equally important indirect impact on mechanisms of dissipation. We demonstrate that driving can partly reverse the natural heat flow of a reservoir to a system as a drastic manifestation. This opens the door to a rigorous treatment of non-equilibrium mesoscopic heat engines.

Acknowledgments

We thank Tommaso Calarco and Antonio Negretti for valuable contributions to earlier stages of this project. Financial support was provided by Landesgraduiertenstiftung Baden-Württemberg and Deutsche Forschungsgemeinschaft (AN 336/6-1).

References

[1] Montangero S, Calarco T and Fazio R 2007 Robust optimal quantum gates for Josephson charge qubits *Phys. Rev. Lett.* **99** 170501
[2] Tesch C M and de Vivie-Riedle R 2002 Quantum computation with vibrationally excited molecules *Phys. Rev. Lett.* **89** 157901
[3] Spörl A, Schulte-Herbrüggen T, Glaser S J, Bergholm V, Storcz M J, Ferber J and Wilhelm F K 2007 Optimal control of coupled Josephson qubits *Phys. Rev.* A **75** 012302
[4] Nigmatullin R and Schirmer S G 2009 Implementation of fault-tolerant quantum logic gates via optimal control *New J. Phys.* **11** 105032
[5] Palao J P and Kosloff R 2002 Quantum computing by an optimal control algorithm for unitary transformations *Phys. Rev. Lett.* **89** 188301
[6] Treutlein P, Hänsch T W, Reichel J, Negretti A, Cirone M A and Calarco T 2006 Microwave potentials and optimal control for robust quantum gates on an atom chip *Phys. Rev.* A **74** 022312
[7] Kofman A G and Kurizki G 2004 Unified theory of dynamically suppressed qubit decoherence in thermal baths *Phys. Rev. Lett.* **93** 130406
[8] Xu R X, Yan Y J, Ohtsuki Y, Fujimura Y and Rabitz H 2004 Optimal control of quantum non-Markovian dissipation: reduced Liouville-space theory *J. Chem. Phys.* **120** 6600
[9] Stockburger J T and Grabert H 2002 Exact *c*-number representation of non-Markovian quantum dissipation *Phys. Rev. Lett.* **88** 170407
[10] Schmidt R, Negretti A, Ankerhold J, Calarco T and Stockburger J T 2011 Optimal control of open quantum systems: cooperative effects of driving and dissipation *Phys. Rev. Lett.* **107** 130404
[11] Caldeira A O and Leggett A J 1983 Path integral approach to quantum Brownian motion *Physica* A **121** 587
[12] Feynman R P and Vernon F L Jr 1963 The theory of a general quantum system interacting with a linear dissipative system *Ann. Phys.* **24** 118
[13] Krotov V F 1996 Global methods in optimal control theory *Pure and Applied Mathematics* (New York: Dekker)
[14] Sklarz S E and Tannor D J 2004 Optimal control of quantum dissipative dynamics: analytic solution for cooling the three-level λ system *Phys. Rev.* A **69** 53408
[15] Vacchini B 2000 Completely positive quantum dissipation *Phys. Rev. Lett.* **84** 1374

Copyright Royal Swedish Academy of Sciences

7.3.

Title:	Quasi-local generation of EPR entanglement in non-equilibrium
Authors:	R. Schmidt, J.T. Stockburger, and J. Ankerhold
Journal:	arXiv:1305.6566 [quant-ph]
Year:	2013
Copyright[3]:	see footnote

[3]Meanwhile, a modified version of the article has been published in Phys. Rev. A**88**, 052321 (2013), the copyright have been transferred to APS. The use of articles in the framework of a PhD thesis is kindly allowed by APS, according to the copyright policies of APS: http://publish.aps.org/copyrightFAQ.html.

Quasi-local generation of EPR entanglement in non-equilibrium

Rebecca Schmidt,* Jürgen T. Stockburger, and Joachim Ankerhold
Institut für Theoretische Physik, Universität Ulm, Albert Einstein-Allee 11, 89069 Ulm, Germany
(Dated: May 28, 2013)

The generation of entanglement is studied in a minimal model consisting of two independent Gaussian parties embedded in a common heat bath and subject to local control signals. Neither the reservoir alone nor the external driving can induce quantum non-locality but only the cooperative impact of both in non-equilibrium. It is shown that this corresponds to a dynamical symmetry breaking between the modes. By applying optimal control protocols substantial entanglement is generated even for single-site control and at higher temperatures and is preserved after the control is switched off.

PACS numbers: 03.65.Yz, 03.67.Bg, 02.30.Yz

Introduction.- Entanglement is one of the most fascinating manifestations of quantum non-locality in systems with more than one degree of freedom. It has thus been investigated as a key resource for quantum information in case of both discrete [1, 2] and continuous variables [3–5]. Implementations in actual devices have induced a deeper understanding of entanglement in open quantum systems [6–11], particularly in presence of decoherence, but also in presence of external control signals [12–15]. As the generation of entanglement asks for non-local interactions [16], the commonly exploited strategy is a direct coupling between the sub-units either static [7] or modulated in time [12]. A paradigmatic model is that of two Gaussian agents in contact with heat baths which provides an accurate description for a vast class of experiments and moreover offers fundamental insight into the mechanisms of entanglement [4, 5, 17, 18]. Quantumness basically appears only as the result of a composite effect since the individual sub-units live close to the classical limit.

The question we address in this Letter is, whether the control of *local* parameters may prompt entanglement generation in a setting where non-local interactions by themselves are *not* suitable for entanglement generation. For this purpose, two independent harmonic modes are considered embedded in a common heat bath such that the surrounding itself does not mediate quantum non-locality. The same is true for control fields acting on these sub-units locally (see Fig. 1). Entanglement, if existent, can thus only be a result of the cooperative impact of decoherence *and* external driving. In fact, it turns out that the symmetry breaking between the modes, required for the appearance of entangled states, occurs dynamically, i.e. only under non-equilibrium conditions. By combining techniques to capture the non-Markovian quantum dynamics of the compound exactly with optimal control algorithm [19], it is shown that entanglement is efficiently generated even for single-site control and at higher temperatures. Moreover, this entanglement does not decay even after the control is turned off. These findings are of potential relevance for current experiments with ultracold atomic gases and superconducting circuits. They also open new possibilities for teleportation without state transfer.

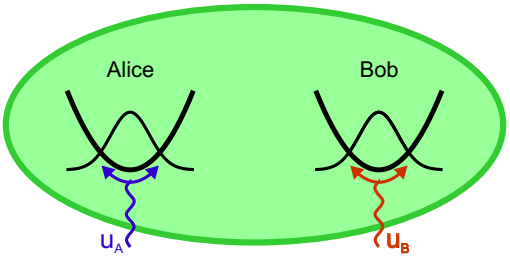

FIG. 1. Two independent harmonic modes A and B are embedded in a common reservoir (green) with no entanglement in thermal equilibrium. Tailored control signals are applied locally to the A and B.

Open system dynamics.- The Hamiltonian of the total compound is given by $H = H_S(t) + H_I + H_R$, where the system part consists of two independent harmonic sub-units

$$H_S(t) \equiv H_A(t) + H_B(t) = \sum_{j=A,B} \frac{p_j^2}{2M} + \frac{M\Omega^2}{2} q_j^2 + \frac{u_j(t)}{2} q_j^2 \tag{1}$$

of equal mass M and frequency Ω and subject to local parametric control signals $u_j(t)$. These units are embedded in a common reservoir according to

$$H_R = \sum_k \frac{p_k^2}{2m_k} + \frac{m_k \omega_k^2}{2} x_k^2 \tag{2}$$

$$H_I = (q_A + q_B) \sum_k c_k x_k + (q_A + q_B)^2 \sum_k \frac{c_k^2}{2m_k\omega_k^2} . \tag{3}$$

Here, the last part in H_I is the usual counter term [20] which removes a reservoir-induced static coupling between the sub-units so that the environment has dynamic impact only according to typical realizations. Its absence may give rise to static entanglement [7, 21], a situation we

thus want to avoid. In the continuum limit the system-reservoir interaction is described by a spectral density $J(\omega) = \pi \sum_k c_k^2/(2m_k\omega_k)\delta(\omega - \omega_k)$.

While the density operator of the full structure obeys the standard Liouville-von Neumann equation, the treatment of the dynamics of the relevant reduced density is a formidable challenge. This is particularly true in case of low temperatures and *a priori* unknown control signals where conventional perturbative expansions like Born-Markov master equations fail. In this situation stochastic Liouville von-Neumann equations (SLN) have been proven as formally exact and numerically powerful tools to capture on the same footing the non-Markovianity of the reduced time evolution and arbitrary external driving fields also for nonlinear systems. They are based on a stochastic representation of the Feynman-Vernon influence functional such that the physical reduced density is obtained by averaging the time evolution according to the SLN over proper noise realizations [22].

For Gaussian modes, the reduced density matrix is fully determined by the first and second cumulants of the elements $x_j, j = 1, \ldots 4$ of the vector $x = (q_A, p_A, q_B, p_B)$ of phase space operators. Since first moments can always be adjusted by local unitary operations, they cannot affect entanglement properties. The central quantity is thus the covariance matrix σ with $\sigma_{ij} = \frac{1}{2}\langle x_i x_j + x_j x_i\rangle - \langle x_i\rangle\langle x_j\rangle$. In the 2×2 block structure [6]

$$\sigma = \begin{pmatrix} \alpha & \gamma \\ \gamma^T & \beta \end{pmatrix}, \tag{4}$$

α, β correspond to the covariance matrices of the respective sub-units A and B, while γ (transpose γ^T) carries the mixed cumulants and thus non-local information. Now, a well-defined measure for entanglement in bipartite Gaussian systems is given by the logarithmic negativity [6, 23]

$$E_{\mathcal{N}} = \max\{0, -\ln(\tilde{\nu}_-)\}, \tag{5}$$

with $\tilde{\nu}_-$ being the smallest symplectic eigenvalue of the partially transposed density matrix. Entanglement only exists if $E_{\mathcal{N}} > 0$ while $E_{\mathcal{N}} = 0$ corresponds to purely classical and/or local quantum correlations. Note that $\det\gamma < 0$ is necessary for $E_{\mathcal{N}}$ to be positive [24].

The dynamical coupling mediated by the reservoir resembles mutual drag between the oscillators, an interaction not able to induce entanglement [25]. Without external driving, any initially separable two-mode state will remain separable indefinitely in the scenario considered here. This applies in particular to the thermal equilibrium state, which can be calculated non-perturbatively exactly [20]. The resulting expression $\tilde{\nu}_-^2 = \langle(q_A + q_B)^2\rangle_\beta\langle(p_A + p_B)^2\rangle_\beta/(\hbar/2)^2$ contains an uncertainty product of the thermal variances *always* exceeding the ground state limit (cf. Fig. 2) so that $\det\gamma > 0$. It is to be noted, however, that this does not preclude discord as a further type of non-classical correlations [26, 27].

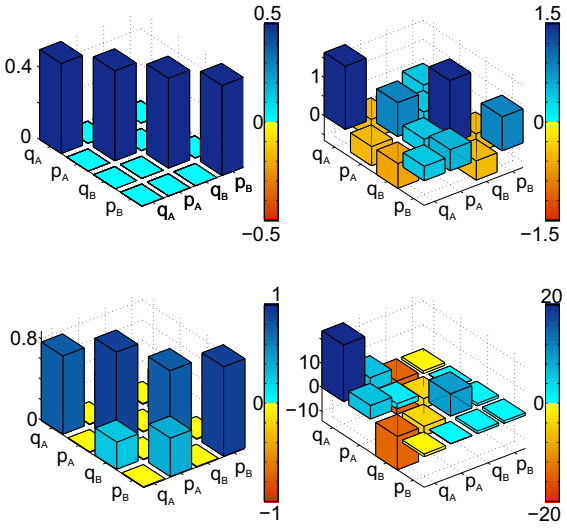

FIG. 2. Covariance matrix for $\beta = 1$, $\eta = 0.1$, and $\omega_c = 50$. Left: no control with harmonic modes in individual ground states (top) and in total thermal equilibrium (bottom). Right: parametric control of both harmonic modes with $u_A = u_B$ (top) and of A only with $u_A \neq 0$, $u_B = 0$ (bottom) at $t_f = 6\pi$. Dimensionless units are used, see text for details.

Optimal control of entanglement.- Although we have stated that interaction with a common reservoir alone is not sufficient to generate entangled states, it nevertheless plays a key role in the generation of entanglement through an external control signal: Since the Hamiltonian (1) provides no two-body interactions (neither static nor controlled), it is needed as an additional ingredient beyond local controls. In the sequel, we not only show that entangled states can be created by this combination of factors, but also perform a numerical search for the maximal entanglement that can be achieved in finite time. For this purpose, the recently developed optimal control formalism for open quantum systems [19] is exploited to maximize the entanglement at a given final time t_f, which is a functional of the control fields $u_A(t), u_B(t)$

$$F[u_A(t), u_B(t); \sigma(t)] = E_{\mathcal{N}}(\sigma(t_f)) \,. \tag{6}$$

We consider an initial preparation with both oscillators in the ground state, and without initial correlations between system and reservoir. This is followed by propagation of the system under the influence of control fields $u_A(t)$, $u_B(t)$ and interaction with an Ohmic bath $J(\omega) = \frac{\eta\omega}{(1+(\omega^2/\omega_c^2))^2}$, parameterized by a coupling constant η, high frequency cut-off ω_c and at inverse temperature $\beta = 1/k_B T$. We use dimensionless units with frequencies scaled with Ω and lengths scaled with $\sqrt{\hbar/M\Omega}$.

Fig. 2 displays bar graphs of optimized covariance matrices (right) compared to ground and thermal states

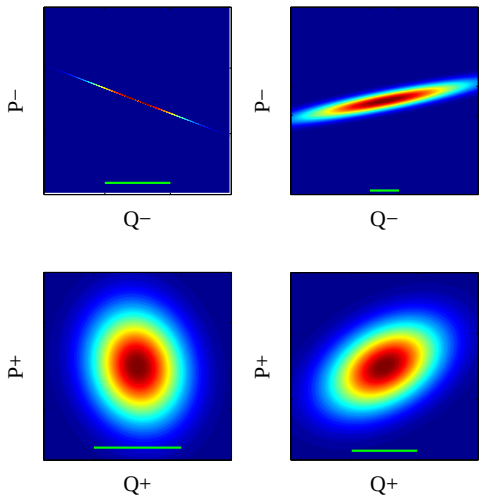

FIG. 3. Reduced Wigner functions for the anti-symmetric Q_-, P_- (top) and symmetric Q_+, P_+ (bottom) normal modes at $t_f = 6\pi$ for two-site (left) and single-site (right) control. The green line indicates the ground state width; parameters are as in Fig. 2.

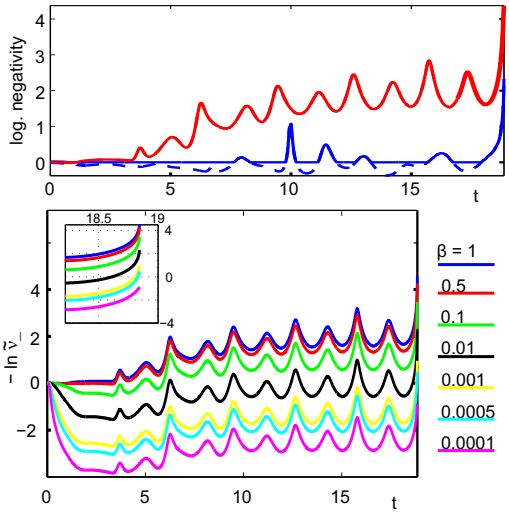

FIG. 4. Top: Logarithmic negativity $E_{\mathcal{N}}(t)$ (solid) for two-site (red) and single-site (blue) control. Negative values for $-\ln(\tilde{\nu}_-)$ corresponding to $E_{\mathcal{N}}(t) = 0$ are also depicted (dashed). Parameters are as in Fig. 2. Bottom: $-\ln(\tilde{\nu}_-)$ for various temperatures (two-site control) with other parameters held fixed. The inset displays the final time range for the control with $E_{\mathcal{N}}(t_f) > 0$ for $\beta \geq 0.0005$.

(left). Apparently, substantial off-diagonal correlations are built up, positive and negative valued, so that one indeed has $\det\gamma < 0$. Notably, the same is true for single-site control ($u_B(t) \equiv 0$).

Further insight is gained through a transformation to normal modes $Q_\pm = (q_A \pm q_B)/\sqrt{2}$, $P_\pm = (p_A \pm p_B)/\sqrt{2}$ which transforms the system Hamiltonian (1) into $H_S = \sum_{\alpha=\pm} \frac{P_\alpha^2}{2} + \frac{1}{2}(1 + \frac{u_A+u_B}{2})Q_\alpha^2 + \frac{1}{2}(u_A - u_B)Q_+Q_-$. Then, for $u_A(t) \equiv u_B(t)$, entanglement ($E_{\mathcal{N}} > 0$) requires

$$4\det\gamma = \Delta_P\,\Delta_Q - [\langle Q_+P_+\rangle - \langle Q_-P_-\rangle]^2 \qquad (7)$$

to be negative, where $\Delta_X = \langle X_+^2\rangle - \langle X_-^2\rangle$, $X = P, Q$. Apparently, this is only possible if the evolution of the two normal modes is not degenerate. Lifting this degeneracy is the decisive role the heat bath plays in this setting. However, external driving is needed as well in order to render the normal mode states dissimilar enough to result in entangled A and B states.

Entanglement generation is thus a *cooperative effect* of local driving and global dissipation in the present setting—either factor by itself is neutral or detrimental to entanglement. A tailored control signal changes the non-local effects of the heat bath from a destructive influence on quantum resources to an asset promoting entanglement.

The correlators in Eq. (7) can be obtained from the Wigner functions plotted in Fig. 3 for the final state under an optimized driving protocol. For symmetric control (left), $u_A \equiv u_B$, a strongly squeezed antisymmetric mode results, while the symmetric mode is close to a thermal state. This leads to opposite signs of the terms Δ_P and Δ_Q, therefore the r.h.s. of Eq. (7) is negative, and the local modes q_A and q_B are entangled. For a more quantitative analysis [28], it is convenient to represent the correlation matrix elements $\langle Q_\pm^2\rangle$, $\langle P_\pm^2\rangle$ and $\langle Q_\pm P_\pm\rangle$ by a different parameter set: squeezing parameters $r_\pm$, squeezing angles $\varphi_\pm$, and width parameters $a_\pm$. Using these parameters, one finds that $\det\gamma < 0$ if the difference $|r_- - r_+|$ is sufficiently large, with a threshold that depends on $\varphi_- - \varphi_+$ and on the ratio a_-/a_+. This observation shows a similarity between the states considered here and two-mode EPR states: EPR states can be seen as factorized pure states of squeezed symmetric and antisymmetric modes, with $r_- = -r_+$ and identical squeezing angles [29]. The states produced in our numerical simulations show strong squeezing in the antisymmetric mode, but *not* in the symmetric mode, which is close to a thermal state. They might therefore be labeled 'semi-EPR' states.

Even using a more rudimentary *single-site* control ($u_A \neq 0, u_B \equiv 0$), we find that the cooperative effect between driving and dissipation persists, although the similarity to EPR states is diminished, see Fig. 3 (right). Moreover, additional correlations between the symmetric and antisymmetric modes are needed to fully characterize the quantum state. The gradual (non-monotonous)

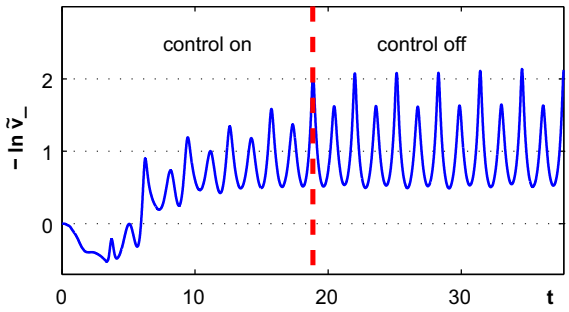

FIG. 5. Entanglement dynamics for $\beta = 0.1$ for a protocol where the control is switched off at $t_f = 6\pi$. Other parameters are as in Fig. 2.

build-up of entanglement over time is shown for the cases of symmetric and single-site control in Fig. 4 (top), with a rapid final approach to values of $E_{\mathcal{N}}(t_f) = 2.33$ (single-site control) and $E_{\mathcal{N}}(t_f) = 4.37$ (symmetric control). Simulations at lower temperatures show further improvements.

The numerical values of the entanglement measure may be related to the number of states involved, allowing a rough comparison to qubit-based entanglement. For two qubits, $E_{\mathcal{N}} = 1$ corresponds to a Bell state. Furthermore, for two-mode squeezed vacuum states with squeezing parameter r and negativity $E_{\mathcal{N}}(r) = 2r$, the number of excited states in each mode dominantly contributing to the entanglement can be estimated as $m \approx \exp[E_{\mathcal{N}}(r)]/2$. While, as discussed above, the situation here is different due to the dissipative Q_+ mode, one may at least estimate that symmetric (single-site) control involves about $m \approx 40$ ($m \approx 5$) states in each of the oscillators.

Let us now discuss the temperature dependence of the protocol. Qualitatively, one may expect quantum non-locality to be quite robust, particularly for $u_A = u_B$. This is indeed seen in Fig. 4 (bottom) where the logarithmic negativity is of order 1 even for inverse temperatures around $\beta = 0.01$. Further understanding can be gained by observing that the fundamental solutions of the classical equation of motion play a prominent role even in the fluctuations of a harmonic oscillator [20]. Generalizing results for the parametrically driven oscillator [30], a semi-analytical theory for the case of symmetric driving $u(t) = u_A(t) = u_B(t)$ can be found based on the fundamental solutions $\phi_{1,2}(t)$ of the equation of motion $\ddot{\phi} + [1 + u(t)]\phi = 0$.

Our analysis in the accompanying supplemental material [28] reveals that the final state of the Q_+ mode differs very little from a thermal state for the parameters covered by our numerical simulations. The condition $\det\gamma < 0$ can thus be re-stated to a good approximation in the simple form

$$\cosh 2r_- > \coth\beta. \tag{8}$$

This indicates that raising temperature does not preclude entanglement *per se*. However, it gives a lower bound on the sqeezing required to obtain entanglement at a given temperature, which becomes more and more stringent as temperature is raised. Given an absolute upper bound of the achievable squeezing r_-, Eq. (8) indicates the highest temperature at which the condition $\det\gamma < 0$ can be fulfilled. This result is largely independent of the dissipative coupling strength; it remains valid as long as the oscillators are underdamped.

Interestingly, the generated entanglement in the present scenario even persists once the external control is switched off, as illustrated in Fig. 5 for $\beta = 0.1$. This feature which may be attractive for potential applications.

Discussion.- We have shown that dynamical symmetry breaking for two-mode Gaussian parties due to the combined impact of common dissipation and local parametric control efficiently generates entanglement. This proves that quantum non-locality can be induced in a minimal model where it is absent in the thermodynamic state and only appears in non-equilibrium. Local optimal control allows to achieve substantial logarithmic negativity in finite time and even at high temperatures and in a simple, experimentally realizable system. The protocol may thus be applicable to various bipartite systems in atomic and solid state physics. Particular examples include two Cooper pair boxes subject to an engineered environment as in [31] or a large Bose-Einstein condensate acting as a reservoir for two impurity fermions in an optical lattice. Potentially, NV centers in diamonds provide an ideal test-bed to dynamically induce entanglement at high temperatures [32]. Beyond these direct realizations, there are also consequences for quantum teleportation to be explored. Namely, Alice does not need to transfer one party of a bipartite entangled state created by her to Bob but rather initially non-entangled parties, one at Alice and one at Bob, are dynamically entangled when a common reservoir dominates against local decoherence.

Acknowledgements. The authors like to thank E. Kajari, T. Häberle and F. Jelezko for valuable discussions. Financial support was provided by Deutsche Forschungsgemeinschaft through AN336/6-1 and SFB/TRR21.

* rebecca.schmidt@uni-ulm.de

[1] C. Bennett, G. Brassard, C. Crépeau, R. Josza, A. Peres, and W. Wooottters, Phys. Rev. Lett. **70**, 1895 (1993)
[2] M. A. Nielsen and I. L. Chuang, *Quantum computation and quantum Information* (Cambridge University Press, 2000)
[3] L. Vaidmann, Phys. Rev. A **49**, 1473 (1994)
[4] B. S.L and P. van Loock, Rev. Mod. Phys. **77**, 513 (2005)
[5] C. Weedbrook, S. Pirandola, R. García-Patrón, N. J. Cerf, T. C. Ralph, J. H. Shapiro, and S. Lloyd, Rev. Mod. Phys. **84**, 621 (2012)

[6] G. Adesso, A. Serafini, and F. Illuminati, Phys. Rev. Lett. **92**, 087901 (2004)
[7] J. P. Paz and A. J. Roncaglia, Phys. Rev. Lett. **100**, 220401 (2008)
[8] J. Eisert and M. B. Plenio, Phys. Rev. Lett. **89**, 137902 (2002)
[9] S. Olivares and M. G. A. Paris, Phys. Rev. Lett. **107**, 170505 (2011)
[10] C. Hörhammer and H. Büttner, Phys. Rev. A **77**, 042305 (2008)
[11] A. Wolf, G. De Chiara, E. Kajari, E. Lutz, and G. Morigi, EPL **95**, 60008 (2011)
[12] F. Galve, L. A. Pachón, and D. Zueco, Phys. Rev. Lett. **105**, 180501 (2010)
[13] S. McEndoo, P. Haikka, G. de Chiara, M. Palma, and S. Maniscalco, EPL **101**, 60005 (2013)
[14] A. Serafini and S. Mancini, Phys. Rev. Lett. **104**, 220501 (2010)
[15] S. Zippilli, M. Paternostro, G. Adesso, and F. Illuminati, Phys. Rev. Lett. **110**, 040503 (2013)
[16] D. Yang, M. Horodecki, R. Horodecki, and B. Synak-Radtke, Phys. Rev. Lett. **95**, 190501 (2005)
[17] V. D'Auria, S. Fornaro, A. Porzio, S. Solimeno, S. Olivares, and M. G. A. Paris, Phys. Rev. Lett. **102**, 020502 (2009)
[18] J. Laurat, G. Keller, J. A. Oliveira-Huguenin, C. Fabre, T. Coudreau, A. Serafini, G. Adesso, and F. Illuminati, J. Opt. B **7**, 577 (2005)
[19] R. Schmidt, A. Negretti, J. Ankerhold, T. Calarco, and J. T. Stockburger, Phys. Rev. Lett. **107**, 130404 (2011)
[20] U. Weiss, *Quantum Dissipative Systems* (World Scientific, 2008)
[21] D. Braun, Phys. Rev.Lett. **89**, 277901 (2002)
[22] J. T. Stockburger and H. Grabert, Phys. Rev. Lett. **88**, 170407 (2002)
[23] G. Vidal and R. Werner, Phys. Rev. A **65**, 032314 (2002)
[24] R. Simon, Phys.Rev.Lett. **84**, 2726 (2000)
[25] For Ohmic friction, the quasistatic interaction scales linearly with the reservoir bandwith, while the dynamical interaction depends only on the friction parameter η.
[26] G. Adesso and A. Datta, Phys. Rev. Lett. **105**, 030501 (2010)
[27] P. Giorda and M. G. A. Paris, Phys. Rev. Lett. **105**, 020503 (2010)
[28] See Supplemental at XXX for details on the description of a paramterically driven quantum oscillator.
[29] U. Leonhardt, *Essential Quantum Optics: From Quantum Measurements to Black Holes* (Cambridge University Press, 2010)
[30] C. Zerbe and P. Hänggi, Phys. Rev. E **52**, 1533 (1995)
[31] P. Solinas, M. Möttönen, J. Salmilehto, and J. Pekola, Phys. Rev. B **82**, 134517 (2010)
[32] P.-B. Li, S.-Y. Gao, H.-R. Li, S.-L. Ma, and F.-L. Li, arXiv:1106718v3

Quasi-local generation of EPR entanglement in non-equilibrium: Supplemental Material

Rebecca Schmidt,* Jürgen T. Stockburger, and Joachim Ankerhold

Institut für Theoretische Physik, Universität Ulm,

Albert Einstein-Allee 11, 89069 Ulm, Germany

(Dated: May 28, 2013)

Abstract

In this supplemental material to our article 'Quasi-local generation of EPR entanglement in non-equilibrium' [ref: article] the dynamics of the parametric quantum oscillator is reviewed with emphasis on the time evolution of the covariance matrix. We also outline some technical details of the optimization algorithm we use.

* rebecca.schmidt@uni-ulm.de

I. PARAMETRIC QUANTUM OSCILLATOR

A. Classical dynamics

The classical equation of motion for a damped harmonic oscillator parametrically driven by a control field $u(t)$ reads in dimensionless units as used in the main text

$$\ddot{q}(t) + \eta\dot{q}(t) + \omega(t)^2 q(t) = 0 \tag{1}$$

where $\omega(t)^2 = 1 + u(t)$. In the sequel, friction is considered as weak $\eta \ll 1$ and about the control signal we only assume that it is sufficiently smooth and bounded from below such that $\omega(t)^2 \geq 0$. Then, solutions to (1) can be written in the form $q(t) = \mathrm{e}^{-\eta t/2} Q(t)$ where

$$\ddot{Q}(t) + \tilde{\omega}(t)^2 Q(t) = 0 \tag{2}$$

with $\tilde{\omega}(t)^2 = \omega(t)^2 - \eta^2/4 \approx \omega(t)^2$ in the weak friction limit. Relevant observables can then be expressed in terms of the independent solutions $\phi_k(t), k = 1, 2$ of (2) with initial conditions $\phi_1 = 0, \dot{\phi}_1(0) = 1$ and $\phi_2(0) = 1, \dot{\phi}_2(0) = 0$. According to Abel's identity [1] the corresponding Wronskian then obeys

$$\phi_2(t)\dot{\phi}_1(t) - \phi_1(t)\dot{\phi}_2(t) = 1\,. \tag{3}$$

Further properties about the ϕ_i are known only in case of a purely periodic drive, e.g. $u(t) = a\cos(2\omega_0 t)$ (see [2]). Even though typical optimal control signals are *not* of this

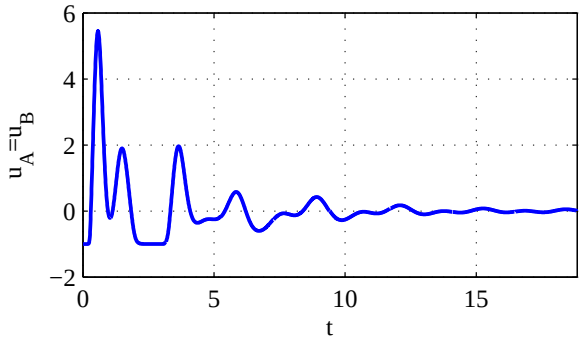

FIG. 1. Optimized control signal for symmetric two-site control for the parameters in Fig. 2 of the main text.

simple form (cf. Fig. 1), it is instructive to recall some results: solutions are of the form $\phi_1(t) = [F_\nu(t) - F_\nu(-t)]/[2\dot{F}_\nu(0)]$ and $\phi_2(t) = [F_\nu(t) + F_\nu(-t)]/[2F_\nu(0)]$ where the Mathieu function $F_\nu(t) = \exp(i\nu t)\, p(t)$ contains the Floquet exponent ν and a periodic function $p(t) = p(t + \pi/\omega_0)$; orbits of (1) are found to be unstable if $|\mathrm{Im}\{\nu\}| > \eta/2$.

B. Parametrization of Gaussian quantum states

A Gaussian state is fully characterized the expectation values of conjugate variables q and p, and by its covariance matrix $\sigma_{xy} = \frac{1}{2}\langle xy+yx\rangle - \langle x\rangle\langle y\rangle$, $x, y \in \{q, p\}$. The matrix elements of σ themselves are suitable as dynamical variables (see below), however, the parametrization

$$\sigma_{qq} = a^2\,(\cosh 2r + \cos 2\varphi \sinh 2r) \tag{4}$$

$$\sigma_{qp} = -a^2 \sin 2\varphi \sinh 2r \tag{5}$$

$$\sigma_{pp} = a^2\,(\cosh 2r - \cos 2\varphi \sinh 2r) \tag{6}$$

through a squeezing parameter r, a squeezing angle φ, and a width parameter a with $\sigma_{qq}\sigma_{pp} - \sigma_{qp}^2 = a^4$ is often more suitable to discuss qualitative properties of a quantum state [3]. Alternatively, the width parameter a can be replaced by an effective temperature parameter through

$$a^2 = \frac{1}{2}\coth\frac{\beta}{2}. \tag{7}$$

For the case of symmetric driving discussed in the main paper, the two-mode covariance matrix factorizes when transformed to normal modes. It is therefore determined by the parameter set $r_\pm$, $\varphi_\pm$, $a_\pm$. Using this parameter set, and reverting to local modes, the quantity $\det\gamma$ (see main paper), takes the form

$$\det\gamma = \frac{1}{2}\left[a_+^4 + a_-^4 - 2a_+^2 a_-^2(\cosh 2r_- \cosh 2r_+ - \cos(2\varphi_- - \varphi_+)\sinh 2r_- \sinh 2r_+)\right] \tag{8}$$

The condition $\det\gamma < 0$ translates thus into

$$\cosh 2r_- \cosh 2r_+ - \cos(2\varphi_- - 2\varphi+)\sinh 2r_- \sinh 2r_+ > \frac{1}{2}\left(\frac{a_+^2}{a_-^2} + \frac{a_-^2}{a_+^2}\right). \tag{9}$$

C. Quantum dynamics

In the quantum regime, the variances $\sigma_{xy} = \frac{1}{2}\langle xy + yx\rangle - \langle x\rangle\langle y\rangle$, $x, y \in \{q, p\}$ of the conjugate operators q, p are the interesting quantities. In the undamped case ($\eta = 0$) they

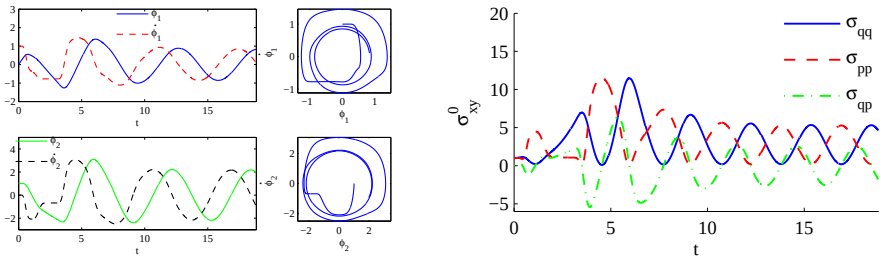

FIG. 2. Left: Time evolution of functions $\phi_1(t)$ and $\phi_2(t)$ (solid) and their respective derivatives (dashed) for the optimal control signal $u(t)$ obtained for the two-site controlled quantum dynamics with parameters as in Fig. 2 of the main text. Middle: Corresponding phase space orbits. Right: Time evolution of the quadrature variances of a non-dissipative parametric quantum oscillator driven by the same optimal control signal $u(t)$.

obey the following set of equations

$$\dot{\sigma}^{(0)}_{qq} = 2\sigma^{(0)}_{qp} \ , \ \dot{\sigma}^{(0)}_{pp} = -2\omega(t)^2\sigma^{(0)}_{qp} \ , \ \dot{\sigma}^{(0)}_{qp} = \sigma^{(0)}_{pp} - \omega(t)^2\sigma^{(0)}_{qq} \, . \tag{10}$$

For a ground state as initial state one has $\sigma_{qq}(0) = \sigma_{pp} = 1, \sigma_{qp} = 0$ and finds

$$\sigma^{(0)}_{qq}(t) = \phi_1(t)^2 + \phi_2(t)^2 \ , \ \sigma^{(0)}_{pp}(t) = \dot{\phi}_1(t)^2 + \dot{\phi}_2(t)^2 \ , \ \sigma^{(0)}_{qp}(t) = \phi_1(t)\dot{\phi}_1(t) + \phi_2(t)\dot{\phi}_2(t) \, . \tag{11}$$

The calculation for a dissipative system is much more cumbersome. It can conveniently be performed using techniques from [4] in terms of the path integral representation of the reduced density operator of the system. For the variances one then obtains $\sigma_{xy}(t) = \sigma_{xy,0}(t) + \sigma_{xy,\beta}(t)$, where the first transient part depends on the initial state but is independent of temperature while the second non-decaying part depends on temperature only. Approximately, in the weak friction limit one has $\sigma_{xy,0}(t) \sim \exp(-\eta t)\sigma^{(0)}_{xy}(t)$. Further, the non-decaying parts of the variances take the form [4] $\sigma_{qq,\beta}(t) = a_{qq}(t)$ so that $\sigma_{pp,\beta}(t) = \ddot{a}_{qq}(t)$, and $\sigma_{qp,\beta}(t) = \dot{a}_{qq}(t)$ where

$$a_{qq}(t) = \int_0^t ds \int_0^s du \, \varphi(t,s) \, K(s-u) \, \varphi(t,u) \, \mathrm{e}^{-\eta[t-(s+u)/2]} \, . \tag{12}$$

This includes the real part of the reservoir force-force correlation

$$K(s) = \int_0^\infty \frac{d\omega}{\pi} \, J(\omega) \, \coth(\omega\hbar\beta/2) \, \cos(\omega s) \tag{13}$$

and a function $\varphi(t,s) = [\phi_1(t)\phi_2(s) - \phi_1(s)\phi_2(t)]$ which obeys the classical equation (2) with boundary conditions $\varphi(t,0) = \phi_1(t)$, $\varphi(t,t) = 0$. Further, $d\varphi(t,s)/ds|_{s=t} = -1$ according to (3).

The momentum variance reads $\sigma_{pp,\beta}(t) = a_{pp}(t) + 2a_{qq}(t)\dot{\phi}_1(t)^2/\phi_1(t)^2 + a_{qp}(t)\dot{\phi}_1(t)/\phi_1(t)$ with

$$a_{pp}(t) = \int_0^t ds \int_0^s du \frac{\phi_1(s)}{\phi_1(t)} K(s-u) \frac{\phi_1(u)}{\phi_1(t)} \mathrm{e}^{-\eta[t-(s+u)/2]} \tag{14}$$

and

$$a_{qp}(t) = \int_0^t ds \int_0^s du \frac{\phi_1(s)}{\phi_1(t)} K(s-u)\, \varphi(t,u)\, \mathrm{e}^{-\eta[t-(s+u)/2]}\,. \tag{15}$$

For the mixed variance one finds $\sigma_{qp,\beta}(t) = a_{qq}(t)\dot{\phi}_1(t)/\phi_1(t) + a_{qp}(t)$.

In case of a vanishing drive, this reduces with the known equilibrium variances of the dissipative quantum oscillator. For weak to moderate friction, $J(\omega) = \omega\eta\omega_c^2/(\omega^2+\omega_c^2)^2$ with a large cut-off ω_c, these differ by slight shifts [5] from the values predicted in the canonical ensemble. The position correlations σ_{qq} are somewhat smaller (quantum Zeno effect), and the momentum correlations σ_{pp} are increased by a correction $\propto \ln\omega_c$. The equilibrium squeezing parameter r_β is thus slightly negative. In the high temperature limit or for very weak friction, all parameters revert to their standard equilibrium values, which are characterized by $r_\beta = 0$, $\varphi_\beta = 0$, and width a related to the physical reservoir temperature by Eq. (7).

This can also be verified in case of finite driving. We first mention that the bath kernel takes for very low temperatures the form $K(s) \sim \eta/s^2, s > 1/\omega_c$ and in the high temperature regime becomes local in time, i.e. $K(s) \sim (\eta/\beta)\,\delta(s)$. Further, for optimized control over an interval $[0,t_f]$ with t_f covering at least a few periods of the bare oscillator, signals $u(t)$ typically consist of an initial segment (about at most two periods of the bare oscillator) with large amplitudes and a second segment with low amplitudes and quasi-periodic behavior, see Fig. 1. Correspondingly, the functions $\phi_1(s), \phi_2(s)$ show an oscillatory behavior similiar to the non-driven case for times $s > \tau$ with $t_f \gg \tau$ as displayed in Fig. 2. This in turn splits the range of the time integration in (12) in a short time domain ($s < \tau$) and a range where the damping dependent exponential dictates the decay. Typically, the contribution of the latter range dominates so that one can write $a_{qq}(t_f) = \langle q^2\rangle_\beta + \epsilon_q(t_f)$ with a smaller time-varying part $\epsilon(t_f)$ of order $\eta\mathrm{e}^{-\eta t_f}\phi_1(t)^2$. A similar analysis shows that a_{pp} in leading order approaches, i.e., $a_{pp}(t_f) = \langle p^2\rangle_\beta + \epsilon_p(t_f)$, while the mixed variances remain smaller

than of order 1. Neglecting these small thermal and dynamical corrections, one may insert the thermal-state parameters $r_+ = 0$, $\phi_+ = 0$, and $a_+ = 1/2 \coth(\beta/2)$ into (9). Observing that the antisymmetric mode is a pure state ($a_- = 1/2$), Eq. (9) then reduces to

$$\cosh 2r_- > \coth \beta, \tag{16}$$

which is Eq. (8) of the main text. This indicates that sufficiently strong squeezing can cancel the destructive effect of thermal fluctuations. However, in any experimental setting there is a highest attainable squeezing parameter r_-. Eq. (16) then defines an upper limit for the temperature range that allows entanglement generation.

II. OPTIMIZATION ALGORITHM FOR ENTANGLEMENT CREATION IN OPEN BIPARTITE GAUSSIAN SYSTEMS

The optimization algorithm used in the main text is an extended version of what has been developed for open quantum dynamics in [6], including the respective supplemental material. In the present case, the Hamiltonian Eqs. (1-3) in the main text

$$\begin{aligned} H = &\sum_{j=A,B} \frac{p_j^2}{2M} + \frac{M\Omega^2}{2} q_j^2 + \frac{u_j(t)}{2} q_j^2 \\ &+ (q_A + q_B) \sum_k c_k x_k + (q_A + q_B)^2 \sum_k \frac{c_k^2}{2m_k\omega_k^2} + \sum_k \frac{p_k^2}{2m_k} + \frac{m_k\omega_k^2}{2} x_k^2 \end{aligned} \tag{17}$$

gives rise to the following stochastic Liouville-von Neumann equation for a single noise realization ξ:

$$\begin{aligned} \dot{\rho}_{AB,\xi} = &-\frac{\mathrm{i}}{\hbar}[H_A \otimes \mathbf{1}_B, \rho_{AB,\xi}] - \frac{\mathrm{i}}{\hbar}[\mathbf{1}_A \otimes H_B, \rho_{AB,\xi}] + \frac{\mathrm{i}}{\hbar}\xi(t)[q_A + q_B, \rho_{AB,\xi}] \\ &- \frac{\mathrm{i}}{\hbar}\frac{\eta}{2}[q_A + q_B, \{p_A + p_B, \rho_{AB,\xi}\}]\,. \end{aligned} \tag{18}$$

Here, $\rho_{AB,\xi}$ denotes the density operator for one stochastic realization with the *physical* reduced density operator ρ_{AB} obtained after averaging over sufficiently many realizations, i.e., $\rho_{AB} = \mathbb{E}\left[\rho_{AB,\xi}\right]$. The statistics of the noise variable $\xi(t)$ is governed by the quantum correlation function of the environmental fluctuations [7]. From (18) corresponding equations of motions for the first and second cumulants in position and in momentum are easily derived. As shown in the main text (Eq. (6)), the for the optimal control procedure the objective is to maximize the entanglement. Variation of the influence functional

$$F[u_A(t), u_B(t); \sigma(t)] = E_{\mathcal{N}}(\sigma(t_f)) \tag{19}$$

with respect to the control fields and to the state and under the constraint that the equations of motion derived from (18) are to be obeyed, provides us with:

- a set of stochastic equations of motion for the cumulants of the co-state Λ with an end time boundary condition (backward propagation)
- an update formula for the control signals.

This system of equations (forward propagation, backward propagation and control update) has to be solved consistently and iteratively. For further details we refer to the supplemental material of [6].

Practically, maximizing the logarithmic negativity $E_{\mathcal{N}} = \max\{0, -\ln(\tilde{\nu}_-)\}$ and thus searching iteratively for solutions with arguments in the log-function decreasing towards zero, poses a numerical problem. Namely, for arguments sufficiently close to zero, the optimization procedure becomes extremely sensitive to the noise averaging. It turns out that for the system in question (two identical oscillators, coupled to a common reservoir) minimizing $\det\gamma$ leads as well to the optimization goal but without numerical instabilities.

---

[1] W. E. Boyce and R. C. DiPrima. *Elementary Differential Equations and Boundary Value Problems*. Wiley, 1986.

[2] N. W. McLachlan. *Theory and Application of Mathieu Functions*. Dover, 1964.

[3] C. Weedbrook, S. Pirandola, R. García-Patrón, N. J. Cerf, T. C. Ralph, J. H. Shapiro, and S. Lloyd. *Rev. Mod. Phys.*, 84:621, 2012.

[4] C. Zerbe and P. Hänggi. *Phys. Rev. E*, 52:1533, 1995.

[5] U. Weiss. *Quantum Dissipative Systems*. World Scientific, 2008.

[6] R. Schmidt, A. Negretti, J. Ankerhold, T. Calarco, and J. T. Stockburger. *Phys. Rev. Lett.*, 107:130404, 2011.

[7] J. T. Stockburger and H. Grabert. *Phys. Rev. Lett.*, 88:170407, 2002.

Part III.

Appendix

A. Cumulant dynamics

As Gaussian systems are fully decribed by their first and second cumulants, the propagation of the reduced densitiy matrix can be replaced by the propagation of these cumulants. In the following, the equation of motions, we implemented, are given.

A.1. one harmonic mode

For our results we used a stochastic Liouville-von Neumann equation, the SLED equation, cf. Subsection 1.3.1. We compared these results with both a Lindblad equation and the Caldeira-Leggett master equation.

SLED

dynamics of the state

Combining the SLED equation 1.3.1 with driving:

$$\begin{aligned}\frac{\mathrm{d}}{\mathrm{d}t}\rho_\xi &= \mathcal{L}^{(SLED)}\rho_\xi \\ &= -\frac{i}{\hbar}[H_S,\rho_\xi] - \frac{i}{\hbar}[H_C,\rho_\xi] + \frac{i}{\hbar}\xi(t)[q,\rho_\xi] - \frac{i}{\hbar}\frac{\gamma_0}{2}\left[q,\{p,\rho_\xi\}\right], \qquad \text{(A.1)}\end{aligned}$$

with $H_C := -u_1 q + \frac{1}{2}u_2 q^2$, gives rise to the following stochastic equations of motion[1] for the first and second cumulants:

$$\begin{aligned}\frac{\mathrm{d}}{\mathrm{d}t}\langle q\rangle_c &= \frac{1}{m}\langle p\rangle_c & \text{(A.2)}\\ \frac{\mathrm{d}}{\mathrm{d}t}\langle p\rangle_c &= -(m\omega_0^2+u_2)\langle q\rangle_c - \gamma_0\langle p\rangle_c + \xi + u_1 & \text{(A.3)}\\ \frac{\mathrm{d}}{\mathrm{d}t}\langle q^2\rangle_c &= \frac{2}{m}\left\langle\frac{pq+qp}{2}\right\rangle_c & \text{(A.4)}\\ \frac{\mathrm{d}}{\mathrm{d}t}\langle p^2\rangle_c &= -(2m\omega_0^2+u_2)\left\langle\frac{pq+qp}{2}\right\rangle_c - 2\gamma_0\langle p^2\rangle_c & \text{(A.5)}\\ \frac{\mathrm{d}}{\mathrm{d}t}\left\langle\frac{pq+qp}{2}\right\rangle_c &= \frac{1}{m}\langle p^2\rangle_c - (m\omega_0^2+u_2)\langle q^2\rangle_c - \gamma_0\left\langle\frac{pq+qp}{2}\right\rangle_c & \text{(A.6)}\end{aligned}$$

[1] The equations hold for one stochastic realisation ξ, for the sake of readabiltiy the index $\cdot_\xi$ had been left away. The averaging indicated by $\langle\cdot\rangle_c$ is the quantum mechanical one.

dynamics of the co-state

With the ansatz:

$$\tilde{\Lambda}_\xi(t) = \Lambda_\xi(t) \cdot \mathrm{e}^{\gamma(t-T)} \tag{A.7}$$

we get the same equations of motion as (A.2) for the backward propagation of $\tilde{\Lambda}_\xi$ with the final time values, as statet in eq. (A.9), beeing the negative values of the cumulants of the objective state.

Boundary condition

$$F[\rho, T] = A = |\alpha\rangle\langle\alpha| \tag{A.8}$$

The initial value of the backward propagation becomes:

$$\Lambda_z(T) = -A \tag{A.9}$$

Lindblad master equation

dynamics of the state

Based on the Lindblad Master equation:

$$\frac{\mathrm{d}}{\mathrm{d}t}\rho = -i[H_S + H_C, \rho] + \gamma_0(N_\beta + 1)\left(a\rho a^\dagger - \frac{1}{2}\{a^\dagger a, \rho\}\right) + \gamma_0 N_\beta\left(a^\dagger \rho a - \frac{1}{2}\{aa^\dagger, \rho\}\right) \tag{A.10}$$

in dimensionless units, where a, $a^\dagger$ are the annihilation and the creation operator of the harmonic oscillator, respectively, and $N_\beta = \frac{1}{e^\beta - 1}$ is the thermal occupation number of the unpertubated oscillator, the following equations of motion for the first and second cumulants are derived:

$$\frac{\mathrm{d}}{\mathrm{d}t}\langle q\rangle_c = \langle p\rangle_c - \frac{\gamma_0}{2}\langle q\rangle_c \tag{A.11}$$

$$\frac{\mathrm{d}}{\mathrm{d}t}\langle p\rangle_c = -(1+u_2)\langle q\rangle_c - \frac{\gamma_0}{2}\langle p\rangle_c + u_1 \tag{A.12}$$

$$\frac{\mathrm{d}}{\mathrm{d}t}\langle q^2\rangle_c = 2\left\langle\frac{pq+qp}{2}\right\rangle_c - \gamma_0\left(\langle q^2\rangle_c - \frac{1}{2}\coth\frac{\beta}{2}\right) \tag{A.13}$$

$$\frac{\mathrm{d}}{\mathrm{d}t}\langle p^2\rangle_c = -(2+u_2)\left\langle\frac{pq+qp}{2}\right\rangle_c - \gamma_0\left(\langle p^2\rangle_c - \frac{1}{2}\coth\frac{\beta}{2}\right) \tag{A.14}$$

$$\frac{\mathrm{d}}{\mathrm{d}t}\left\langle\frac{pq+qp}{2}\right\rangle_c = \langle p^2\rangle_c - (1+u_2)\langle q^2\rangle_c - \gamma_0\left\langle\frac{pq+qp}{2}\right\rangle_c \tag{A.15}$$

With ω_0, m equal to one.

dynamics of the co-state

Here, the backward propagation is the same as the forward one.

Caldeira-Leggett master equation

dynamics of the state

The Caldeira-Leggett master equation:

$$\frac{\mathrm{d}}{\mathrm{d}t}\rho = -\frac{i}{\hbar}[H_S + H_C, \rho] - \frac{i\eta}{2m\hbar}\left[q, \{p, \rho\}\right] - \frac{\eta}{\hbar^2\beta}\left[q, [q, \rho]\right] \tag{A.16}$$

gives rise to the following equations of motion for the first and second cumulants:

$$\begin{aligned}
\frac{\mathrm{d}}{\mathrm{d}t}\langle q\rangle_c &= \frac{1}{m}\langle p\rangle_c && \text{(A.17)}\\
\frac{\mathrm{d}}{\mathrm{d}t}\langle p\rangle_c &= -(m\omega_0^2 + u_2)\langle q\rangle_c - \gamma_0\langle p\rangle_c + u_1 && \text{(A.18)}\\
\frac{\mathrm{d}}{\mathrm{d}t}\langle q^2\rangle_c &= \frac{2}{m}\left\langle\frac{pq+qp}{2}\right\rangle_c && \text{(A.19)}\\
\frac{\mathrm{d}}{\mathrm{d}t}\langle p^2\rangle_c &= -(2m\omega_0^2 + u_2)\left\langle\frac{pq+qp}{2}\right\rangle_c - 2\gamma_0\langle p^2\rangle_c + \gamma kT && \text{(A.20)}\\
\frac{\mathrm{d}}{\mathrm{d}t}\left\langle\frac{pq+qp}{2}\right\rangle_c &= \frac{1}{m}\langle p^2\rangle_c - (m\omega_0^2 + u_2)\langle q^2\rangle_c - \gamma_0\left\langle\frac{pq+qp}{2}\right\rangle_c && \text{(A.21)}
\end{aligned}$$

dynamics of the co-state

For calculating the dynamics of the co-state, the following influence functional is used:

$$J[\vec{x}, \vec{u}, \vec{\lambda}] = E(T) + \int_0^T \vec{\lambda}\left(\dot{\vec{x}} - \left(A\vec{x} + \vec{b}\right)\right)dt, \tag{A.22}$$

where $\vec{x} = (\langle q\rangle_c, \langle p\rangle_c, \langle q^2\rangle_c, \langle p^2\rangle_c, \langle\frac{pq+qp}{2}\rangle_c)^T$, the dynamics of the state is $\dot{\vec{x}} = A\vec{x} + \vec{b}$. The objective is energy $E(T) = 1/2$ in natural units. This gives rise to the following equations for the backward propagation:

$$\frac{\mathrm{d}}{\mathrm{d}t}\langle q\rangle_c = (m\omega_0^2 + u_2)\langle p\rangle_c \tag{A.23}$$

$$\frac{\mathrm{d}}{\mathrm{d}t}\langle p\rangle_c = -\frac{1}{m}\langle q\rangle_c + \gamma_0\langle p\rangle_c \tag{A.24}$$

$$\frac{\mathrm{d}}{\mathrm{d}t}\langle q^2\rangle_c = (m\omega_0^2 + u_2)\left\langle \frac{pq+qp}{2}\right\rangle_c \tag{A.25}$$

$$\frac{\mathrm{d}}{\mathrm{d}t}\langle p^2\rangle_c = 2\gamma_0\langle p^2\rangle_c - \frac{1}{m}\left\langle \frac{pq+qp}{2}\right\rangle_c \tag{A.26}$$

$$\frac{\mathrm{d}}{\mathrm{d}t}\left\langle \frac{pq+qp}{2}\right\rangle_c = -\frac{2}{m}\langle q^2\rangle_c + 2(m\omega_0^2 + u_2)\langle p^2\rangle_c + \gamma_0\left\langle \frac{pq+qp}{2}\right\rangle_c \tag{A.27}$$

A.2. two harmonic modes

For two harmonic modes A and B, subject to the same reservoir, but not directly coupled to each other, the dynamics are gouverned by the following equations[2]:

SLED

dynamics of the state

with i, $j = A$, B and $i \neq j$:

$$\frac{\mathrm{d}}{\mathrm{d}t}\langle q_i\rangle_c = \frac{1}{m_i}\langle p_i\rangle_c \tag{A.28}$$

$$\frac{\mathrm{d}}{\mathrm{d}t}\langle p_i\rangle_c = -(m_i\omega_{0,i}^2 + u_{2,i})\langle q_i\rangle_c - \gamma_0\left(\langle p_i\rangle_c + \langle p_j\rangle_c\right) + \xi \tag{A.29}$$

$$\frac{\mathrm{d}}{\mathrm{d}t}\langle q_i^2\rangle_c = \frac{2}{m_i}\left\langle \frac{p_iq_i + q_ip_i}{2}\right\rangle_c \tag{A.30}$$

$$\frac{\mathrm{d}}{\mathrm{d}t}\langle p_i^2\rangle_c = -2(m_i\omega_{0,i}^2 + u_{2,i})\left\langle \frac{p_iq_i + q_ip_i}{2}\right\rangle_c - 2\gamma_0\left(\langle p_i^2\rangle_c + \langle p_jp_i\rangle_c\right) \tag{A.31}$$

$$\frac{\mathrm{d}}{\mathrm{d}t}\left\langle \frac{q_ip_i + p_iq_i}{2}\right\rangle_c = \frac{1}{m_i}\langle p_i^2\rangle_c - (m_i\omega_{0,i}^2 + u_{2,i})\langle q_i^2\rangle_c$$

[2]Again, the equations hold for one stochastic realisation ξ, for the sake of readabiltiy the index $\cdot_\xi$ had been left away. The averaging indicated by $\langle\cdot\rangle_c$ is the quantum mechanical one.

$$-\gamma_0 \left(\left\langle \frac{p_i q_i + q_i p_i}{2} \right\rangle_c + \langle q_i p_j \rangle_c \right) \tag{A.32}$$

$$\frac{\mathrm{d}}{\mathrm{d}t}\langle q_A q_B \rangle_c = \frac{1}{m_A} \langle q_B p_A \rangle_c + \frac{1}{m_B} \langle q_A p_B \rangle_c \tag{A.33}$$

$$\begin{aligned} \frac{\mathrm{d}}{\mathrm{d}t}\langle p_A p_B \rangle_c &= -(m_A \omega_{0,A}^2 + u_{2,A}(t)) \langle q_A p_B \rangle_c - (m_B \omega_{0,B}^2 + u_{2,B}(t)) \langle q_B p_A \rangle_c \\ &\quad -\gamma_0 \left(\langle p_A^2 \rangle_c + 2 \langle p_A p_B \rangle_c + \langle p_B^2 \rangle_c \right) \end{aligned} \tag{A.34}$$

$$\begin{aligned} \frac{\mathrm{d}}{\mathrm{d}t}\langle q_i p_j \rangle_c &= \frac{1}{m_i} \langle p_i p_j \rangle_c - \left(m_j \omega_{0,j}^2 + u_{2,j} \right) \langle q_i q_j \rangle_c \\ &\quad -\gamma_0 \left(\langle q_i p_j \rangle_c + \left\langle \frac{p_i q_i + q_i p_i}{2} \right\rangle_c \right) \end{aligned} \tag{A.35}$$

dynamics of the co-state

With $\vec{\lambda}(t)$ given by:

$$\begin{aligned} \vec{\lambda}(t) = \; & (\langle q_A \rangle_{c,\lambda}, \langle p_A \rangle_{c,\lambda}, \langle q_B \rangle_{c,\lambda}, \langle p_B \rangle_{c,\lambda}, \\ & \langle q_A^2 \rangle_{c,\lambda}, \langle p_A^2 \rangle_{c,\lambda}, \left\langle \frac{p_A q_A + q_A p_A}{2} \right\rangle_{c,\lambda}, \langle q_B^2 \rangle_{c,\lambda}, \langle p_B^2 \rangle_{c,\lambda}, \left\langle \frac{p_B q_B + q_B p_B}{2} \right\rangle_{c,\lambda}, \\ & \langle q_A q_B \rangle_{c,\lambda}, \langle p_A p_B \rangle_{c,\lambda}, \langle p_A q_B \rangle_{c,\lambda}, \langle q_A p_B \rangle_{c,\lambda})^T \end{aligned} \tag{A.36}$$

the equations of motions for the backward propagation for the first cumulants are:

$$\begin{aligned} \dot{\lambda}_1 &= -\eta_A \lambda_2 \\ \dot{\lambda}_2 &= \frac{1}{m_A} \lambda_1 - \gamma_0 (\lambda_2 - \lambda_4) \\ \dot{\lambda}_3 &= -\eta_B \lambda_4 \\ \dot{\lambda}_4 &= \frac{1}{m_B} \lambda_3 + \gamma_0 (\lambda_2 - \lambda_4). \end{aligned}$$

and, with $\eta_i = m_i \omega_i^2 + u_{2,i}$, $i = \{A, B\}$, for the second cumulants:

$$\dot{\lambda}_5 = -\eta_A \lambda_7 \tag{A.37}$$

$$\dot{\lambda}_6 = -2\gamma_0 \lambda_6 + \frac{1}{m_A} \lambda_7 + \alpha \lambda_{12} \tag{A.38}$$

$$\dot{\lambda}_7 = \frac{2}{m_A} \lambda_5 - 2\eta_A \lambda_6 - \gamma_0 (\lambda_7 + \lambda_{13}) \tag{A.39}$$

$$\dot{\lambda}_8 = -\eta_B \lambda_{10} \tag{A.40}$$

$$\dot{\lambda}_9 = -2\gamma_0 \lambda_9 + \frac{1}{m_B} \lambda_{10} + \gamma_0 \lambda_{12} \tag{A.41}$$

$$\dot{\lambda}_{10} = \frac{2}{m_B}\lambda_8 - 2\eta_B\lambda_9 - \gamma_0(\lambda_{10} + \lambda_{14}) \tag{A.42}$$

$$\dot{\lambda}_{11} = -\eta_B\lambda_{13} - \eta_A\lambda_{14} \tag{A.43}$$

$$\dot{\lambda}_{12} = 2\gamma_0\left(\lambda_6 + \lambda_9 - \lambda_{12}\right) + \frac{1}{m_A}\lambda_{13} + \frac{1}{m_B}\lambda_{14} \tag{A.44}$$

$$\dot{\lambda}_{13} = \gamma_0\lambda_7 + \frac{1}{m_B}\lambda_{11} - \eta_A\lambda_{12} - \gamma_0\lambda_{13} \tag{A.45}$$

$$\dot{\lambda}_{14} = \gamma_0\lambda_{10} + \frac{1}{m_A}\lambda_{11} - \eta_B\lambda_{12} - \gamma_0\lambda_{14} \tag{A.46}$$

B. Dissipative optimal control algorithm

Schematically, our dissipative optimal control algorithm (cf. Section 2.3) works as following:

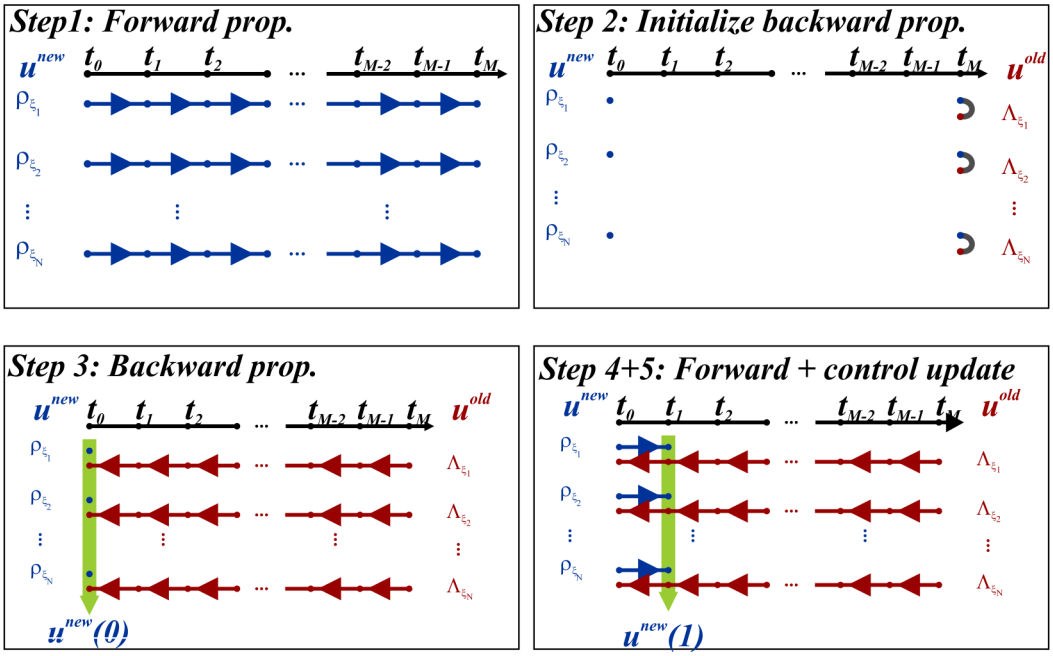

Figure B.1.: Dissipative optimal control (DOCT) algorithm.

1. Forward propagation of $\rho_z(t)$ for all realisations with an initial control $\mathbf{u}^{new}(t)$, at $t = T$: $\mathbf{u}^{old}(t) \leftarrow \mathbf{u}^{new}(t)$,

2. Calculate initial value $\Lambda_z(T)$ of backward propagation for all realisations with the old control $\mathbf{u}^{old}(t)$,

3. Backward propagation of $\Lambda_z(t)$ for all realisations, store all intermediate values, and calculate $\mathbf{u}^{new}(t = 0)$ by avering over all contributions of pairs $(\rho_z(t = 0), \Lambda_z(t = 0))$.

4. Forward propagation of $\rho_z(t) \rightarrow \rho_z(t+1)$ for one timestep for all realisations with the new control $\mathbf{u}^{new}(t)$
5. calculate $\mathbf{u}^{new}(t+1)$ by avering over all contributions of pairs $(\rho_z(t+1), \Lambda_z(t+1))$.
6. repeat steps 4 and 5 for all timesteps,
7. $\mathbf{u}^{old}(t) \leftarrow \mathbf{u}^{new}(t)$,
8. Repeat steps 2 to 7 until some specified stop criterion is fullfilled

Bibliography

[ABB+98] A Assion, T. Baumert, M. Bergt, T. Brixner, B. Kiefer, V. Seyfried, M. Strehle, and G. Gerber. Control of Chemical Reactions by Feedback-Optimized Phase-Shaped Femtosecond Laser Pulses. *Science*, 282:919, 1998.

[ACVM13] Christian Arenz, Cecilia Cormick, David Vitali, and Giovanna Morigi. Generation of two-mode entangled states by quantum reservoir engineering. *arXiv:1303.1977v1 [quant-ph]*, 2013.

[AD10] Gerardo Adesso and Animesh Datta. Quantum versus classical correlations in gaussian states. *Phys. Rev. Lett.*, 105:030501, 2010.

[Ade06] Gerardo Adesso. *Entanglement of Gaussian states*. PhD thesis, Universita degli studi di Salerno, 2006.

[AEM+95] M.H. Anderson, J.R. Ensher, M.R. Matthews, C.E. Wieman, and E.A. Cornell. Observation of Bose-Einstein condensation in a Dilute Atomic Vapor. *Science*, 269:198, 1995.

[ARJ+12] O. Abah, J. Roßnagel, G. Jacob, S. Deffner, F. Schmidt-Kaler, K. Singer, and E. Lutz. Single-ion heat engine at maximum power. *Phys. Rev. Lett.*, 109:203006, Nov 2012.

[AS84] Milton Abramowitz and Irene A. Stegun, editors. *Pocketbook of Mathematical Functions*. Verlag Harri Deutsch, 1984.

[ASI04] Gerardo Adesso, Alessio Serafini, and Fabrizio Illuminati. Determination of continuous variable entanglement by purity measurements. *Phys. Rev. Lett.*, 92:087901, 2004.

[Aud05] Jürgen Audretsch. *Verschränkte Systeme - Die Quantenphysik auf neuen Wegen*. Wiley-VCH Verlag, 2005.

[BBC+93] Charles H. Bennett, Gilles Brassard, Claude Crépeau, Richard Jozsa, Asher Peres, and William K. Wootters. Teleporting an unknown quantum state via dual classical and einstein-podolsky-rosen channels. *Phys. Rev. Lett.*, 70:1895, 1993.

[BBG+91] R. Blümel, A. Buchleitner, R. Graham, L. Sirko, U. Smilansky, and H. Walther. Dynamical localization in the microwave interaction of rydberg atoms: The influence of noise. *Phys. Rev. A*, 44:4521, 1991.

[BCR10] Constantin Brif, Raj Charkrabarti, and Herschel Rabitz. Control of quantum phenomena: past, present and future. *New Journal of Physics*, 12:075008, 2010.

[BD86] W. E. Boyce and R. C. DiPrima. *Elementary Differential Equations and Boundary Value Problems*. Wiley, 1986.

[BD12] R. Biele and R. D'Agosta. A stochastic approach to open quantum systems. *J. Phys.: Condens. Matter*, 24:273201, 2012.

[BFP03] Fabio Benatti, Roberto Floreanini, and Marco Piani. Environment induced Entanglement in Markovian Dissipative Dynamics. *Physical Review Letters*, 91:070402, 2003.

[BH69] Arthur E. Bryson and Yu-Chi Ho. *Applied Optimal Control*. Ginn and Company, 1969.

[BMM+10] Daniel Burgarth, Koji Maruyama, Michael Murphy, Simone Montangero, Tommaso Calarco, Franco Nori, and Martin B. Plenio. Scalable quantum computation via local control of only two qubits. *Phys. Rev. A*, 81:040303, 2010.

[BMS+11] Julio T. Barreiro, Markus Müller, Philipp Schindler, Daniel Nigg, Thomas Monz, Michael Chwalla, Markus Hennrich, Christian F. Roos, Peter Zoller, and Rainer Blatt. An open-system quantum simulator with trapped ions. *Nature*, 470:486, 2011.

[BP06] Heinz-Peter Breuer and Francesco Petruccione. *The theory of open quantum systems*. Oxford University Press, 2006.

[Bra02] Daniel Braun. Creation of entanglement by interaction with a common heat bath. *Phys. Rev.Lett.*, 89:277901, 2002.

[BSMM99] I. N. Bronstein, K. A. Semendjajew, Gerhard Musiol, and Heiner Mühlig. *Taschenbuch der Mathematik*. Verlag Harri Deutsch, 1999.

[BvL05] Samuel L. Braunstein and Peter van Look. Quantum information with continuous variables. *Rev Mod Phys*, 77:513, 2005.

[CBK12] Jens Clausen, Guy Bensky, and Gershon Kurizki. Task-optimized control of open quantum systems. *Phys. Rev. A*, 85:052105, May 2012.

[CCM11] Tommaso Caneva, Tommaso Calarco, and Simone Montangero. Chopped random-basis quantum optimization. *Phys. Rev. A*, 84:022326, 2011.

[CCM12] Tommaso Caneva, Tommaso Calarco, and Simone Montangero. Entanglement storage units. *arXiv:1108.3200v2 [quant-ph]*, 2012.

[CHJ+00] T. Calarco, E. A. Hinds, D. Jaksch, J. Schmiedmayer, J. I. Cirac, and P. Zoller. Quantum gates with neutral atoms: Controlling collisional interactions in time-dependent traps. *Phys. Rev. A*, 61:022304, 2000.

[CL83] Amir O. Caldeira and Anthony J. Leggett. Path integral approach to quantum brownian motion. *Physica*, 121A:587, 1983.

[CMC+09] T. Caneva, M. Murphy, T. Calarco, R. Fazio, S. Montangero, V. Giovannetti, and G. E. Santoro. Optimal Control at the Quantum Speed Limit. *Phys. Rev. Lett.*, 103:240501, 2009.

[CMC+12] F. Caruso, S. Montangero, T. Calarco, S. F. Huelga, and M. B. Plenio. Coherent optimal control of photosynthetic molecules. *Phys. Rev. A*, 85:042331, 2012.

[Dav02] Jon H. Davis. *Foundations of Deterministic and Stochastic Control*. Birkhäuser Boston, 2002.

[DCM11] Patrick Doria, Tommaso Calarco, and Simone Montangero. Optimal control technique for many-body quantum dynamics. *Phys. Rev. Lett.*, 106:190501, 2011.

[DFP+09] V. D'Auria, S. Fornaro, A. Porzio, S. Solimeno, S. Olivares, and M. G. A. Paris. Full characterization of gaussian bipartite entangled states by a single homodyne detector. *Phys. Rev. Lett.*, 102:020502, 2009.

[DMB+09] I. Dotsenko, M. Mirrahimi, M. Brune, S. Haroche, J.-M. Raimond, and P. Rouchon. Quantum feedback by discrete quantum nondemolition measurements: Towards on-demand generation of photon-number states. *Phys. Rev. A*, 80:013805, 2009.

[EP02] Jens Eisert and Martin B. Plenio. Quantum and classical correlations in quantum brownian motion. *Physical Review Letters*, 89:137902, 2002.

[EPR35] A. Einstein, B. Podolsky, and N. Rosen. Can Quantum-Mechanical Description of Physical Reality Be Consired Complete? *Physical Review*, 47:777, 1935.

[EW13] Daniel J. Egger and Frank K. Wilhelm. Optimized controlled Z gates for two superconducting qubits coupled through a resonator. *arXiv:1306.6894v1[quant-ph]*, 2013.

[FdFS12] Frederik F. Floether, Pierre de Fouquieres, and Sophie G. Schirmer. Robust quantum gates for open systems via optimal control: Markovian versus non-Markovian. *New Journal of Physics*, 14:073023, 2012.

[FDT+09] G.D. Fuchs, V.V. Dobrovitski, D.M. Toyli, F.J. Heremans, and D.D. Awschalom. Gigahertz Dynamics of a Strongly Driven Single Quantum Spin. *Science*, 326:1520, 2009.

[FH65] Richard P. Feynman and A.R. Hibbs. *Quantum mechanics and path integrals*. McGraw-Hill Book Company, 1965.

[FV63] Richard P. Feynman and F. L. jr. Vernon. The theory of a general quantum system interacting with a linear dissipative system. *Annals of Physics*, 24:118, 1963.

[GP10] Paolo Giorda and Matteo G. A. Paris. Gaussian quantum discord. *Phys. Rev. Lett.*, 105:020503, Jul 2010.

[GPZ10] Fernando Galve, Leonardo A. Pachón, and David Zueco. Bringing entanglement to the high temperature limit. *Phys. Rev. Lett.*, 105:180501, 2010.

[GSHS+98] Steffen J. Glaser, T. Schulte-Herbrüggen, M. Sieveking, O. Schedletzky, N.C. Nielsen, O.W. Sørensen, and C. Griesinger. Unitary Control in Quantum Ensembles: Maximizing Signal Intensity in Coherent Spectroscopy. *Science*, 280:421, 1998.

[GSI88] Hermann Grabert, Peter Schramm, and Gert-Ludwig Ingold. Quantum Brownian motion: The functional integral approach. *Phys. Rep.*, 168:115, 1988.

[GWT84] Hermann Grabert, Ulrich Weiss, and Peter Talkner. Quantum theory of the damped harmonic oscillator. *Zeitschrift für Physik B*, 55:87, 1984.

[Häb08] Thomas Häberle. Kontrolltheorie und Verschränkung quantenmechanischer Systeme. Master's thesis, Universität Ulm, 2008.

[HB08] Christian Hörhammer and Helmut Büttner. Enviroment-induced two-mode entanglement in quantum brownian motion. *Physical Review A*, 2008.

[HG12] Bin Hwang and Hsi-Sheng Goan. Optimal control for non-markovian open quantum systems. *Phys. Rev. A*, 85:032321, Mar 2012.

[HHH96] M. Horodecki, P. Horodecki, and R. Horodecki. Separability of mixed states: necessary and sufficient conditions. *Physics Letters A*, 223:1, 1996.

[Hol75] Alexander S. Holevo. Some statistical problems for quantum Gaussian states. *IEEE Transactions on Information Theory*, 21:533, 1975.

[HSH99] A. S. Holevo, M. Sohma, and O. Hirota. Capacity of quantum gaussian channels. *Phys. Rev. A*, 59:1820–1828, Mar 1999.

[HWA+09] M. Hofheinz, H. Wang, M. Ansmann, R.C. Bialczak, E. Lucero, M. Neeley, A.D. O'Connell, John M. Martinis, and A.N. Cleland. Synthesizing arbitrary quantum states in a superconducting resonator. *Nature*, 459:546, 2009.

[ICJ+05] G. Ithier, E. Collin, P. Joyez, P.J. Meeson, Denis Vion, Daniel Esteve, F. Chiarello, A. Shnirman, Y. Makhlin, J. Schriefl, and G. Schön. Decoherence in a superconducting quantum bit circuit. *Physical Review B*, 72:134549, 2005.

[JBA+03] S. Jochim, M. Bartenstein, A. Altenmeyer, G. Hendl, S. Riedl, C. Chin, Johannes Hecker Denschlag, and R. Grimm. Bose-Einstein Condensation of Molecules. *Science*, 302:2101, 2003.

[JGP+04] F. Jelezko, T. Gaebel, I. Popa, M. Domhan, A. Gruber, and J. Wrachtrup. Observation of coherent oscillation of a single nuclear spin and realization of a two-qubit conditional quantum gate. *Phys. Rev. Lett.*, 93:130501, Sep 2004.

[KF83] Vadim Krotov and I.N. Feldman. An iterative method for solving optimal control problem. *Engineering cybernetics*, 17:123ff, 1983.

[KGAS09] Werner Koch, Frank Grossmann, Joachim Ankerhold, and Jürgen T. Stockburger. Semiclassical formulation of non-markovian quantum brownian motion. *Physica E*, 2009.

[KGSA08] Werner Koch, Frank Großmann, Jürgen T. Stockburger, and Joachim Ankerhold. Non-markovian dissipative semiclassical dynamics. *Physical Review Letters*, 100:230402, 2008.

[KK99] A.I. Konnov and Vadim F. Krotov. On global methods of successive improvement of controlled processes. *Automation and Remote Control*, 60:1427, 1999.

[KK04] A. G. Kofman and G. Kurizki. Unified theory of dynamically suppressed qubit decoherence in thermal baths. *Phys. Rev. Lett.*, 93:130406, 2004.

[KKC+11] Alexander Karabanov, Ilya Kuprov, G. T. P. Charnock, Anniek van der Drift, Luke J. Edwards, and Walter Köckenberger. On the accuracy of the state space restriction approximation for spin dynamics simulations. *Journal of Chemical Physics*, 135:084106, 2011.

[Kro96] Vadim F. Krotov. *Global Methods in Optimal Control Theory*. Pure and applied mathematics. Marcel Dekker, INC, 1996.

[KSK+08] Kyryl Kobzar, Thomas E. Skinner, Navin Khaneja, Steffen J. Glaser, and Burkhard Luy. Exploring the limits of broadband excitation and inversion: II. Rf-power optimized pulses. *Journal of Magnetic Resonance*, 194:58, 2008.

[Leo10] U. Leonhardt. *Essential Quantum Optics: From Quantum Measurements to Black Holes*. Cambridge University Press, 2010.

[LGL+11] Peng-Bo Li, Shao-Yan Gao, Hong-Rong Li, Sheng-Li Ma, and Fu-Li Li. Dissipative preparation of entangled states between two spacially separated nitrogen-vacancy centers. *arXiv:1106718v3*, 2011.

[LKOH+05] Julien Laurat, Gaëlle Keller, Jose Augusto Oliveira-Huguenin, Claude Fabre, Thomas Coudreau, Alessio Serafini, Gerardo Adesso, and Fabrizio Illuminati. Entanglement of two-mode Gaussian states: characterization and experimental production and manipulation. *Journal of Optics B*, 7:577, 2005.

[MAK05] L. Mühlbacher, J. Ankerhold, and A. Komnik. Nonequilibrium dynamics of correlated electron transfer in molecular chains. *Phys. Rev. Lett.*, 95:220404, 2005.

[MCF07] Simone Montangero, Tommaso Calarco, and Rosario Fazio. Robust optimal quantum gates for josephson charge qubits. *Physical Review Letters*, 99:170501, 2007.

[McL64] N. W. McLachlan. *Theory and Application of Mathieu Functions*. Dover, 1964.

[MHdC+13] Suzanne McEndoo, Pinja Haikka, Gabriele de Chiara, Massimo Palma, and Sabrina Maniscalco. Entanglement control via reservoir engineering in ultracold atomic gases. *EPL*, 101:60005, 2013.

[Min12] Florian Mintert. Smooth, optimal control. *arXiv:1205.5142v1[quant-ph]*, 2012.

[MJKC09] Michael Murphy, L. Jiang, N. Khaneja, and Tommaso Calarco. High-fidelity fast quantum transport with imperfect controls. *Physical Review A*, 79:020301, 2009.

[MKL+13] M. M. Müller, A. Kölle, R. Löw, T. Pfau, T. Calarco, and S. Montangero. Room-temperature Rydberg single-photon source. *Phys. Rev. A*, 87:053412, 2013.

[MMC+11] Michael Murphy, Simone Montangero, Tommaso Calarco, Philippe Grangier, and Antoine Browaeys. Towards an experimentally feasible controlled-phase gate on two blockaded Rydberg atoms. *arXiv:1111.6083v1[quant-ph]*, 2011.

[MRM+11] Matthias M. Müller, Daniel M. Reich, Michael Murphy, H. Yuan, J. Vala, K.B. Whaley, Tommaso Calarco, and Christiane Koch. Optimizing entangling quantum gates for physical systems. *Physical Review A*, 84:042315, 2011.

[MSS01] Yuriy Makhlin, Gerd Schön, and Alexander Shnirman. Quantum-state engineering with josephson-junction devices. *Rev. Mod. Phys.*, 73:357, 2001.

[NC00] Michael A. Nielsen and Isaac L. Chuang. *Quantum computation and quantum Information*. Cambridge University Press, 2000.

[NLKS13] Mamadou Ndong, Marc Lapert, Christiane P. Koch, and Dominique Sugny. Comparative study of monotonically convergent optimization algorithms for the control of molecular rotation. *Phys. Rev. A*, 87:043416, Apr 2013.

[NRO+99] G. Nogues, A. Rauschenbeutel, S. Osnaghi, M. Brune, J.M. Raimond, and S. Haroche. Seeing a single photon without destroying it. *Nature*, 400:239, 1999.

[NS09] R. Nigmatullin and S. G. Schirmer. Implementation of fault-tolerant quantum logic gates via optimal control. *New Journal of Physics*, 11:105032, 2009.

[OHA+10] A.D. O'Connell, M. Hofheinz, M. Ansmann, R.C. Bialczak, M. Lenanader, E. Lucero, M. Neeley, D. Sank, H. Wang, M. Weides, J. Wenner, John M. Martinis, and A.N. Cleland. Quantum ground state and single-phonon control of mechanical oscillator. *Nature*, 464:697, 2010.

[OP11] Stefano Olivares and Matteo G. A. Paris. Fidelity matters: The birth of entanglement in the mixing of gaussian states. *Phys. Rev. Lett.*, 107:170505, Oct 2011.

[OZ01] Harold Ollivier and Wojciech H. Zurek. Quantum discord: A measure of the quantumness of correlations. *Phys. Rev. Lett.*, 88:017901, Dec 2001.

[PDR88] Anthony P. Peirce, Mohammed A. Dahleh, and Herschel Rabitz. Optimal control of quantum-mechanical systems: Existence, nummerical approximation, and applications. *Physical Review A*, 37:4950, 1988.

[Pec11] Alexander Pechen. Engineering arbitrary pure and mixed quantum states. *Physical Review A*, 84:042106, 2011.

[Per96] Asher Peres. Separability criterion for density matrices. *Physical Review Letters*, 77:1413, 1996.

[PH07] J. P. Pekola and F. W. J. Hekking. Normal-Metal-Superconductor Tunnel Junction as a Brownian Refrigerator. *Phys. Rev. Lett.*, 98:210604, May 2007.

[PK02] J. P. Palao and R. Kosloff. Quantum computing by an optimal control algorithm for unitary transformations. *Phys. Rev. Lett.*, 89:188301, 2002.

[Ple05] M. B. Plenio. Logarithmic negativity: A full entanglement monotone that is not convex. *Phys. Rev. Lett.*, 95:090503, 2005.

[PMB10] Felix Platzer, Florian Mintert, and Andreas Buchleitner. Optimal Dynamical Control of Many-Body Entanglement. *Phys. Rev. Lett.*, 105:020501, Jul 2010.

[PR08] Juan Pablo Paz and Augusto J. Roncaglia. Dynamics of the Entanglement between Two Oscillators in the Same Environment. *Phys. Rev. Lett.*, 100:220401, 2008.

[RdVRMK00] Herschel Rabitz, Regina de Vivie-Riedle, Markus Motzkus, and Karl Kompa. Whither the Future of Controlling Quantum Phenomena. *Science*, 288:824, 200.

[RNK12] Daniel M. Reich, Mamadou Ndong, and Christiane P. Koch. Monotonically convergent optimization in quantum control using krotov's method. *Journal of Chemical Physics*, 136:104103, 2012.

[Roh11] Selina Rohrer. Optimale Kontrolle offener dynamischer Systeme. Master's thesis, Universität Ulm, 2011.

[RSK+07] Miguel Rey, Michael Strass, Sigmund Kohler, Peter Hänggi, and Fernando Sols. Nonadiabatic electron heat pump. *Phys. Rev. B*, 76:085337, Aug 2007.

[RSSHW09] P. Rebentrost, I. Serban, T. Schulte-Herbrüggen, and F.K. Wilhelm. Optimal control of a qubit coupled to an non-markovian enviroment. *Physical Review Letters*, 102:090401, 2009.

[Sch35] Erwin Schrödinger. Die gegenwärtige Situation der Quantenmechanik. *Die Naturwissenschaften*, 50:844, 1935.

[Sch01] Wolfgang P. Schleich. *Quantum Optics in Phase Space*. Wiley-VCH Verlag, 2001.

[Sch09] Rebecca Schmidt. Kontrollprobleme in offenen Quantensystemen und deren Lösung im Rahmen stochastischer semiklassischer Dynamik. Master's thesis, Universität Ulm, 2009.

[SdF11] S. G. Schirmer and Pierre de Fouquieres. Efficient algorithms for optimal control of quantum dynamics: the Krotov method unencumbered. *New Journal of Physics*, 13:073029, 2011.

[SG02] Jürgen T. Stockburger and Hermann Grabert. Exact c-number representation of non-markovian quantum dissipation. *Physical Review Letters*, 88:170407, 2002.

[SG08] R.J. Schoelkopf and S.M. Girvin. Wiring up quantum systems. *Nature*, 451:664, 2008.

[SHSKG05] T. Schulte-Herbrüggen, A. Spörl, N. Khaneja, and S. J. Glaser. Optimal control-based efficient synthesis of building blocks of quantum algorithms: A perspective from network complexity towards time complexity. *Phys. Rev. A*, 72:042331, 2005.

[SHSKG11] T. Schulte-Herbrüggen, A. Spörl, N. Khaneja, and S. J. Glaser. Optimal control for generating quantum gates in open dissipative systems. *Journal of Physics B*, 44:154013, 2011.

[Sim00] R. Simon. Peres-horodecki seperability criterion for continuous variable systems. *Phys.Rev.Lett.*, 84:2726, 2000.

[SKHR+03] Ferdinand Schmidt-Kaler, Hartmut Häffner, Mark Riebe, Stephan Gulde, Gavin P. T. Lancaster, Thomas Deuschle, Christoph Becher, Christian F. Roos, Jürgen Eschner, and Rainer Blatt. Realization of the Cirac–Zoller controlled-NOT quantum gate. *Nature*, 422:408, 2003.

[SM99] Jürgen T. Stockburger and C. H. Mak. Stochastic liouvillian algorithm to simulate dissipative quantum dynamics with arbitrary precision. *Journal of Chemical Physics*, 110 (11):4983ff, 1999.

[SM10] Alessio Serafini and Stefano Mancini. Determination of Maximal Gaussian entanglement achievable by Feedback-Controlled Dynamics. *Physical Review Letters*, 104:220501, 2010.

[SMSP10] P. Solinas, M. Möttönen, J. Salmilehto, and Jukka P. Pekola. Decoherence of adiabatically steered quantum systems. *Physical Review B*, 82:134517, 2010.

[SNA+11a] Rebecca Schmidt, Antonio Negretti, Joachim Ankerhold, Tommaso Calarco, and Jürgen T. Stockburger. Optimal control of open quantum systems: Cooperative effects of driving and dissipation. *Physical Review Letters*, 107:130404, 2011.

[SNA+11b] Rebecca Schmidt, Antonio Negretti, Joachim Ankerhold, Tommaso Calarco, and Jürgen T. Stockburger. Supplemental material to: Optimal control of open quantum systems: Cooperative effects of driving and dissipation, 2011.

[SR90] Shengua Shi and Herschel Rabitz. Quantum mechanical optimal control of physical observables in microsystems. *J. Chem. Phys.*, 92:364, 1990.

[SRAS12] R. Schmidt, Selina Rohrer, J. Ankerhold, and J. T. Stockburger. Cooling of quantum systems through optimal control and dissipation. *Phys. Scr.*, T151:014034, 2012.

[SRL+03] Thomas E. Skinner, Timo O. Reiss, Burkhard Luy, Navin Khaneja, and Steffen J. Glaser. Application of optimal control theory to the design of broadband excitation pulses for high-resolution NMR. *Journal of Magnetic Resonance*, 163:8, 2003.

[SRP09] Alessio Serafini, Alexander Retzker, and Martin B. Plenio. Manipulating the quantum information of the radial modes of trapped ions: linear phononics, entanglement generation, quantum state transmission and non-locality tests. *New Journal of Physics*, 11:023007, 2009.

[SSA13a] Rebecca Schmidt, Jürgen T. Stockburger, and Joachim Ankerhold. Quasi-local generation of EPR entanglement in non-equilibrium. *arXiv:1305.6566 [quant-ph]*, 2013.

[SSA13b] Rebecca Schmidt, Jürgen T. Stockburger, and Joachim Ankerhold. Supplemental material to: Quasi-local generation of EPR entanglement in non-equilibrium, 2013.

[SSHG+07] A. Spörl, T. Schulte-Herbrüggen, S. J. Glaser, V. Bergholm, M. J. Storcz, J. Ferber, and F. K. Wilhelm. Optimal control of coupled josephson qubits. *Phys. Rev. A*, 75:012302, 2007.

[ST02] Shlomo E. Sklarz and David J. Tannor. Loading a bose-einstein condensate onto a optical lattice: An application of optimal control theory to the nonlinear schrödinger equation. *Physical Review A*, 66:053619, 2002.

[ST04] Shlomo E. Sklarz and David J. Tannor. Optimal control of quantum dissipative dynamics: Analytic solution for cooling the three-level λ system. *Physical Review A*, 69:53408, 2004.

[Sto03] Jürgen T. Stockburger. Stochastic and numerical approaches to dissipative quantum dynamics: path integrals and beyond. *phys. stat. sol. (b)*, 237:146, 2003.

[Sto04] Jürgen T. Stockburger. Simulating spin-boson dynamics with stochastic Liouville-von Neumann equations. *Chemical Physics*, 296:159–169, 2004.

[Sto06] Jürgen T. Stockburger. *Stochastic methods for the dynamics of open quantum systems*. Habilitationsschrift, Unversität Stuttgart, 2006.

[Sto13a] Jürgen T. Stockburger. Vorlesungsskript Nichtgleichgewichtsstatistik WS12/13, 2013.

[Sto13b] Jürgen T. Stockburger. Vorlesungsskript Numerische Simulationsmethoden, SoSe, 2013.

[STP+10] Joel Stettenheim, Madhu Thalakulam, Feng Pan, Mustafa Bal, Zhonqing Ji, Weiwei Xue, Loren Pfeiffer, K. W. West, M. P. Blencowe, and A. J. Rimberg. A macroscopic mechanical resonator driven by mesoscopic electrical back-action. *Nature*, 466:86, 2010.

[Suz93] M. Suzuki, editor. *Quantum Monte Carlo Methods in Condensed Matter Physics*. World Scientific Singapore, 1993.

[Tan06] Yoshitaka Tanimura. Stochastic Liouville, Langevin, Fokker-Planck, and Master Equation Approaches to Quantum Dissipative Systems. *Journal of the Physical Society of Japan*, 75:8, 2006.

[TdVR02] Carmen M. Tesch and Regina de Vivie-Riedle. Quantum computation with vibrationally exited molecules. *Phys. Rev. Lett.*, 89:157901, 2002.

[THR+06] Philipp Treutlein, Theodor W. Hänsch, Jakob Reichel, Antonio Negretti, Markus A. Cirone, and Tommaso Calarco. Microwave potentials and optimal control for robust quantum gates on an atom chip. *Phys. Rev. A*, 74:022312, 2006.

[THS+04] Philipp Treutlein, Peter Hommelhoff, Tilo Steinmetz, Theodor W. Hänsch, and Jakob Reichel. Coherence in microchip traps. *Phys. Rev. Lett.*, 92:203005, May 2004.

[TKR86] David J. Tannor, Ronnie Kosloff, and Stuart A. Rice. Coherent pulse sequence induced control of selectivity of reactions: Exact quantum mechanical calculations. *Journal of Chemical Physics*, 85:5805, 1986.

[Vac00] Bassano Vacchini. Completely positive quantum dissipation. *Phys. Rev. Lett.*, 84:1374, 2000.

[VAC+02] Denis Vion, A. Aassime, A. Cottet, P. Joyez, H. Pothier, C. Urbina, D. Esteve, and M.H. Devoret. Manipulating the Quantum State of an Electrical Circuit. *Science*, 296:886, 2002.

[VL98] Lorenza Viola and Seth Lloyd. Dynamical suppression of decoherence in two-state quantum systems. *Phys. Rev. A*, 58:2733, 1998.

[VW02] G. Vidal and R.F. Werner. Computable measure of entanglement. *Physical Review A*, 65:032314, 2002.

[WC13] Ying-Dan Wang and Aashish A. Clerk. Reservoir-engineered entanglement in optomechanical systems. *Phys. Rev. Lett.*, 110:253601, Jun 2013.

[WDCK+11] Alexander Wolf, G. De Chiara, Endre Kajari, Eric Lutz, and Giovanna Morigi. Entangling two distant oscillators with a quantum reservoir. *Euro Physics Letters*, 95:60008, 2011.

[Wei12] Ulrich Weiss. *Quantum Dissipative Systems*. Series in Modern Condensed Matter Physics. World Scientific Publishing Co. Pte. Ltd, 4 edition, 2012.

[WG07] J. Werschnik and E.K.U. Gross. Quantum optimal control theory. *J. Phys. B: At. Mol. Opt. Phys.*, 40:R175, 2007.

[WPGP+12] Christian Weedbrook, Stefano Pirandola, Raúl García-Patrón, Nicolas J. Cerf, Timothy C. Ralph, Jeffrey H. Shapiro, and Seth Lloyd. Gaussian quantum information. *Rev. Mod. Phys.*, 84:621, 2012.

[WR03] Ian Walmsley and Herschel Rabitz. Quantum physics under control. *Physics Today*, page 43, 2003.

[XYO+04] Riuxue Xu, YiJing Yan, Yukiyoshi Ohtsuki, Yuichi Fujimura, and Herschel Rabitz. Optimal control of quantum non-Markovian dissipation: Reduced Liouville-space theory. *Journal of Chemical Physics*, 120:6600, 2004.

[YHHSR05] Dong Yang, Michał Horodecki, Ryszard Horodecki, and Barbara Synak-Radtke. Irreversibility for All Bound Entangled States. *Phys. Rev. Lett.*, 95:190501, 2005.

[YPA+03] T. Yamamoto, Yu. A. Pashkin, O. Astafiev, Y. Nakamura, and J.S. Tsai. Demonstration of conditional gate operation using superconducting charge qubits. *Nature*, 425:941, 2003.

[ZH95] Christine Zerbe and Peter Hänggi. Brownian parametric quantum oszillator with dissipation. *Physical Review E*, 52:1533, 1995.

[ZPAI13] S. Zippilli, M. Paternostro, G. Adesso, and F. Illuminati. Entanglement replication in driven dissipative many-body systems. *Phys. Rev. Lett.*, 110:040503, 2013.

Aus Gründen des Datenschutzes wurde der Lebenslauf aus der elektronischen Version entfernt.
For the sake of privacy protection the curriculum is not part of the electronic version.

Aus Gründen des Datenschutzes wurde die Danksagung aus der elektronischen Version entfernt.
For the sake of privacy protection the acknowledgements are not part of the electronic version.

Diese Arbeit ist entstanden am Institut für Theoretische Physik, Abteilung Kondensierte Materie, an der Universität Ulm in Zusammenarbeit mit Jürgen Stockburger und Joachim Ankerhold. Teile der Arbeit sind in Kooperation mit Tommaso Calarco und Antonio Negretti (Institut für Quanteninformationsverarbeitung,Universität Ulm) sowie Selina Rohrer (Institut für Theoretische Physik, Abteilung Kondensierte Materie) entstanden.
Finanziell wurde diese Promotion durch die Landesstiftung Baden-Württemberg und die Deutsche Forschungsgemeinschaft gefördert.

Hiermit erkläre ich, dass ich die vorliegende Arbeit selbstständig angefertigt sowie keine anderen als die angegebenen Quellen und Hilfmitteln benutzt, sowie wörtlich oder inhaltlich übernommene Stellen als solche kenntlich gemacht und die Satzung der Universität Ulm zur Sicherung guter wissenschaftlicher Praxis in der aktuell gültigen Fassung vom 16.10.2009 beachtet habe.

Ulm, den 25. Juli 2013 _____